


Title	Mesenchymal stem cell therapy for the treatment of myocardial infarction
Author(s)	Gleeson, Birgitta
Publication date	2014
Original citation	Gleeson, B. 2014. Mesenchymal stem cell therapy for the treatment of myocardial infarction. PhD Thesis, University College Cork.
Type of publication	Doctoral thesis
Rights	<p>© 2014, Birgitta Gleeson.</p> <p>http://creativecommons.org/licenses/by-nc-nd/3.0/</p> 
Embargo information	No embargo required
Item downloaded from	http://hdl.handle.net/10468/2003

Downloaded on 2017-02-12T09:18:49Z

Mesenchymal Stem Cell Therapy for the Treatment of Myocardial Infarction

Submitted to the National University of Ireland in fulfilment of the requirements
for the degree of

Doctor of Philosophy

By

Gleeson, Birgitta

Centre for Research in Vascular Biology,
Biosciences Institute

National University of Ireland, Cork,
Ireland.

Thesis Supervisor: Prof. Noel M Caplice MD PhD

August 2014

DECLARATION

This thesis has not been previously submitted, in whole or in part, to this or any other University or Institution for any degree, and is, unless otherwise stated, the original work of the author.

Signed _____

CHAPTER1	1
INTRODUCTION	1
1.1 Myocardial Infarction	2
1.1-1 Epidemiology of Myocardial Infarction	2
1.1.1 Cardiac Anatomy	2
1.1.2 Pathophysiology of Myocardial Infarction	3
1.1.3 Atherogenesis and Vascular Occlusion	6
1.1.4 Myocardial Ischemia and Reperfusion	8
1.1.5 Current treatments for Myocardial Infarction	9
1.2 Emerging treatments for MI	13
1.2.1 Bone Marrow Progenitors	14
1.2.2 Cardiac Stem cells	15
1.3 Mesenchymal stem cells	16
1.3.1 Introduction	16
1.3.2 Mesenchymal stem cells engraftment and transdifferentiation post myocardial Infarction (Figure 1.6)	18
1.3.3 Mesenchymal stem cell secreted factors and their effect post Myocardial Infarction (Figure 1.6)	20
1.3.4 MSC and Apoptosis	21
1.3.5 MSC and cardiac inflammation post MI	22
1.3.6 MSC and cardiac remodelling	24
1.3.7 Allogeneic vs. Autologous MSC	25
1.4 MSC delivery strategies	26
1.4.1 Introduction	26
1.4.2 Intravenous MSC delivery	27
1.4.3 Intramyocardial MSC Delivery	28
1.4.4 Intracoronary MSC delivery	31

1.5	Tissue Factor	32
1.6	Aims	35
	CHAPTER 2	36
	MATERIALS AND METHODS	36
2.1	Isolation of Porcine Bone Marrow	37
2.1.1	MSC culturing and preparation	38
2.2	Characterisation of MSC differentiation capacity	39
2.2.1	Characterisation of MSC osteogenic differentiation capacity	39
2.2.2	Characterisation of MSC adipogenic differentiation capacity	39
2.2.3	Characterisation of MSC chondrogenic differentiation capacity	40
2.3	Staining of MSC with DiI	41
2.4	MSC delivery and Infarct model	42
2.4.1	MSC preparation	42
2.4.2	Myocardial Infarction model	42
2.4.3	Anaesthesia and intubation	44
2.4.4	Treating Arrhythmias and maintenance of arterial pressure	45
2.4.5	Animal Housing	45
2.4.6	Coronary Flow Reserve	46
2.4.7	Intracoronary MSC delivery	47
2.4.8	Sacrifice and tissue collection	47
2.5	Tissue sampling	49
2.5.1	Apoptosis and cell infiltration in border zone	49
2.5.2	Trichrome staining for analysis of microvascular plugging	50
2.6	Analysis of Tissue Factor	51
2.6.1	Surface Tissue Factor expression by immunocytochemistry	51

2.6.2	Analysis of surface Tissue Factor expression by FACS	52
2.6.3	Assessment of Tissue factor Protein Expression by Immunoblotting	52
2.6.4	Analysis of thrombin generation and coverage under physiological flow conditions [163, 164]	53
2.6.5	Analysis of Tissue Factor activity	54
2.6.6	Thrombin generation.	55
2.7	Analysis of secretome of porcine and human MSC	55
2.8	Sparcl1 study	56
2.8.1	Sparcl1 ELISA	56
2.8.2	Sparcl1 MI model	57
2.8.3	Dose of SPARCL1	57
2.9	Statistics	57
2.9.1	Power calculation	57
2.9.2	Analysis	57
CHAPTER 3		60
PORCINE MSC ISOLATION AND CELL DELIVERY OPTIMIZATION		
IN MI		60
3.1	Introduction	61
3.2	Results	65
3.2.1	Isolation and expansion of porcine MSC	65
3.2.2	MSC differentiation and surface marker expression	65
3.2.3	Efficiency of Dil cell labelling and viability of MSC	69
3.2.4	Initial dosing studies	69

3.3	Discussion	76
CHAPTER 4		80
IDENTIFYING THE <i>IN VITRO</i> PROCOAGULANT NATURE OF MESENCHYMAL STEM CELLS		80
4.1	Introduction	81
4.2	Results	82
4.2.1	MSC expressed significant surface TF	82
4.2.2	TF expressed by MSC was catalytically active and supported thrombin generation <i>in vitro</i>	86
4.2.3	MSC augment thrombus build-up under flow conditions	86
4.3	Discussion	90
CHAPTER 5		94
THE ACUTE EFFECT OF INTRACORONARY DELIVERY OF TF EXPRESSING MSC IN A PORCINE MODEL OF MI		94
5.1	Introduction	95
5.2	Results	97
5.2.1	MSC administration was associated with intramyocardial haemorrhage and reduced coronary flow reserve.	97
5.2.2	Intracoronary MSC administration was associated with <i>in situ</i> microvascular thrombosis and ameliorated by heparin co-administration	100
5.2.3	MSC delivery has no effect on acute infarct size or on acute hemodynamic function	103

5.3	Discussion	107
5.3.1	Mechanisms of Tissue Factor induced adverse events post MSC delivery	107
5.3.2	Heparin effect on MSC procoagulative activity	109
5.3.3	Tissue Factor induced Microvascular Obstruction	111
CHAPTER 6		113
LONG TERM CARDIAC FUNCTIONAL BENEFIT OF MSC WHEN DELIVERED IN THE PRESENCE OF HEPARIN		113
6.1	Introduction	114
6.2	Results	116
6.2.1	Chronic effect of heparin assisted intracoronary MSC delivery on chronic infarct size and global ventricular remodelling	116
6.2.2	MSC delivery in the presence of heparin improved cardiac wall motion at 6 week s.	116
6.2.3	MSC delivery decreased infarct fibrosis	121
6.3	Discussion	122
CHAPTER 7		125
MSC SECRETED PARACRINE FACTORS AND THEIR ROLE IN CARDIAC REPAIR		125
7.1	Introduction	126
7.2	Results	129
7.2.1	MSC secrete SPARCL1	129
7.2.2	SPARCL1 has no effect on cardiac functional parameters.	129
7.2.3	MSC secrete a wide array of paracrine factors.	129

7.3	Discussion	137
CHAPTER 8		142
DISCUSSION AND FUTURE DIRECTIONS		142
8.1	Discussion	143
8.1.1	Optimising MSC delivery	143
8.1.2	Safety concerns surrounding MSC therapy	143
8.1.3	The effect of heparin on MSC	146
8.1.4	The role of MSC associated TF	147
8.1.5	Clinical implications	147
8.2	Future Directions	149
CHAPTER 9	APPENDIX	175
9.1	MSC DiI Labelling	176
9.2	7AAD Staining	177
9.3	Coronary Flow Researve Theroy[156]	178
9.4	TF Activity Assay	179
9.5	Thrombin Generation Assay	183
9.6	Sparcl1 ELISA	187
9.7	CM Ctokine Arrays	191
9.8	Cardiac Functional Parameters	198

PUBLICATIONS

Bone marrow-derived mesenchymal stem cells have innate procoagulant activity and cause microvascular obstruction following intracoronary delivery: amelioration by heparin co-administration.

Birgitta M Gleeson MSc, Kenneth Martin, PhD, Arun HS Kumar, DVM PhD
Mohammed T Ali, MD, Gopala Krishnan, BRIT, Frank P Barry, PhD, Timothy
O'Brien, MD PhD, Noel M Caplice, MD PhD

Stem cells, 2014 (In revision)

Intravascular cell delivery device for therapeutic VEGF-induced angiogenesis in chronic vascular occlusion.

Noel M Caplice MD PhD, Brendan Doyle MD, Arun HS Kumar DVM, Kenneth
Martin PhD, Mohammed T Ali MD, Kimberly A Skelding MD, Birgitta M
Gleeson MSc, Shaohua Wang MD, Gopal Krishnan BS, Erik L Ritman MD
PhD, Stephen J Russell MD PhD.

Biomaterials, 2014 (Accepted)

A Novel CX3CR1 antagonist eluting stent prevents In-Stent neointimal hyperplasia and has similar re-endothelialization profile to bare metal stents.

Mohammed T Ali MB, Arun HS Kumar DVM PhD, Kenneth Martin PhD,
William L. McPheat, Stefan Pierrou, Birgitta M Gleeson MSc, Chien Ling Huang
PhD Elizebeth C Turner Ph.D, Carl Vaughan MD, Noel M Caplice MD PhD.

JACC (In revision)

PRESENTATIONS

Bone marrow-derived mesenchymal stem cells have innate procoagulant activity and cause microvascular obstruction following intracoronary delivery: amelioration by heparin co-administration.

Birgitta M Gleeson MSc, Kenneth Martin, PhD, Arun HS Kumar, DVM PhD, Mohammed T Ali, MD, Gopala Krishnan, BRIT, Frank P Barry, PhD, Timothy O'Brien, MD PhD, Noel M Caplice, MD PhD

American Heart Association Scientific Sessions in Dallas, TX, November 16-20, 2013

Intravascular cell delivery device for therapeutic VEGF-induced angiogenesis in chronic vascular occlusion.

Noel M Caplice MD PhD, Brendan Doyle MD, Arun HS Kumar DVM, Kenneth Martin PhD, Mohammed T Ali MD, Kimberly A Skelding MD, **Birgitta M Gleeson MSc**, Shaohua Wang MD, Gopal Krishnan BS, Erik L Ritman MD PhD, Stephen J Russell MD PhD.

American Heart Association Scientific Sessions in Dallas, TX, November 16-20, 2013

ACKNOWLEDGEMENTS

Firstly, I would like to express my gratitude to my supervisor Professor Noel Caplice for giving me the opportunity to undertake my PhD in the CRVB, for the motivation, mentorship and for always maintaining a high standard of workmanship. I want to thank him for his support in pursuing a career in medicine and for providing and solid grounding to do so.

I also want to thank everyone else at the CRVB over the past three years. In particular I would like to thank Ken who has been there from start to finish, for all his support and knowledge, for his love of GPIb-beta and for always asking the hard question, what would Carl Sagan do? I also want to thank him for his meticulous proof reading of everything that I wrote for the duration of my PhD, including this thesis. I would like to thank Arun for all his help with the animal work, without his unfaltering patience, guidance and knowledge the completion for this PhD would have been impossible. I would also like to thank Mohammad for all his help with the animal work and for persevering even when it was all going against us. I would like to thank Sujit for all those trips to Fermoy and for enduring the smell! I want to thank Vincent whose innovative ideas in the animal lab always make the work just that little but easier for all involved. I want to thank Gopal for his extensive knowledge of CT. I also want to thank Chien-ling and Libby for providing support and advice on everything from the molecular science to women in science. I want to thank Sharon and Janet for all the genuine support, for always looking out for my best interests and for always just getting things done. I also must acknowledge all the PhDs that have been through the lab since I began, sometimes just being in the same boat can make a world of difference. I

also want to thank Dan for helping me get through it and for being there. I would like to thank Maj for her love and support over the years for which a simple thanks cannot suffice. Finally, I want to thank my dad for his constant support and guidance from day one. His love of life and knowledge has certainly rubbed off and to him I dedicate this thesis.

ABSTRACT

Mesenchymal stem cells (MSCs) are currently under investigation as repair agents in the preservation of cardiac function following myocardial infarction (MI). However concerns have emerged regarding the safety of acute intracoronary (IC) MSC delivery specifically related to mortality, micro-infarction and microvascular flow restriction post cell therapy in animal models. This thesis aimed to firstly identify an optimal dose of MSC that could be tolerated when delivered via the coronary artery in a porcine model of acute MI (AMI). Initial dosing studies identified 25×10^6 MSC to be a safe MSC cell dose, however, angiographic observations from these studies recognised that on delivery of MSC there was a significant adverse decrease in distal blood flow within the artery. This observation along with additional supportive data in the literature (published during the course of this thesis) suggested MSC may be contributing to such adverse events through the propagation of thrombosis. Therefore further studies aimed to investigate the innate prothrombotic activity of MSC. Expression of the initiator of the coagulation cascade initiator tissue factor (TF) on MSC was detected in high levels on the surface of these cells. MSC-derived TF antigen was catalytically active, capable of supporting thrombin generation *in vitro* and enhancing platelet-driven thrombus deposition on collagen under flow. Infusion of MSC via IC route was associated with a decreased coronary flow reserve when delivered but not when coadministered with an anti-thrombin agent heparin. Heparin also reduced MSC-associated in situ thrombosis incorporating platelets and VWF in the microvasculature. Heparin-assisted MSC delivery reduced acute apoptosis and significantly improved infarct size, left ventricular ejection fraction,

LV volumes, wall motion and scar formation at 6 weeks post AMI. In addition, this thesis investigated the paracrine factors secreted by MSC, in particular focusing on the effect on cardiac repair of a novel MSC-paracrine factor SPARCL1. In summary this work provides new insight into the mechanism by which MSC may be deleterious when delivered by an IC route and a means of abrogating this effect. Moreover we present new data on the MSC secretome with elucidation of the challenges encountered using a single paracrine factor cardiac repair strategy.

ABBREVIATIONS

7AAD	7-aminoactinomycin D
ACE	Angiotensin converting enzyme
ADSC	Adipose Derived Stromal Cells
BM	Bone Marrow
BM-MNC	Bone Marrow Mononuclear Cells
BMP2	Bone morphogenetic protein-2
BZ	Border Zone
CF	Cardiac fibroblasts
CFR	Coronary Flow Reserve
CRVB	Centre for Research in Vascular Biology
CSC	Cardiac Stem cells
CT	Computed Tomography
DAPI	4',6-Diamidino-2-phenylindole
DMSO	Dimethyl sulfoxide
D-PBS	Dulbecco's Phosphate-Buffered Saline
EC	Endothelial Cell
ECG	Electrocardiography
ECM	Extracellular Matrix
EDTA	Ethylenediaminetetraacetic acid
EDV	End Diastolic Volume
EF	Ejection Fraction
ELISA	Enzyme-linked immunosorbent assay

EPC	Endothelial Progenitor Cell
FACS	Fluorescence-activated cell sorting
FB	Fibroblasts
FGF	Fibroblast Growth Factor
FISH	Fluorescent in situ hybridization
GP	Glycoprotein
hALPC	Human Adult Liver derived mesenchymal Progenitor Cells
HDL	High-density lipoprotein
HF	Heart Failure
HGF	Hepatocyte growth factor
HSC	Haemopoietic Stem Cells
I/R	Ischemia/Reperfusion
IC	Intracoronary
IFN- γ	Interferon gamma
IGF-1	Insulin Growth Factor
IgG	Immunoglobulin G
IL	Interleukin
IM	Intramyocardial
ISCT	International Society for Cellular Therapy
IV	Intravenous
IZ	Infarct Zone
LAD	Left Anterior Descending Artery
LDL	Low-density lipoprotein

LIF	Leukaemia Inhibitory Factor
LV	Left Ventricle
MAPC	Multipotent Adult Progenitor Cells
MDCT	Multidetector computed tomography
MEF-2C	Myocyte enhancer factor 2C
MI	Myocardial Infarction
miRNA	microRNA
MMP	matrix metalloproteinase
MRI	Magnetic resonance imaging
MSC	Mesenchymal Stem Cells
MVO	Microvascular Obstruction
NADPH	Nicotinamide adenine dinucleotide phosphate
NCS	Neural Stem Cells
NF κ B	Nuclear Factor kappa-light-chain-enhancer of activated B cells
OCT	Optimal Cutting Temperature compound
PAR	Protease-activated receptors
PBS	Phosphate-Buffered Saline
PCA	Procoagulant Activity
PDGF	Platelet Derived Growth Factor
PET/CT	Positron Emission Tomography/Computed Tomography,
PFA	Paraformaldehyde
PI3K	Phosphoinositide 3-kinase
PKC	Protein kinase C

pMSC	Porcine Mesenchymal Stem Cells
PPCI	Primary Percutaneous Coronary Intervention
PTCA	Percutaneous transluminal coronary angioplasty
RV	Right Ventricle
RZ	Remote Zone
SDF-1	Stromal-derived factor-1
SPARC	Secreted Protein Acidic and Rich in Cysteine
SPARCL1	SPARC like-1
SPECT	Single-photon emission computed tomography
STAT-3	Signal transducer and activator of transcription-3
TEF-1	Transcriptional Enhancer Factor 1
TF	Tissue Factor
TGF- β	Transforming growth factor beta
TGS-6	NF- α -stimulated gene 6 protein
TIMP	Tissue inhibitor of metalloproteinase
TNF- α	Tumour necrosis factor- α
TTC	2,3,5-Triphenyl-tetrazolium chloride solution
TUNEL	Terminal deoxynucleotidyl transferase dUTP nick end labelling
VCAM	Vascular cell adhesion protein 1
VEGF	Vascular endothelial growth factor
VF	ventricular fibrillation
α -MEM	Minimum Essential Medium- α

FIGURES AND TABLES

Figure 1.1 The heart wall	4
Figure 1.2 Cardiac Anatomy.	5
Figure 1.3 Progression of Atherosclerosis.	7
Figure 1.4 Ventricular remodelling after myocardial infarction post MI	10
Figure 1.5 Effects of ischemia and reperfusion on infarct size over time.	12
Figure 1.6 MSC Mechanisms of action in Cardiac Repair	21
Figure 1.7 MSC delivery routes	27
Figure 1.8 Extrinsic coagulation cascade	35
Figure 2.1 Ibidi Flow system	54
Figure 3.1 Porcine MSC Isolation	67
Figure 3.2 MSC surface marker expression	68
Figure 3.3 Porcine MSC are capable of tri-lineage differentiation	69
Figure 3.4 Infarct and MSC delivery protocol	71
Figure 3.5 MSC DiI labelling	72
Figure 3.6 Macroscopic images of infarcted porcine heart	73
Figure 3.7 MSC tissue extravasation	77
Figure 3.8 Angiography at MI, during MSC delivery and post MSC delivery	76
Figure 4.1. MSC expression of TF by immunocytochemistry	84
Figure 4.2 MSC expression of surface TF	85
Figure 4.3 MSC express TF	86
Figure 4.4 MSCs express active TF	88
Figure 4.5 MSC are capable of inducing thrombin generation <i>in vitro</i>	89
Figure 4.6 MSC potentiate thrombus build-up on collagen during <i>ex-vivo</i> flow at arterial shear	90
Figure 4.7 TF role in thrombus build up on collagen during <i>ex-vivo</i> flow at arterial shear	92
Figure 5.1 MSC delivery increases myocardial haemorrhage at 24 hours post intracoronary administration in a porcine model of acute MI	99
Figure 5.2. MSC delivery reduces coronary flow reserve 24 hours post intracoronary administration in a porcine model of acute MI.	100
Figure 5.3: MSC promote microvascular thrombus formation <i>in vivo</i> post MI	102
Figure 5.4 MSC are associated with in situ microvascular thrombosis post MI	103
Figure 5.5 Heparin increases MSC infiltration in infarct border zone and decreases apoptosis post MI	105
Figure 5.6 Acutely MSC delivery has no impact on acute infarct size post MI	106
Figure 5.7 Acutely MSC delivery has no impact on cardiac function	107
Figure 6.1 Chronic MI model	116
Figure 6.2 MSC therapy rescues Infarct size at 6 weeks post MI.	117
Figure 6.3 MSC therapy significantly improves LV ejection fraction at 6 weeks post MI	118
Figure 6.4 MSC therapy significantly improves LV function at 6 weeks post MI	119

Figure 6.5 MSC therapy significantly improves wall motion at 6 weeks post MI	120
Figure 6.6 MSC delivery is associated with decreased collagen deposition at 6 weeks post MI	121
Figure 7.1 SPARC and SPARCL1 homology	127
Figure 7.2 MSC <i>in vitro</i> expression of SPARCL1	130
Figure 7.3 CT functional cardiac analysis 6 weeks post SPARCL1 delivery	131
Figure 7.4 MSC cytokine analysis	132
Figure 7.5 MSC cytokine analysis	133
Figure 7.6 MSC cytokine analysis	134
Figure 7.7 MSC cytokine analysis	135
Figure 7. 8 MSC cytokine analysis	136
Table 2.1 Animal numbers	45
Table 2.2 Osteogenic Media	59
Table 2.2 Adipogenic Induction Media	59
Table 2.3 Adipogenic Maintenance Media	59
Table 2.4 Incomplete Chondrogenic Media	60
Table 3.1 Pre-clinical MSC cell studies	65
Table 3.2 MSC Dosing Study	74

Chapter1

Introduction

1.1 Myocardial Infarction

1.1-1 Epidemiology of Myocardial Infarction

Ischemic heart disease is the leading cause of mortality and morbidity in the world, accounting for over 7 million deaths annually [1]. In the western world due to improvements in primary prevention and also in acute coronary care [2] mortality associated with acute events are on the decline however, figures indicate that the number of patients suffering from progressive heart failure (HF) are on the rise [3]. HF is now considered to be a substantial economic burden and in 2007 the US health care expenditure devoted \$30.2 billion to HF alone [4]. In developing countries increased adoption of adverse behavioural and metabolic risk factors linked to ischemic heart disease has led to an overall increase in the number of associated deaths and disabilities [5]. To date, current medical strategies for the treatment of myocardial damage in the setting of myocardial infarction have only achieved modest improvements and in recent times new efforts have pursued cellular therapeutic strategies aimed at preservation, regeneration or repair of cardiac tissue post myocardial infarction (MI).

1.1.1 Cardiac Anatomy

The heart is a predominantly muscular organ which is responsible for homeostasis by providing adequate circulation of oxygenated blood throughout the body. The heart is divided into four chambers, consisting of two atria and two ventricles. The left ventricle (LV) which receives oxygenated blood from the pulmonary circulation via the left atrium is responsible for pumping blood to every organ in the body except the lungs. The right ventricle (RV), which is separated from the LV by the intraventricular septum, receives deoxygenated blood from the

systemic circulation through the right atrium which it then sends to the lungs. The heart wall of each chamber is arranged into three main layers; the pericardium, the myocardium and the endocardium (**Figure 1.1**). The myocardium is the main functioning body of the heart and hosts striated muscle cells known as cardiomyocytes which are embedded within a matrix of connective tissue. Cardiomyocytes are responsible for the involuntary contraction of the heart and like all cells within the body require a constant supply of oxygen and nutrients to order to function. Within the heart, blood is supplied to these cells via the coronary arteries which are found on the surface and embedded within the myocardium. There are two main coronary arteries which originate above the right and left cusp of the aorta, namely the left main and the right main coronary arteries. The right coronary artery branches into the right posterior and acute marginal arteries and these are responsible for supplying blood to the right ventricle, the right atrium and the sinoatrial and atrioventricular nodes. The left main coronary artery supplies the left ventricle and the left atrium and divides into the Left Anterior Descending (LAD) artery which supplies the antero-lateral part of the LV and the circumflex artery which supplies the poster-lateral region of the heart (**Figure 1.2**).

1.1.2 Pathophysiology of Myocardial Infarction

Cardiac ischemic events due to the interruption of blood flow within the coronary arteries preventing blood supply to a region of the heart muscle may lead to myocardial infarction [6]. Cardiac ischemia is predominantly a result of coronary rupture or erosion of atherosclerotic plaque, which is a term used to describe the slow and progressive hardening or narrowing of the coronary arteries.

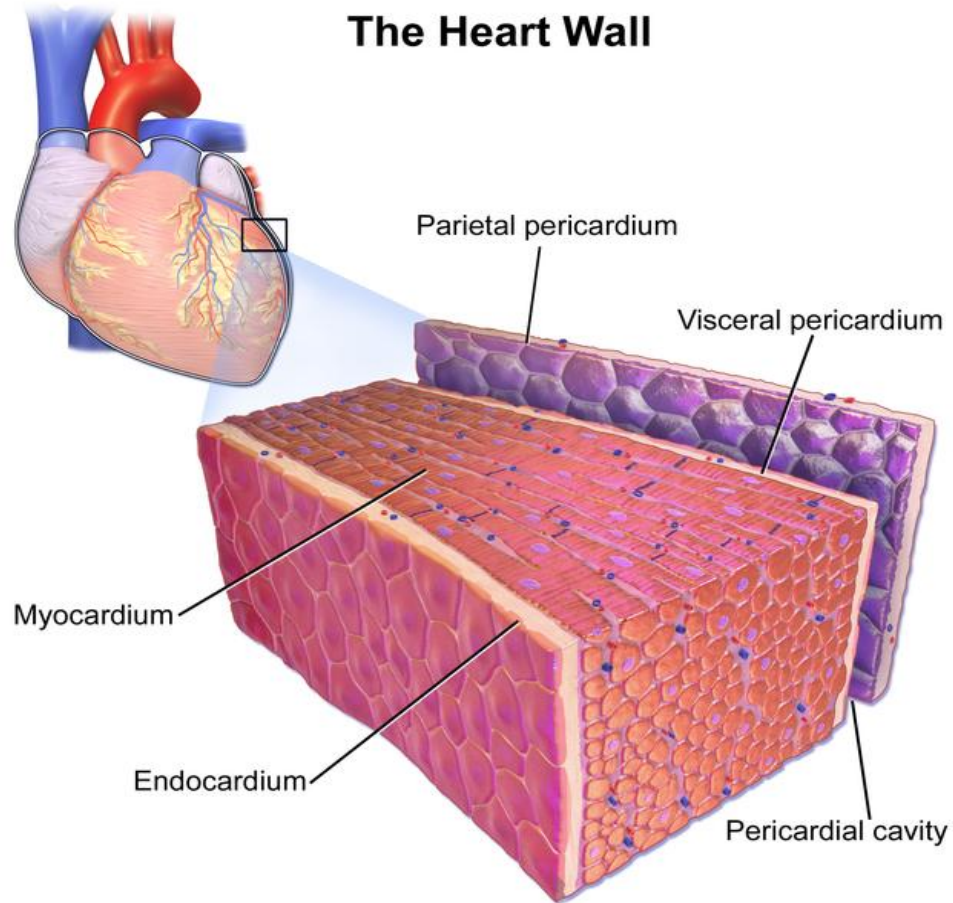
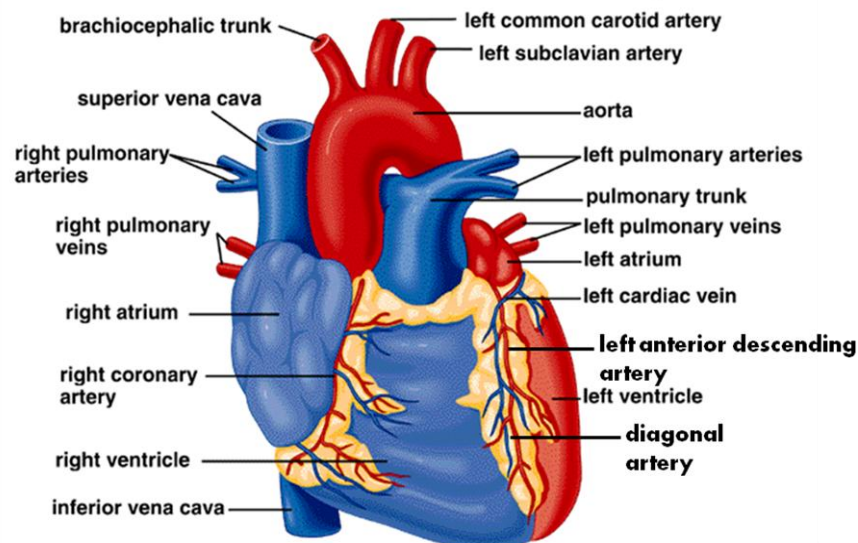


Figure 1.1 The Heart Wall

The heart is made up of three main layers, the outermost layer the Pericardium, the middle layer known as the Myocardium and the inner layer the endocardium.

Obtained from Blausen 0470, Heart Wall.png, Wikimedia Commons, the free media repository

External Heart Anatomy



Internal View of Heart

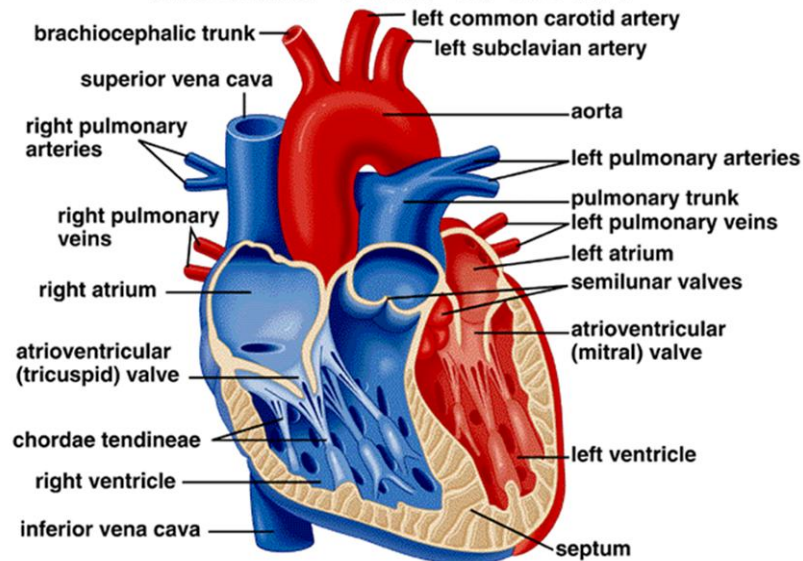


Figure 1.2 Cardiac Anatomy

The heart consists of four chambers, namely two atria and two ventricles. The left ventricle (LV) receives oxygenated blood from the pulmonary circulation via the left atrium and sends this blood to the rest of the body via the aorta. The right ventricle (RV) receives deoxygenated blood from the systemic circulation through the right atrium which it then sends to the lungs via the pulmonary arteries.

Adapted from-Sylvia S. Mader, *Inquiry into life*, 8th Edition,
Copyright©1997

1.1.3 Atherogenesis and Vascular Occlusion

Atherosclerosis is a chronic disease that can remain asymptomatic for decades. Pathological risk factors for atherosclerosis include, LDL cholesterol, smoking, systolic blood pressure, family history of premature MI, diabetes mellitus, and the presence of triglycerides [7]. The onset of atherosclerosis can occur as young as 15 years of age [8] and it is thought to be initiated by disruptions to the endothelial layer of the coronary arteries[9]. Analysis of early plaque formation indicates that this endothelial dysfunction allows for the infiltration and accumulation of LDL cholesterol within the arterial sublayer (**Figure 1.3**) [10, 11]. Infiltration of LDL cholesterol elicits local inflammatory responses which further activates endothelial cells and results in the migration and infiltration of circulating monocytes into the arterial wall [12, 13]. Within the artery wall the monocytes present mature into a macrophage phenotype where they begin to phagocytose the LDL to become what are known as foam cells. As these foam cells mature further they begin to deposit their lipids, resulting in the progressive formation a rich necrotic lipid core beneath the endothelial layer [14, 15]. Subsequently, over many years, a fibrous cap consisting of vascular smooth muscle cells and matrix [16] form over this lipid core. As the lipid core increases in size, the plaque begins to protrude, reducing the size of the artery lumen and thus the flow of blood to the myocardium. As the plaque matures further, it may become more vulnerable to rupture, however, in some cases due to compensatory enlargement of the vessels, plaque progression can occur with no effect [17, 18]. If a plaque rupture or erosion does occur, matrix proteins such as collagen, VWF and laminin present within the exposed endothelium come in contact with the blood, triggering platelet adhesion and activation [19].

Activation of platelets causes the release of modulating factors that recruit additional platelets and mediate the process of platelet aggregation. Activated integrins on the surface of platelets bind fibrinogen, crosslinking platelets and leading to consequences including in situ complete or subtotal occlusion of the artery [19].

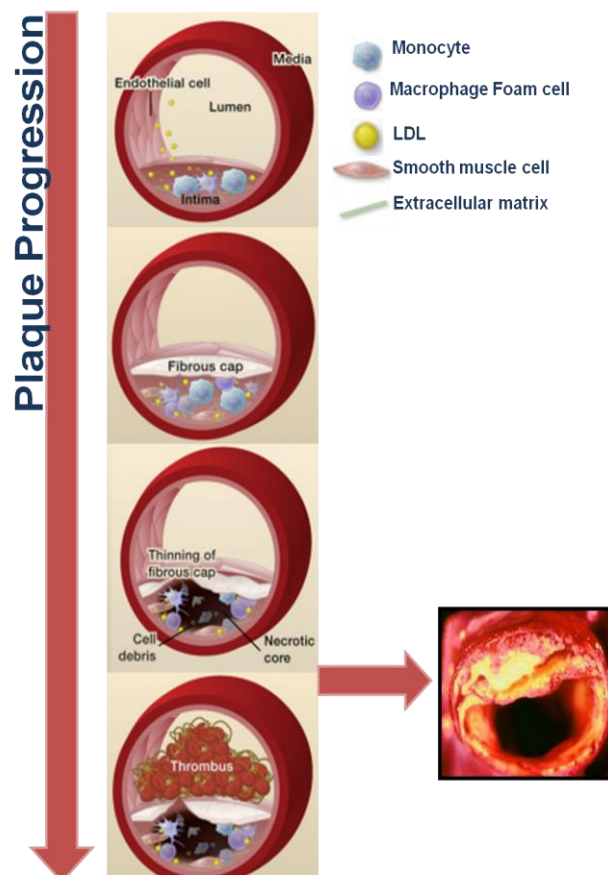


Figure 1.3 Progression of Atherosclerosis

Endothelial dysfunction causes the infiltration of LDL cholesterol into the endothelial sub-layer causing a local inflammatory response. Monocytes adhere and migrate into the vessel wall and develop into lipid laden macrophages known as foam cells. Foam cell, in turn releases chemokines and cytokines that promote the recruitment of smooth muscle cells which along with other matrix protein form a fibrous cap. Over time this fibrous cap may become vulnerable to rupture. If a plaque rupture does occur it exposes circulating platelets and coagulants to the underlying matrix which initiates thrombosis and the triggering of a cascade of events that can lead to partial or complete occlusion of the artery and thus MI.

Adapted from Kathryn J. Moore and Ira Tabas, Macrophages in the pathogenesis of atherosclerosis. Cell, 2011;145(3):341-355.

1.1.4 Myocardial Ischemia and Reperfusion

The physiological result of coronary occlusion is dependent on several factors, including the anatomical location of the occlusion, the degree of occlusion and the duration of time until reperfusion is achieved [20]. Cardiomyocytes, due to lack of oxygen, begin to undergo apoptotic and necrotic cell death within the first 20 minutes of coronary artery occlusion [21]. If the occlusion persists the ability to salvage the myocardium is decreased considerably [22]. An average human infarct can result in the loss up to 1.7 billion cardiomyocytes (30%) [23]. Data shows that endogenous cardiac regeneration, through cardiomyocyte renewal, occurs at a rate of 1% at the age of 25 which declines to a rate of around 0.45% at the age of 75, [24] therefore, the heart is unable to regenerate enough cardiomyocytes to compensate for the those lost during MI. Ischemic events as a result of arterial occlusion trigger a cascade of endogenous reparative processes. These process occur in three over lapping phases, an initial inflammatory phase, a proliferative phase and a healing phase [25].

In the initial phase, myocardial ischemia induces immediate complement activation and free radical generation, triggering a cytokine cascade with induces the migration of inflammatory cells such as neutrophils, monocytes and leukocytes into the necrosing infarcted region [26].

In the initial part of the repair process these cells are involved in the clearance of necrotic cell tissue and matrix debris. Approximately 3-4 four days following the onset of MI inhibition of inflammation is achieved primarily though the release of TGF- β and IL-10 within the myocardium [25]. Pro-inflammatory monocytes which are initially involved in cellular clearance undergo a phenotypic switch at

approximately day 4 and begin to suppress local inflammation and aid in repair [27]. The proliferative phase of repair is characterised by angiogenesis and the formation of granulation tissue consisting of proliferative myofibroblasts. The local cytokine milieu stimulates increased cardiac fibroblast infiltration and proliferation and collagen production which over time assemble to form a fibrotic scar within the infarct zone, replacing in part lost cardiomyocytes [26] (**Figure 1.4**). Infarct area expansion associated with scar formation results in the myocardial wall thinning, distortion of the ventricular shape and some compensatory cardiomyocyte hypertrophy [28]. This adverse remodelling renders the muscle incapable of tolerating the stress involved in performing its normal physiological contractile function. Over time this results in a negative cycle of progressive dilation and further scar expansion. As adverse remodelling continues cardiac function deteriorates further leading to decreased ejection fraction (EF) and changes in diastolic and systolic volumes which can eventually lead to HF. Currently available medical treatments for MI and subsequent HF can only achieve modest results in abrogating this negative remodelling pathology and will be discussed in detail in section 1.1.5 (**Figure 1.4**).

1.1.5 Current treatments for Myocardial Infarction

Over the past 30 years there have been major medical advancements in both the diagnosis and treatment of MI. The first line of treatment for an acute MI event is always restoration of blood flow to the myocardium, through the use of either pharmacological agents and mechanical interventions [29].

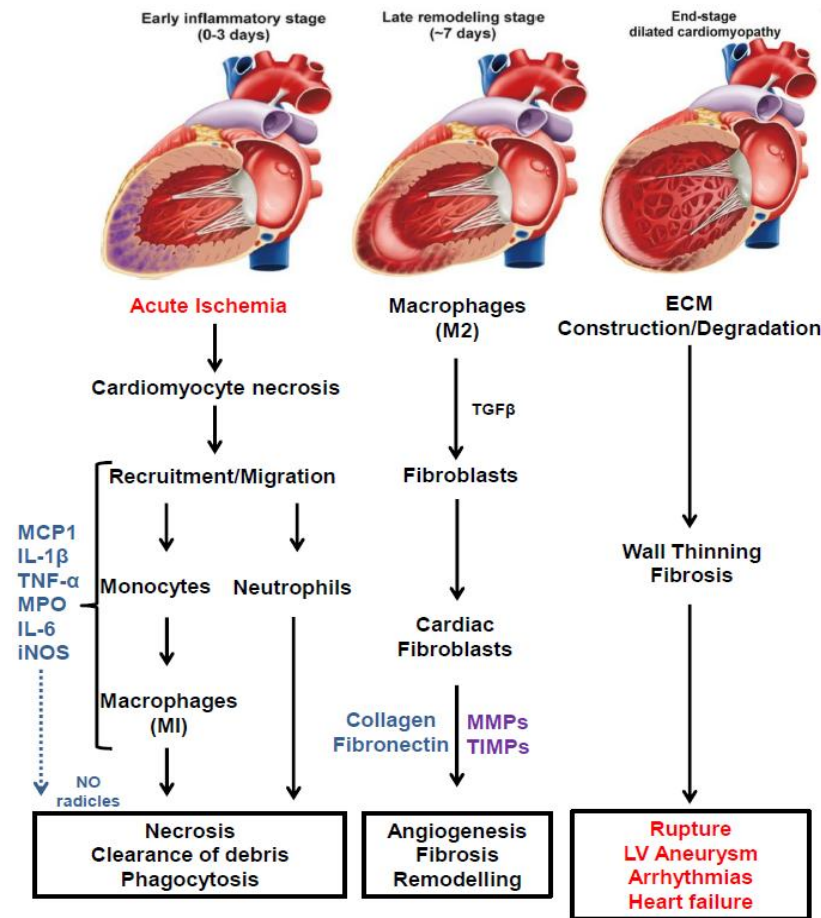


Figure 1.4 Ventricular remodelling after myocardial infarction

Acute ischemia is followed by a number of cellular and molecular events that result in pathological ventricular remodelling. Initially repair and remodelling is characterised by the influx of a pro-inflammatory cells such as neutrophils and monocytes which secrete an array of molecules that aid in initial repair process. Monocytes are then activated to become M2 macrophages known to be anti-inflammatory and play a phagocytic and reparative role within the myocardium post MI. Cardiac fibroblasts also infiltrate and proliferate within the myocardium, in order to replace the lost myocytes these CFs form an immature scar to try and maintain cardiac function. However as these cell do not have the contractile ability of myocytes the region of myocardium loses its ability to contract which results if the alteration of the global myocardium and subsequently leads to functional deterioration of the heart and in many cases results in HF.

Adapted from Yan X et al. J Am Heart Assoc 2012;1(5)

Thrombolytics such as tissue plasminogen activator and streptokinase achieve reperfusion by lysing occlusive thrombi thus restoring coronary blood flow [30]. Mechanical restoration of flow is achieved through primary percutaneous coronary interventions (PPCI), in which the artery at the site of thrombosis or occlusion is wired and then dilated by means of balloon inflation or through the placing of a stent. Both methods have proven successful in decreasing mortality however adverse events such as haemorrhagic stroke, and significant time related acute failure and reocclusion rates associated with the administration of thrombolytics have resulted in PPCI being the preferred method of clinical MI reperfusion [31].

The benefits of reperfusion therapy are reduced dramatically if patency is not achieved rapidly and in recent times there have been great efforts to shorten the time between onset of symptoms and the time to PPCI known as symptom onset-to-Balloon times [32] (**Figure 1.5**). Despite PPCI being effective at preserving LV function and reducing the incidence of progressive HF, the process of reperfusion can itself cause additional injury to the myocardium [33] (**Figure 1.5**). Reperfusion can independently accelerate inflammatory responses, induce ventricular arrhythmias and myocardial stunning, increase microvascular obstruction and cause additional cell necrosis within the infarct border zone [33]. In addition reactive oxygen species (ROS) which are generated in the ischemic myocardium especially after reperfusion are also capable of directly or indirectly causing additional cell death. The main sources of ROS in the post ischemic environment include mitochondria, xanthine oxidase and phagocyte nicotinamide adenine dinucleotide phosphate (NADPH) oxidase[34]. As ROS are generated they can stimulate the production of inflammatory cytokines and which are then in

turn capable of stimulating further ROS formation[35]. Cytokines such as TNF α , IL-1 β and IL-6 stimulate apoptosis through a TNF- α receptor/caspase pathway, however ROS generation causes necrosis by causing a CA²⁺ overload, enhancing mitochondrial membrane permeability and inducing cell death[34]. At present, there is no successful cardioprotective therapeutic strategy available for preventing this additional injury associated with reperfusion [36]. Other pharmacological agents' routinely used in treating events post MI, include beta-adrenergic blockers and angiotensin converting enzyme (ACE) inhibitors.

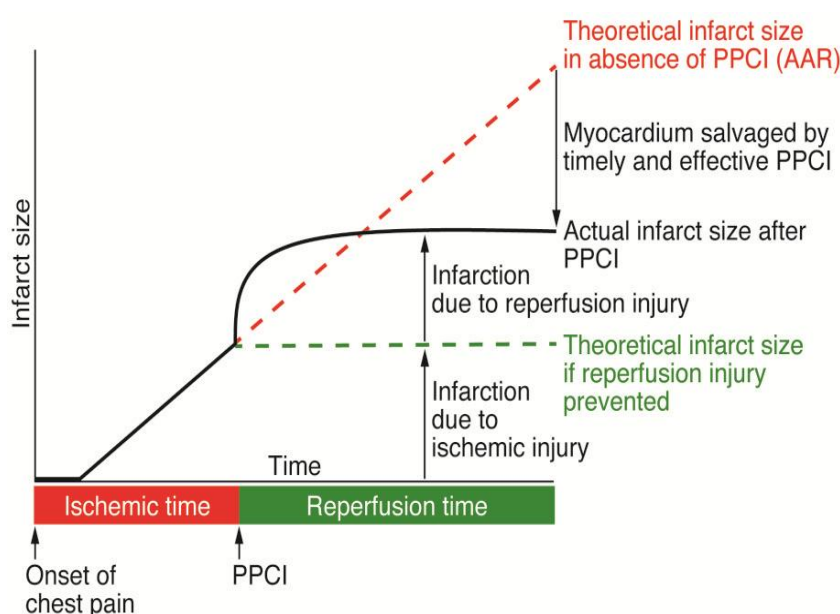


Figure 1.5 Effects of ischemia and reperfusion on infarct size over time

Contributions of acute myocardial ischemic injury and myocardial reperfusion injury to final MI size (expressed in arbitrary units) in STEMI patients up to 24 hours following PPCI. The black solid line depicts the individual contributions to final MI size of acute myocardial ischemic injury and of myocardial reperfusion injury. The green dashed line depicts the theoretical MI size following PPCI based on acute myocardial ischemia alone in the absence of myocardial reperfusion injury. The red dashed line depicts the theoretical MI size based on acute myocardial ischemia alone in the absence of PPCI. The presence of myocardial reperfusion injury attenuates the benefit of PPCI in terms of the reduction of MI size. Therefore, the administration of a therapeutic strategy as an adjunct to PPCI that is capable of reducing myocardial reperfusion injury would result in a smaller MI size (as depicted by the green dashed line) and take advantage of full benefits of myocardial reperfusion.

Obtained from Derek J. Hausenloy, Derek M. Yellon, Myocardial ischemia-reperfusion injury: a neglected therapeutic target, J Clin Invest, 2013;123(1):92-100.

Beta-adrenergic blockers act by decreasing cardiac afterload associated with excessive catecholamine levels and decrease injury by limiting cardiac hypertrophy post MI [37]. ACE inhibitors act as an angiotensin II antagonist and decrease hypertension, cardiac hypertrophy and cardiac fibrosis associated with the renin-angiotensin-aldosterone system [38]. Although these therapies are capable of successfully modulating post MI hemodynamics they do not facilitate extensive regeneration which is required in order to prevent HF associated with large MIs that present late for reperfusion. The annual mortality of patients with MI and resultant left ventricular systolic dysfunction currently stands at 13% and rehospitalisation for HF in this cohort is approximately 6-8% annually [39].

1.2 Emerging treatments for MI

In the last decade scientific research has strived to find new therapeutic strategies to successfully repair the damage caused post MI. This research has focused mainly on attempting to harness the potential of stem and progenitor cells in the area of cardiac regeneration and repair. It was first identified in 1997 by Asahara *et al* that cell therapy may be a viable option for the treatment of ischemic disease [40]. Ashara illustrated the ability of CD34+ cells to induce therapeutic neovascularisation, achieved through CD34+ endothelial cell differentiation [40]. Since then different cell types have been evaluated for use in myocardial regeneration and repair post MI.

Skeletal myoblasts were one of the first cells tested for their ability to induce cardiac repair. Pre-clinically, skeletal myoblast obtained via a skeletal muscle biopsies were shown to be capable of differentiating into myotubes within the infarct region, resulting in improved cardiac functions[41]. Promising pre-clinical

results prompted the undertaking of a phase I clinical trial known as the MAGIC trial [41]. However, results from this trial did not live up to pre-clinical experimental data, as myoblasts failed to improve global or LV function and patients receiving these cells experienced increased incidences of ventricular arrhythmias. Based on the findings of this trial the use of skeletal myoblasts for cardiac repair was abandoned.

1.2.1 Bone Marrow Progenitors

Both pre-clinically and clinically, the predominant source of cells used for cardiac repair and regeneration has been the bone marrow (BM) [42]. To date, cell isolates have been delivered as unfractionated whole BM, as selected subpopulations or as culture-derived out growth cells [43]. Unfractionated BM cells are used largely due to the fact that they are unselected, allowing for delivery of a cocktail of putative stem cells, their relative ease of harvest and the lack of required *ex vivo* expansion[42]. The first clinical trial using unfractionated BM cells or BM-MNCs for the treatment of MI began in 2001[44]. Initial safety results from this trial were positive and BM-MNC transplantation did result in improved cardiac function. However, further BM-MNC trials have come to varied conclusions. Trials such as the REPAIR-AMI [45] and the BOOST trial did demonstrate significant improvement in ejection fraction (EF) at 6 months after cell therapy [46], however the BOOST trial reported that this difference in EF was no longer significant between the control and cell group at 18 months post therapy [47] and recent evidence from the 5 year follow up has revealed a similar trend [48]. Subsequently, two other BM trials did not report any significant changes in LV function at 4-6 months after BM-MNC treatment [49, 50]. A large

multi-centre trial, the BAMI (NCT01569178) trial is now underway to determine if BM cells can reduce all cause mortality associated with MI.

1.2.2 Cardiac Stem cells

Since their discovery, cardiac stem cells (CSC) have proven to be a promising candidate for cardiac regeneration post MI. CSC are isolated from cardiac tissue removed during heart surgery, expanded in culture and delivered back into the infarcted heart. CSCs are described as multipotent clonogenic cells that are capable of both cardiomyocyte and vascular cell differentiation [51]. Although, no definitive markers for CSC isolation and characterisation have yet been identified the expression of C-kit and Sca-1 have been used extensively [52]. The efficacy of CSC in cardiac repair has been evaluated in two major clinical trials; the first-in-human, phase I SCIPIO trial demonstrated that C-kit⁺ CSC, isolated from the right atrial appendage during surgery and expanded in culture were capable of improving global cardiac performance [53]. CSC delivered via intracoronary injection increased LVEF by ~12% and significantly reduced infarct size one year after cell delivery [54]. In another phase I clinical trial, the CADUCEUS trial, patients received intracoronary injection of autologous cells grown from endomyocardial biopsies 1.5-3 months after MI. The 6 month follow up analysed by MRI revealed that although there was no significant difference with regard global cardiac function there was a significant reduction in infarct scar mass and an increase in viable cardiac tissue [55]. Although CSC have been demonstrated to improve cardiac function, the invasive protocol required for CSC harvesting and the labour intensive cell expansion required has mitigated against their routine use and may be a hindrance when translating these progenitors to clinical practice.

Another potential candidate for cardiac regeneration over the last number of years has been the use of culture derived Mesenchymal Stem Cells (MSC). MSC are the main focus of research of this thesis and their therapeutic potential thus will be discussed in detail.

1.3 Mesenchymal stem cells

1.3.1 Introduction

Mesenchymal stem cells (MSC) were first described by Friedenstein and Petrakova in 1970 as multipotent stem cells capable of differentiating into a variety of different mesenchymal lineages both *in vitro* and after transfer *in vivo* [56]. Friedenstein identified a heterogeneous, adherent, non-hematopoietic cell population capable of forming fibroblast colony-forming units (CFU-Fs) and referred to them initially as Mesenchymal stromal cells [56, 57]. The term “Mesenchymal Stem Cells” was first used by Caplan in 1991, so called because of their ability of differentiate into not fibroblast-like cells but osteoblasts, chondrocytes and adipocytes. [58, 59].

MSC were initially thought to exist solely in the bone marrow but have since been cultured from many other tissues, including adipose, cord and liver blood, and lung tissue [60]. MSC are considered as rare, slow cycling cells and are thought to represent approximately 0.01–0.001% of total cells in human bone marrow[58]. Since their discovery, MSC have been isolated from a number of non-human species, including mice, rats, rabbits, dogs, pigs and primates [61-66]. Isolated MSC have the ability to expand readily as plastic adherent cells in culture yet retain their growth and multi-lineage potential. However, cultured human MSC display signs of senescence after a limited number of cell doublings, ranging from

15-50 depending on the study [67, 68]. This phenomenon has raised questions surrounding the actual 'stemness' of MSC and clonal studies of MSC populations have highlighted the extent of heterogeneity between cultured MSC. Cultured MSC display varying morphologies and express varying degrees of surface markers that in fact vary between passages. [69]

In an attempt to exclusively define MSC, the International Society of Cellular Therapy (ISCT) recommended minimal criteria for characterising MSC. *In vitro* cultured MSC are required to be plastic adherent, be capable of differentiating into adipocytes, osteocytes and chondrocytes and be positive for the surface markers CD73, CD90 and CD105 and the negative hematopoietic and co-stimulatory markers CD11b, CD14, CD 19 CD34, CD45, CD79a, HLA-DR and Stro-1 [70]. The ISCT recommended the use of the nomenclature multipotent Mesenchymal Stromal Cells when referring to MSC and this is due to their restricted tri-lineage 'stemness'. Although the ability of MSC to differentiate into bone and cartilage *in vivo* has been evident since the early 1980s, their ability to differentiate into other lineages has been somewhat more controversial. Studies have shown their ability to differentiate into non-mesodermal lineages such as neural cells, cardiomyocytes and endothelial cells but the lack of universal standards with regard to markers of differentiation and inability to reproduce these findings in multiple studies have cast doubt on MSC's actual ability to differentiate into other lineages. [71-75] One of the most important properties of transplanted MSC is their ability to home to sites of injury and aid in the repair of these sites both by transdifferentiating, by suppressing local inflammation and also by secreting trophic factors that simulate local and systemic repair [76-78]. MSC have a number of advantages including low immunogenicity, ease of isolation and expansion, reproducible

characteristics, high reparative potential and few ethical concerns such as those surrounding embryonic stem cells. Cumulatively, these properties make MSC an interesting candidate cell type for tissue engineering and regenerative medicine.

1.3.2 Mesenchymal stem cells engraftment and transdifferentiation post myocardial Infarction (Figure 1.6)

When MSC were initially suggested as a therapy post MI it was hypothesised that the benefits of MSC occurred through their ability to replace cells that are lost as a result of MI. BM cells were first posited to be capable of differentiating along cardiac lineages by Orlic *et al* in 2001,[79] who suggested that the transplanted cells responded to signals within the myocardium causing them to differentiate into myocytes, endothelial cells and smooth muscle cells which in turn resulted in the regeneration of a new and functional myocardium [79]. This, along with *in vitro* studies which also showed the capacity of MSC to differentiate along cardiac lineages [71] prompted investigators to test the efficacy of MSC on tissue regeneration within the heart. The first cardiac related MSC study demonstrated that when human MSC were injected into a mouse heart they were capable of engrafting into the myocardium where they appeared to differentiate into cardiomyocytes [73]. Following on from this initial study numerous *in vivo* animal studies have also revealed the ability of MSC to engraft and transdifferentiate [73, 80-82]. MSC were tested first in a porcine models in 2002, in which 6 billion MSC were directly injected into the infarcted region two weeks post MI. MSC showed robust engraftment and muscle specific differentiation which resulted in significant functional and structural improvements within the MSC treated groups [80]. In a porcine model of myocardial infarction, Quevedo *et al* hypothesised the observed repair effect of MSC was solely due to their

engraftment and tri-lineage differentiation potential [82]. Twelve weeks post MI, 200 million MSC were delivered via endocardial injection and followed out for a period of 3 months at which time MSC engraftment was still observable within infarct regions [82]. Additionally 14% of the tracked cells showed co-expression with the cardiac associated factors such as GATA-4, Nkx2.5, sarcomeric actinin and tropomyosin. MRI data indicated increased contractile function and decreased infarct size in the MSC treated animals when compared to saline treated controls [82]. Due to modest observable MSC engraftment and cardiac lineage differentiation *in vivo* subsequent studies were aimed at trying to improve the engraftment and differentiation potential of MSC [83]. Stimulation of MSC *ex vivo* with various cytokines and growth factors, such as 5-azacytidine which is capable of demethylation of genes implicated in cardiac differentiation [71, 84], induced MSC expression of the cardiac specific markers Nkx2.5/Csx, GATA4, TEF-1, and MEF-2C mRNA [71]. This group also claimed that after three weeks in culture stimulated MSC were capable of forming myotube structures and beating spontaneously. Ultimately delivery of these cells *in vivo* resulted in engrafted MSC displaying the expression of myosin heavy chain, myosin light chain and α -actin [71]. However, MSCs capability for cardiomyocyte differentiation remains controversial within the field and a number of groups have been unable to reproduce similar results regarding *in vitro* and *in vivo* MSC differentiation. [85, 86].

In addition to cardiomyocyte differentiation MSC have also displayed capacity for endothelial differentiation and new vessel formation. *In vitro* when exposed to stimulation such as VEGF [74], MSC are capable of acquiring an endothelial phenotype, capable of forming *de novo* tubular structures and of secreting pro-

angiogenic cytokines [87-89]. *In vivo* evidence supporting neovascularisation was illustrated by Barbash *et al* who showed that the observed therapeutic benefit of MSC was achieved through both smooth muscle and endothelial cell differentiation [81]. There continues to be interstudy variability and lack of consensus with regard to the engraftment and differentiation potential of MSC, however, evidence supporting the paracrine effects of MSC therapy is more robust.

1.3.3 Mesenchymal stem cell secreted factors and their effect post Myocardial Infarction (Figure 1.6)

The paracrine hypothesis surrounding MSC ability for regeneration and repair was first reported as far back as 1996 [90]. Since then, MSC have been shown to secrete a wide array of reparative growth factors, cytokines, chemokines, extracellular matrix proteases and hormones. Due to their extensive secretory profile, Caplan, who first coined the term ‘MSC’, has now suggested changing the acronym MSC to mean ‘Medical Signalling Cell’ [91]. Factors released from MSC have pro-angiogenic, immunomodulating, anti-scarring and anti-apoptotic properties [92]. The secretory profile of MSC varies considerably depending on the local microenvironment and *ex vivo* modification of MSC using methods such as hypoxia or mechanical stress has been used to enhance the therapeutic benefit of MSC in relation to cardiac repair [93]. *In vitro* studies have shown that MSC secretory profile includes Vascular endothelial growth factor (VEGF), Hepatocyte Growth Factor (HGF), Insulin Growth Factor (IGF-1), Transforming Growth Factor- β (TGF- β), Leukaemia Inhibitory Factor (LIF), Stromal cell-derived Factor-1 (SDF-1) [92].

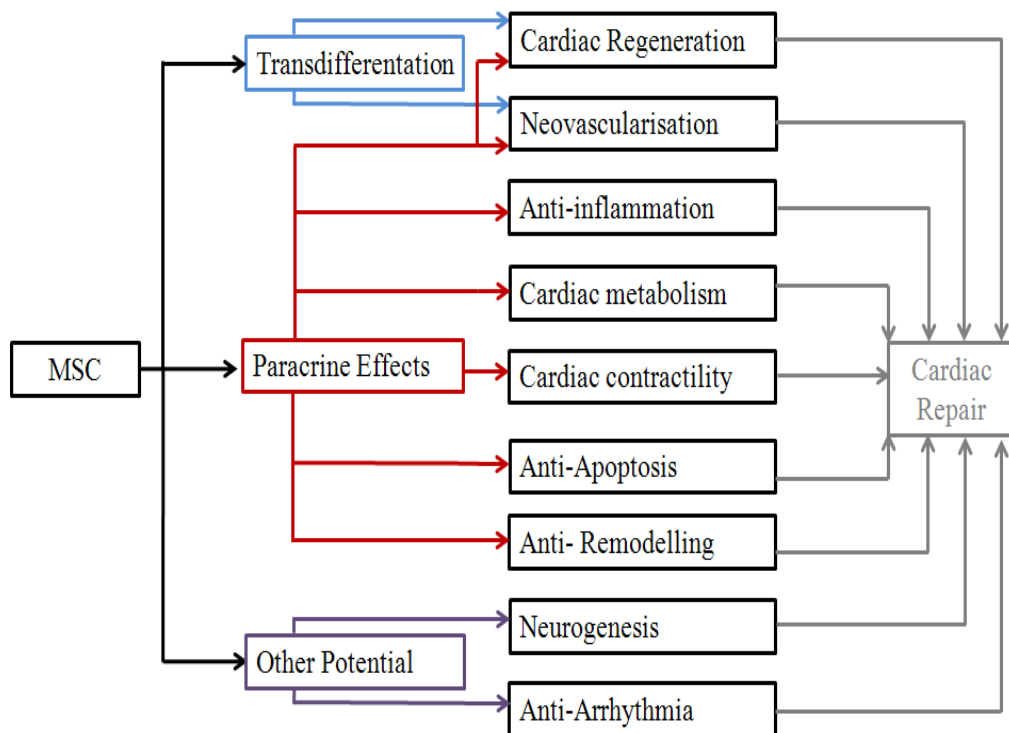


Figure 1.6 MSC Mechanisms of Action in Cardiac Repair

MSC mechanisms of repair were considered originally to occur through transdifferentiation and vascular regeneration. More recently however, it has been demonstrated that paracrine factors released from MSC strongly influence the cardiac repair benefits observed after their delivery post MI.

Adapted from Wen *et al*, Repair mechanisms of bone marrow mesenchymal stem cells in myocardial infarction, J. Cell. Mol. Med, 2013; 15(5):1032-1043.

1.3.4 MSC and Apoptosis

Cardiomyocyte apoptosis is a form of cell death that occurs as a result of ischemic events within the infarcted myocardium. The ability to salvage cardiomyocytes from apoptotic cell death represents one strategy in preventing the progression of MI related adverse remodelling and subsequent HF [94]. Therefore the capacity to prevent apoptosis is an important property of MSC that may be exploited with regards cardiac repair.

The anti-apoptotic benefits of MSC were first established in a rat model of acute kidney injury, these initial studies observed that infused MSC attached to the renal microvascular circulation and induced a renoprotective effect through prevention

of apoptosis [95]. In an attempt to elucidate the factors responsible for the observed renoprotective effect subsequent MSC-conditioned media experiments focused on the presence of cytokines VEGF, HGF and IGF [95].

Within the cardiac field, Gnecchi *et al* provided novel evidence for the cytoprotective capabilities of the MSC secretome. Initial studies showed that transducing MSC with Akt, a pro-survival gene and delivering them post MI inhibited adverse ventricular remodelling and restored cardiac function. Gnecchi, however suggested that the magnitude of early improvements could not be attributed solely to delivery and engraftment of donor cells and therefore hypothesised that additional mechanisms such as paracrine actions must be at play. In concurrence, conditioned media from Akt transduced MSC when injected into LV in a rat MI model significantly reduced infarct size and improved LV function. It was suggested that these improvements were mediated through the up-regulation of genes such as VEGF, IGF, FGF-2, HGF [96]. Similar results were observed in large animal studies with intracoronary injection of concentrated MSC media reducing cardiac troponin-T levels, improving cardiac functional parameters and decreasing fibrosis [97]. Mechanistically MSC may prevent apoptosis through the activation of multiple pro-survival pathways including, PKC, PI3K/Akt, NF- κ B and STAT3 signalling [98, 99].

1.3.5 MSC and cardiac inflammation post MI

Inflammation after MI is a prerequisite for the initiation of reparative processes, yet activated immune cells can cause additional damage to the infarcted myocardium. Although the negative effects of excess inflammation have been known for decades, no clinical treatment exists that is capable of positively

influencing these responses. Post MI inflammation is considered to be an active process that is influenced by factors secreted from cells and matrix within the myocardium[100]. Through the release of paracrine mediators MSC have exhibited the capacity to modulate cells of the innate and adaptive immune system [92]. MSC may exert their therapeutic benefit post MI, in part, by shifting the local microenvironment from a pro-inflammatory to an anti-inflammatory environment [101-103].

The ability to modulate inflammation has been demonstrated in a rat model of MI, in which MSC inhibit NF- κ B activity, mitigate TNF- α and IL-6 release and subsequently to increase the expression of IL-10 within the heart, preventing both ventricular dilation and cardiac dysfunction [102]. The capacity of MSC delivery to improve cardiac function in a murine model of myocarditis, an inflammatory heart disease, provides further evidence of immunomodulative properties of MSC [104]. IFN- γ primed MSC delivered into the myocardium was associated with decreased TNF- α mRNA expression and decreased cardiac mononuclear cell activation which resulted in improved heart contractility [103]. The observed paracrine anti-inflammatory effect of MSC can also occur systemically. Lee *et al* demonstrated in a murine model of permanent LAD ligation, that TGS-6 secreted remotely from MSC, embolized within the lungs after IV delivery, was capable of decreasing the inflammatory response, decreasing infarct size and improving overall cardiac function.

However, delivering a cultured cell to an unstable *in vivo* environment can also enhance inflammation which may not always be beneficial for cardiac repair. For example, MMP-2, MMP-9 and IL-6 which are known to be secreted by MSC may

hamper the positive effects of MSC delivery by causing additional adverse myocardial damage as opposed to being beneficial [105, 106].

Since their discovery one of the major benefits of MSC therapy has been their ability for potent immunomodulation. However because we still do not fully understand how the local environment influences what MSC secrete and the mechanisms involved, the full potential of MSC as an immunotherapy cannot be fully exploited.

1.3.6 MSC and cardiac remodelling

With an increasing number of patients suffering from HF and with no cardiac regenerative options currently available in current clinical practice, research has focused its attention on improving post MI remodelling. Factors released from MSC may alter the extracellular matrix resulting in improved post infarction remodelling and increased infarct scar strength. MSC secrete an array of cytokines that have anti-fibrotic properties and studies have identified the main factors involved to be hepatocyte growth factor (HGF), IL-10 and adrenomedullin [107-109].

Matrix metalloproteinases (MMPs) are a family of enzymes that are responsible for the degradation of extracellular matrix post MI. Increased amounts of MMPs have been linked to diseased hearts and their expression is tightly regulated by inhibitors known as tissue inhibitors of metalloproteinase (TIMPs). MSC secretory profile includes high levels of TIMPs and altered *in vivo* dynamics of MMPs and TIMPs may be a mechanism for this cells benefit. Delivery of mesenchymal precursor cells in a large model of MI resulted in modified LV remodelling and was associated with decreased collagen and modified TIMP and

MMP expression [110]. Authors suggested, that although the mechanism of action remains speculative, the study does demonstrate that alteration in MMPs associated with MSC delivery can positively influence chamber remodelling [110]. MSCs interaction with ECM components is not the only method of action of MSC with regard to remodelling. MSC have also been shown to suppress the proliferation of and modulate the phenotype of cardiac fibroblasts (CFs) through which adverse remodelling is prevented [111]. CFs play a crucial role in the maintenance of ECM post MI [112]. Experimentally, MSC conditioned media has been shown to decrease the proliferative capacity of CFs which positively alters regional cardiac fibrosis through decreasing both the expression and synthesis of collagen type I and type III [112-114]

MSC have thus been implicated nearly every facet of cardiac repair post MI such as cell differentiation, neovascularisation, apoptosis and cardiac remodelling. However, optimised cell numbers, routes of delivery and source of MSC remain unresolved topics with respect to clinical application.

1.3.7 Allogeneic vs. Autologous MSC

For MSC to be a clinically viable therapy in an acute MI setting they need to be available as an 'off the shelf' product and therefore need to be allogeneic. Autologous cell harvest and required expansion renders MSC delivery for acute MI impractical. Allogeneic cells have a number of important advantages over autologous cells, including; cells can be acquired in large quantities, they are available on demand, they can be obtained from one healthy donor and cell quality and efficiency is not dependent on patient characteristics such as age and health status. As MSC are considered to be immunoprivileged, potentially they

can be used as allogeneic cells. However whether they remain immunoprivileged when injected into the heart remains controversial [115]. With this in mind recent experimental findings have questioned the long term retention and therapeutic potential of allogeneic MSC *in vivo*. One study suggests that autologous MSC may have more persistence potential than allogeneic MSC and that this may be due to the formation of not only alloreactive antibodies but an alteration in HLA antigen expression [116]. Improved cell retention is also observed in models where immunosuppression is used, suggesting an immune clearance reaction may be associated with allogeneic MSC delivery [117]. Despite these findings, Hare *et al* has carried out phase I/II clinical trial evaluating the effect of allogeneic and autologous MSC for the treatment of ischemic cardiomyopathy [118]. Interestingly, this study demonstrated that both allogeneic and autologous cells were deemed safe and that both cell types demonstrated similar regenerative potential and that evidentially the majority of patients receiving allogeneic cells did not experience a reactive antibody response [118]. However, more extensive and sensitive immune tolerance studies may be required in order to address if allogeneic cells illicit immune responses particularly in relation to repeat cell dosing.

1.4 MSC delivery strategies

1.4.1 Introduction

Since their discovery MSC have been delivered to the heart both clinically and pre-clinically via a number of different routes. However, to date, there still has been no universal agreement as to the optimal route of cell delivery. The route by which cells are delivered may influence the engraftment, retention, and survival of the cells and may therefore have a downstream impact on the therapeutic outcome

of the treatment [119]. To date, MSC have been delivered intravenously (IV), via the coronary artery (IC), and intramyocardially (IM) (**Figure 1.7**). Each route has its own advantages and disadvantages.

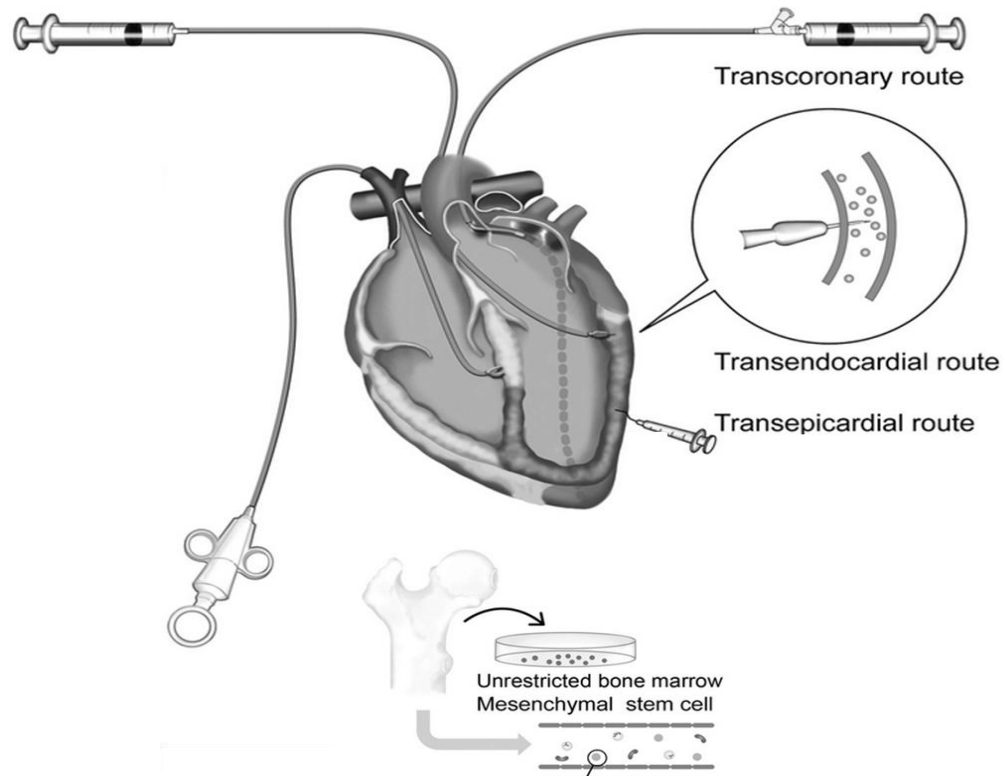


Figure 1.7 MSC delivery routes

To date MSC have been delivered via the coronary artery (IC), via transendocardial and transepiscardial routes (IM) delivery and systemically (IV) (not Illustrated)

Adapted from Naofumi Takehara , Hiroaki Matsubara, Cardiac regeneration therapy: connections to cardiac physiology, *Ajpheart*, 2011;301(6):2169-2180

1.4.2 Intravenous MSC delivery

Although intravenous MSC delivery is the least invasive and least expensive method of cell delivery, it is also the least efficacious. In order for cells to reach the injured myocardium after IV administration they must first pass thorough the systemic circulation, where pulmonary passage may become an issue [78, 120]. Dynamic tracking of MSC using a single-photon emission CT (SPECT)/CT

demonstrated that up to 24 hours after IV administration, the majority of MSC are retained within the lungs [120]. Interestingly however, imaging after 24 hours and up to 8 days after administration revealed that MSC had homed from the lungs to the infarcted region of the myocardium and that this homing ability was only evident in infarcted animals [120]. To determine the therapeutic effect of IV MSC administration Halkos *et al* delivered MSC in increasing doses (1, 3, or 10 million cells/kg) in a porcine model of MI. Endpoint analysis revealed no differences in EF between the groups. There was however a difference in PV loop functional analysis and histological analysis post mortem revealed increased angiogenesis in the MSC treated groups compare to placebo treated group. This study concluded that IV administration is an effective modality for the treatment of myocardial injury despite relatively modest cardiac improvements. A comparative study that set out to identify the optimal route of MSC delivery for cardiac repair demonstrated that 14 days post IV delivery of 50×10^6 MSC, none of the infarcted region of six animals had a detectable number of MSC compared to the other two routes of delivery [119]. Due to low retention and engraftment levels post IV delivery this study recommended that IM and IC delivery are more favourable options than IV delivery [119].

1.4.3 Intramyocardial MSC Delivery

1.4.3.1 Transepicaldial

Cell delivery via transepicaldial IM involves the direct injection of MSC into the epicardium; this route allows for direct visualisation of the infarcted region. However, it requires an open thoracotomy and is usually only performed during coronary artery bypass surgery. The invasive nature of transepicaldial cell

delivery and the risk of myocardial perforation limit the use of this method in patients.

1.4.3.2 Transendocardial

Transendocardial IM delivery involves the direct injection of the MSC in to the endocardium. Transendocardial IM injection can be performed percutaneously using three dimensional electrophysiological mapping which allows for the identification of targeted regions within the myocardial wall. Freyman *et al* [119] has demonstrated that transendocardial IM injection leads to a significant increase in the number of engrafted MSC within the infarct region and that remote organ retention of cells is significantly reduced when compared to IV cell delivery. Transendocardial IM injection of MSC has, in recent years become one of the most widespread methods of MSC administration. In particular, the Hare group have published a number of papers in which MSC are delivered via this route in various porcine infarct models [121-124]. Transendocardial IM administration of MSC 3 days after MI induction was capable of improving cardiac function and decreasing infarct scar by 50% at 8 weeks [121]. A dose escalation study showed similar results in that there was a significant reduction in infarct size at 12 weeks. This observation however was not dose dependent and cell delivery had no sustained effect on EF [125]. In addition to these acute studies further studies aimed at elucidating the effect of transendocardial IM MSC delivery on chronic porcine models of MI. To demonstrate this, cells were delivered to infarct scar region at 3 months post MI and functional analysis at 12 weeks was carried out by MRI. Results showed 30% reduction in scar size, improved contractility and subsequently improved global LV function when compared to placebo treated animals [124].

Despite these positive results there remains a number of safety issues that are associated with IM injections. Experimental evidence has demonstrated that IM injection can lead to increased local inflammation due to mechanical perforation of the myocardium and that inhibiting this inflammation can improve donor cell survival and proliferation. [126] Another established drawback associated with IM delivery is the apparent presence of localised islet like regions of donor cells sequestered within the myocardium post cell administration.[127] Although mainly associated with skeletal myoblast transplantation, these islets are known to induce disturbances to electrical impulses within the myocardium and can therefore be associated with ventricular arrhythmias [128]. Notwithstanding these adverse pre-clinical observations, IM injections have been reported to be safe and feasible in clinical settings. In the phase I/II randomised POSEIDON trial an increasing number of allogeneic or autologous MSC were delivered by transendocardial IM injection to patients with chronic ischemic left ventricular dysfunction. The effects of MSC treatment in this study were modest but the study did confirm that no serious adverse events, including arrhythmias were associated with endocardial delivery [118].

A head to head comparative study of IM and IC infusion of MSC in a porcine MI model suggests no superiority between the routes of delivery [129]. Cell retention was the same between the groups, however, IC delivery did show less variability in efficiency but more remote organ distribution when compared to IM delivery [130].

1.4.4 Intracoronary MSC delivery

IC delivery involves the delivery of cells directly into the coronary circulation. Cells are infused via the lumen of a catheter placed within the target coronary artery. The main benefit of IC delivery is that it can be performed during routine primary PCI and unlike IM delivery that requires specialised electro-physiological mapping most interventional cardiologists are familiar with coronary catheterization techniques. IC MSC delivery has been proven to be therapeutically beneficial post MI in both the preclinical and clinical settings. For instance IC MSC delivery has been shown to decrease infarct size [131, 132], improve cardiac function [132-135], increase cardiac perfusion [133] decrease adverse remodelling [132, 133] and increase angiogenesis post therapy [134, 135]. Despite these beneficial findings however, there has also been a number of safety issues raised regarding MSC delivery via this route.

One of the first publications of IC MSC delivery involved the delivery of 0.5 million MSC/kg via the left circumflex coronary artery into a healthy canine myocardium in the absence of MI. IC delivery was associated with adverse events such as ST segment elevation and T wave changes during cell administration. Post mortem macroscopic and microscopic analysis 7 day after cell administration also revealed the presence of micro-infarctions within the region of cell delivery [136]. Similarly, a study in which sheep received IC delivery of gadolinium labelled MSC, demonstrated, by cardiac magnetic resonance, the presence of cell associated microvascular obstruction and resultant regions of myocardial infarction [137]. Published data comparing IC and IM delivery also allude to adverse cell related events. Although IC delivery did result in comparatively higher cell retention at the 14 day follow up, IC delivery was

associated with a higher incidence of decreased blood flow within the coronary arteries. Histological evaluation of the infarcted region demonstrated capillary plugging due to MSC interactions with neutrophils and red blood cells [119]. Due to these findings, methods for alleviating coronary flow reduction post IC MSC delivery have been proposed. Wilensky *et al* has suggested that delivering cells at high flow rate can prevent reductions in myocardial blood flow and decrease mortality associated with MSC delivery. Wilensky evaluated three cell delivery rates, 5 serial 2 ml infusions, a single 60ml/minute infusion and 20ml/minute infusion. Results revealed that serial infusion of cells significantly reduced coronary blood flow and that this reduction in flow was sustained out to 14 day and was also associated with increased animal mortality. The study however did not show any long term functional benefits of such MSC administration [138].

Many studies have alluded to safety issues surrounding MSC IC delivery but none of these pre-clinical studies have provided a mechanistic reasoning as to why this may be occurring. As reductions in coronary blood flow are associated with microvascular obstruction which is linked with thrombotic events, it is plausible to suggest that MSC augmentation of coagulation in situ may be at play we thus hypothesise that MSC may be causing thrombotic events due to their expression of procoagulant factors such as Tissue Factor

1.5 Tissue Factor

Tissue factor is a 46kDa membrane associated glycoprotein, consisting of a 219-amino-acid extracellular domain, a 23-amino-acid transmembrane domain and an intracellular 21-amino acid C-terminus [139, 140]. Tissue Factor is the principal initiator of the extrinsic coagulation cascade and under normal physiological

conditions contributes to maintaining vascular homeostasis. TF activates coagulation through interaction with factor VIIa, resulting in activation of factors V and X leading ultimately to thrombin generation and fibrin deposition (**Figure 1.8**). TF has been shown to be expressed in both vascular and non-vascular cells[141]. TF is expressed by fibroblasts, smooth muscle cells, and pericytes [141], however TF expression by platelets remains controversial and although resting endothelial cells do not express TF, *ex vivo* stimulation has been shown to induce its expression [141]. It was originally believed that TF was not expressed in the blood however active TF has been recently detected in the circulation [142]. This blood-borne TF has been associated with cell secreted microparticles (MPs) which are small lipoproteins vesicles produced and released from activated or apoptotic eukaryotic cells. MPs have been associated with various cells types including monocytes, endothelial cells, VSMCs and more recently MSC [143, 144].

In addition to coagulation, TF is involved in a number of other biological processes including angiogenesis, cell migration, cell adhesion, wound repair, immunity and embryonic development [145]. TF exerts its biological function through interaction both directly and indirectly with a number of cell receptors. *In vitro* studies have shown that coagulation factor FVIIa, FXa and thrombin are capable of activating protease-activated receptors (PARs) which go on to activate platelets. Expression of TF may have beneficial biological properties, the presence of TF being essential for embryogenesis, since knocking out TF gene results in an embryonic mortality rate of approximately 90% [146]. In wound healing models the presence of excess amounts of TF is associated with angiogenesis through indirect increases in secretion of growth factor such as

VEGF, PDGF, bFGF [147, 148]. TF may also be responsible for cell migration and this property of TF has been implicated in cancer metastasis [149]. Enhanced presence of TF is associated with negative events during atherogenesis, however under normal physiological conditions TF is essential. The role of TF *in vivo* appears to be multifunctional, its role in stem cell delivery has yet to be established. The aim of this thesis was therefore, to establish if TF is associated with MSC and if so what is its impact post MSC cell delivery with respect to immediate intravascular events, MSC homing and late functional effects of MSC post MI therapy.

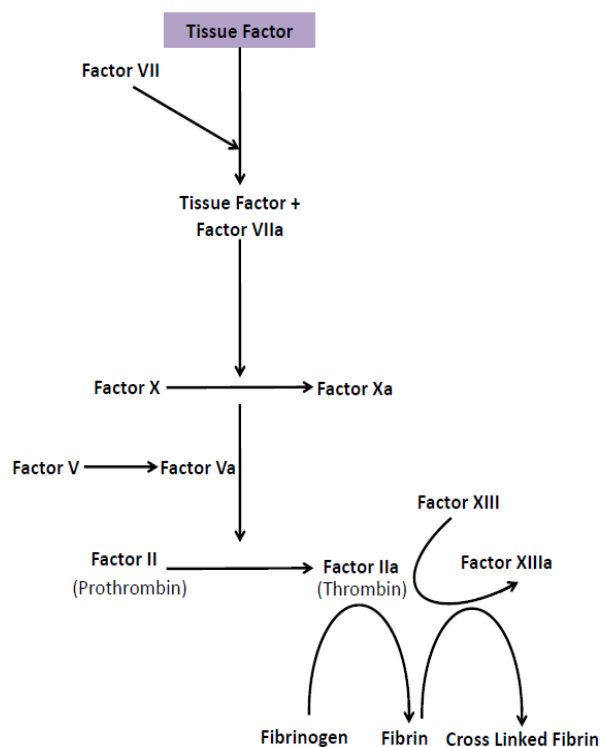


Figure 1.8 Extrinsic coagulation cascade

Model of the extrinsic coagulation cascade. TF initiates coagulation through its initial interaction with FVII which is activated to form a TF-FVIIa complex. This complex then rapidly activates FX to FXa. FV is activated to FVa which is a cofactor in the formation of prothrombin. FXa along with cofactor FVa converts prothrombin to thrombin which in turn converts circulating fibrinogen to fibrin. Fibrin is then stabilised by FXIIIa produced by the conversion of FXII by thrombin.

1.6 Aims

The main objectives of this thesis based are based on the concepts raised throughout the preceding introduction. As it stands, MI and resultant HF are the leading cause of mortality and morbidity in the world. MSC cell therapy, through the various mechanisms discussed is becoming a realistic strategy for improving cardiac function post MI. However, there are still major obstacles facing the efficient application of MSC in a clinical setting. To date, the majority of pre-clinical studies have raised issues surround the safety of MSC therapy. Despite this, clinical trials have gone ahead without understanding the mechanisms behind these observed safety issues. The specific aims of this thesis are as follows.

Specific Aims

1. To establish an expandable and reproducible porcine MSC culture for use in *in vivo* studies
2. Thorough MSC dose ranging studies to determine a dose that can be delivered safely via the coronary artery in a clinically relevant porcine model of AMI
3. To investigate the role of TF in mediating the prothrombotic effect of MSC delivery
4. To determine, *in vivo*, the effect of abrogating TF effects on MSC delivery in a porcine model of AMI
5. To determine the long term benefits of MSC when delivered in the presence of a TF inhibiting agent
6. To determine the *in vivo* cardiac repair effect of the MSC secreted cytokine Sparcl1 and to investigate other possible cardiac repair factors secreted by MSC

Chapter 2

Materials and Methods

2.1 Isolation of Porcine Bone Marrow

Female Landrace Pigs (25-30 kg) were obtained from Teagasc, Moorepark, Fermoy, Co. Cork. Pigs were anaesthetised by intramuscular injection of ketamine (10 mg/kg) (Vetoquinol UK Ltd, Buckingham, UK) and xylazine (2 mg/kg) (Vetoquinol UK Ltd, Buckingham, UK). Ethical approval was obtained for all animal experiments from Cork University animal ethics committee. Bone marrow biopsies were performed as previously described [150]. Firstly, to identify the iliac bone, the animal was placed in either the right or left lateral position and the surgical site is aseptically prepared. The iliac crest is located at the centre of the iliac spine and was identifiable as the projecting structure or ridge at the border of the bone. Once located, the aspiration needle (11 gauge 6") was held horizontally and advanced through the skin until it contacted bone. To engage the bone, the needle was rotated while applying steady pressure and when the bone cavity was entered a change in resistance was observed. Once the needle was in the marrow, the stylet of the aspiration needle was removed and a heparinised luer-lock syringe was attached. Bone marrow (BM) (15-20ml) was collected from the iliac crest in 10ml syringes (BD) and transferred into 9 ml vacuette® containers. Bone marrow was processed according to previous described protocols [151]. Aspirates were maintained at room temperature until further processing was performed under sterile flow conditions in laminar flow hood (ThermoScientific). Approximately 5ml of BM aspirate was added to 45ml of sterile PBS (Fisher Scientific) in a 50ml tube (Sarstedt) and mixed thoroughly before the suspension was centrifuged (Centra®-CL-3 Series) at 900g for 10 minutes. Supernatant was carefully discarded with particular care being taken not to disturb the soft pellet. If multiple tubes were used pellets were combined and washed with approximately

5ml of PBS (Sigma) and total BM suspension was measured. To quantify cell number a diluted BM suspension (1:5) was added to 4% (v/v) acetic acid (Sigma) solution (1:2) and allowed to sit for approximately 1 minute to allow for sufficient lysing of erythrocytes (solution should turn brown). Cell numbers were counted using a haemocytometer. Primary pMSC were plated at a cell density of $41.5\text{--}59.3 \times 10^6$ cells/T175 flask (Sarstedt). Complete pMSC α -MEM (30ml) (PAA #E15832) media consisting of 10%FBS (Gibco-Invitrogen) and 1% penicillin/streptomycin (Sigma) was added to each T175 flask before being placed in an incubator at 37°C, 5% CO₂, 90% (Forma™ Series II 3110) humidity.

At Day 3, 15 ml of complete pMSC media was added to each flask and flasks were incubated again until day 5 when media was removed and flasks were washed with D-PBS (Sigma) in order to remove any unattached cells.

Fresh complete pMSC media (35ml) was added and cells were maintained until confluent monolayer colonies were observed. Cells were then passaged, characterised and expanded until their use in both *in vitro* and *in vivo* experiments.

2.1.1 MSC culturing and preparation

For *in vivo* experiments, cells were expanded in culture using complete pMSC media. pMSC were expanded in round tissue culture flasks (growth area 152cm²) (Sarstedt). In order to have sufficient numbers for *in vivo* experiments 2x the amount of cells required were cultured for the day of *in vivo* studies. Cells were in culture for at least one week after thawing before being used in order to allow cells to recover and to ensure viability.

2.2 Characterisation of MSC differentiation capacity

Tri-lineage differentiation capacity was determined using standard chondrogenic, adipogenic and osteogenic differentiation assays [151, 152]

2.2.1 Characterisation of MSC osteogenic differentiation capacity

Cells were trypsinized using 0.25% trypsin/EDTA (Gibco-Invitrogen) solution and seeded at a density of 2×10^4 cells in 8 wells of a 24 well plate (Sarstedt) with complete pMSC media. Cells were maintained in complete pMSC media for 2-3 days until they reach confluency. Once confluent 1 ml of osteogenic medium (**Table 2.2**) and 1 ml of complete pMSC medium was added to test wells and control wells respectively. Media was changed twice a week and the assay was harvested after 10-17 days depending on the condition of the monolayer. Samples were tested for osteogenic differentiation by staining cells with Alizarin Red (Sigma). In order to stain with Alizarin red the medium was removed and cells washed in PBS and then fixed in 10% (v/v) neutral buffered formalin for 20min at room temperature. Formalin was removed and cells were washed in 2ml of PBS. 1ml of Alizarin Red solution was added to the fixed cells and allowed to stain for 20min. Excess stain was removed and the cells were washed with dH₂O. Finally, 1ml of dH₂O was added to each well and cells were examined under the microscope for red deposits indicating the presence of osteogenesis.

2.2.2 Characterisation of MSC adipogenic differentiation capacity

Cells were trypsinized and seeded at a density of 2×10^4 cells in 8 wells of a 24 well plate with complete pMSC media. Cells were maintained in complete pMSC

media for 2-3 days until they reached confluency. Once confluent 1 ml of adipogenic induction medium (**Table 2.2**) and 1 ml of complete pMSC medium was added to test wells and control well respectively. Test well media was replaced with adipogenic maintenance media (**Table 2.3**) every 3 days for 24 hours to allow cells to recover. This was then repeated until 3 cycles of induction and maintenance were completed. On the final cycle of maintenance, maintenance media was left for a total of 5-7 days. Cells were then stained for adipogenic differentiation by Oil Red O staining. Before cells were first washed in PBS and then fixed in 10% neutral buffered formalin for 20min at room temperature. Formalin was removed and cells were washed in 2ml of PBS. Oil Red O (1ml) was added to the fixed cells and allowed to stain for 20min. Excess stain was removed and the cells were washed with PBS. 60%(v/v) isopropanol (2ml)(Sigma) solution was added to each well and rinsed with tap water, this was then followed by the addition of 1ml of 1:5 Haematoxylin(Cell Path)in distilled H₂O solution for 1 minute. Haematoxylin was washed with warm tap water until water was clear. Finally, 1ml of PBS was added to each well and cells were examined under the light microscope for red fat globules indicating the presence of adipogenesis.

2.2.3 Characterisation of MSC chondrogenic differentiation capacity

pMSC monolayers were trypsinized and counted. Cells ($2-2.5 \times 10^5$) were placed into a 15ml tube (Sarstedt) and pelleted by centrifugation at 500g for 5 minutes. Supernatant was removed and pellet was resuspended in either incomplete chondrogegenic medium (**Table 2.4**) for control tubes or in complete chondrogenic medium (**Table 2.4**) for test tubes. Tubes were centrifuged again at

100g for 5 minutes in a swing out rotor and were then transferred to an incubator and maintained at 37°C, 5% CO₂, 90% humidity. The caps of tubes were loosely closed to allow for adequate gas exchange. Medium was changed every other day for 14-21 days at which time pellets were harvested by aspirating off all medium and washing twice in D-PBS. Pellets were allowed to air dry and fixed in 10% formalin before being embedded in OCT embedding matrix (CellPath) in cryomoulds (TissueTek, Sakura, USA) and placed at -80°C. OCT embedded pellets were then sectioned at 5µm onto superfrost slides (ThermoFisher) using a cryostat (Leica). Toluidine blue staining was then carried out for the detection of glycosaminoglycans in sections of chondrocyte pellets according to the following staining procedure. Sections were initially fixed in 4% PFA for 10 minutes, followed by immersion of slides in the following solutions- 3 x 2 minute in Xylene, and 2x2 minutes in 100%, 95% and 17% ethanol. Slides were then washed in tap water and blotted dry. A 0.5% (w/v) Toluidine blue solution was warmed to 57-60°C and slides were immersed in solution for 5 minutes before being washed with tap water again and immersed in 100% Xylene for 2 minutes. Slides were then mounted with DPX mount and coverslipped before being visualised under light microscopy.

2.3 Staining of MSC with DiI

DiI staining was carried out as per manufactures protocol (**Appendix 9.1**). Accordingly, MSC were trypsinized, counted and centrifuged at 600g for 5 minutes before being resuspended at a density 1×10^6 in 1 ml of serum free media. After cell resuspension 5µl of a 2.5mg/ml DiI in DMSO solution was added per ml of cell solution and mixed well by gentle pipetting. Cells were then incubated for 20 minutes at 37°C. The labelled suspension was centrifuged again at 600g for

5 minutes, supernatant was removed and pellet was resuspended with warm complete pMSC medium to neutralise the DMSO for 10 minutes and to allow cells for cell recovery.

2.4 MSC delivery and Infarct model

2.4.1 MSC preparation

MSC (25×10^6) were trypsinized, counted and centrifuged at 600g for 5 minutes before being resuspended at a density 1×10^6 in 1 ml of serum free α -MEM. Cells were stained with DiI according to methods 1.3. Cells were combined in a single 15 ml falcon tube, counted, centrifuged again at 600g for 5 minutes and washed in PBS twice before being resuspended at a density of 12.5×10^6 cells in 8 ml of Saline in two 10ml luer-lock syringes (BD). 2500IU of heparin (Wochardt®) was added to each cell suspension in experiments where heparin was used. Cells were tested for viability by 7AAD (Sigma) staining (**Appendix 9.2**) before their use *in vivo*.

2.4.2 Myocardial Infarction model

The myocardial infarction protocol was derived from previous porcine MI models performed in our laboratory and others [153, 154]. Pigs were orally administered aspirin 75 mg (Aspar Pharmaceuticals Ltd, Capitol Way, London) daily for two weeks prior to surgery. Anaesthesia was induced by intramuscular injection of ketamine (10 mg/kg) (Vétoquinol UK Ltd, Buckingham, UK) and xylazine (2 mg/kg) (Vétoquinol UK Ltd, Buckingham, UK). IV access is obtained via the posterior auricular vein. Propofol, 40 mg (Fresenius Kabi Ltd, Cheshire, UK) was administered intravenously before intubation. Endotracheal intubation was achieved using a 6.5- to 7.5-mm endotracheal tube. Mechanical ventilation was

maintained using a large animal Harvard Apparatus ventilator and supplemental oxygen (4-6 L/min) combined with isoflurane (1.5%) to maintain general anaesthesia (Abbott Laboratories Ltd, Maidenhead, UK). Heparin (10,000IU) were administered intravenously before starting the procedure. ECG was monitored continuously by way of a 3 lead wire ECG system. In order to gain access to the carotid artery the pig was placed in a dorsal position with its front hooves slightly splayed and secured backwards. A 3-4 cm perpendicular cutdown was then made over the jugular furrow in order to access to the right carotid artery. Once the artery was identified by finger palpation of pulse the artery was isolated and exposed. The artery was then cannulated by the Seldinger technique, briefly, a micropuncture needle is inserted into the artery, upon entry a wire is inserted through the needle and the needle was then removed and replaced by a 6 French sheath. The left anterior descending artery was subsequently catheterised under fluoroscopy guidance using a 6 French JL 4.0 G-stage PTCA guide catheter over a J-type guide wire and a TREK rapid exchange 3.5mm x 8mm/ 2.75x8mm coronary dilation balloon catheter placed in the coronary artery. The balloon was positioned proximal to the second diagonal branch of the LAD and balloon was inflated to 14-15mmHg. Complete LAD occlusion was confirmed by angiography using the contrast agent iodixanol (Visipaque 320, Amersham Health). Arrhythmias were treated by both defibrillation and intravenous administration of 50-100mg of Lidiocaine. The balloon remained inflated for 90 minutes during which time a 64-slice contrast CT (GE Discovery VCT RX scanner) was performed to assess the area of risk. After 90 minutes the balloon was deflated and the LAD was then allowed to reperfuse for 120 minutes before treatment was delivered. Post procedure the sheath was removed and the carotid was tied. The

surgical incision site was then closed and disinfected. The wound was sealed using an aluminium powder based spray (Vétoquinol UK Ltd, Buckingham, UK). All pigs received a subcutaneous post-operative injection of 5mg of Carprofen (Norbrook Laboratories Ltd, Newry, Northern Ireland) for pain relief. At appropriate time points (24 hours for acute MSC study and 6 weeks for chronic MSC and Sparcll study) (**Table 2.1**) animals were sacrificed by IV delivery of 5mg of pentobarbitone (Merial Animal Health Ltd, Essex, UK). Functional parameters analysed by CT included End-Systolic Volume (ESV), End-Diastolic Volume (EDV), Ejection Fraction (EF), Cardiac Output (CO) or Stroke Volume (SV) (See **Appendix 9.8** for additional details).

Animals Used (Table 21)

Acute MSC Study(24 hours)	36 (8 MSC, 15, MSC+H, 12 Saline)
Chronic MSC Study(6 weeks)	12 (6 MSC, 6 Saline)
Chronic Sparcll Study(6 weeks)	8 (4 Sparcll, 4 Saline)

2.4.3 Anaesthesia and intubation

The effect of ketamine and xylazine administration should occur within 5-10 minutes. Once the pig became unresponsive it was transported to the operating table where a mask is applied to deliver 3-4% isoflourane in order to safely administer propofol. After IV administration of propofol immediate intubation and ventilation was required as propofol is a strong respiratory depressant. For adequate intubation the pig was in placed in a prone position and mouth held open. Due to the pig's narrow mouth, its limited jaw movement and profuse salivation visualization of the aditus laryngis can be difficult. To adequately insert the intubation tube the pharynx was illuminated with a laryngoscope, saliva aspirated if required and with the tongue extended the epiglottis was depressed

using the tip of the laryngoscope. The tube was pushed past the closed vocal folds and when the tube was in the right position the pig coughed reflexively and expelled air through the tube.

2.4.4 Treating Arrhythmias and maintenance of arterial pressure

Ventricular arrhythmia and fibrillation (VF) can occur during the induction of MI in porcine models. Most VF episodes occur within the first 30 minutes of induction of the infarction or within the first 10 minutes of reperfusion. All episodes were treated with external electrical defibrillation (Defibrillator, Hewlett-Packard) by using 360 J of shock and repeat applications were applied until arrhythmia ceased. After MI induction and prior to VF a decrease in arterial pressure was usually observed. Decreases in arterial pressure were alleviated by reductions to the dose of isoflourane administered for a period of time until arterial pressure increased.

2.4.5 Animal Housing

Pigs were maintained for 6 weeks post MI. Landrace pig rapidly gain weight and size as they reach maturity, a pig weighing 20-25Kg at the initial procedure would weigh 40-45Kg by week 6. This needs to be kept in mind when housing animals as additional pen numbers may be required. The number of personnel required may also need to be increased due to increased weight burden. During the 6 weeks follow up pigs were observed and their well-being was assessed twice daily by the animal technician. If there were observed behavioural or health changes a veterinarian was contacted

2.4.6 Coronary Flow Reserve

Coronary Flow (Velocity) Reserve (CFR) measurements by thermodilution were carried out post reperfusion and post MSC delivery using commercially available pressure guide wires (PressureWire-3, Radi Medical Systems). CFR is defined as the ratio of hyperemic to baseline blood flow and it is an accurate evaluator of resistance within microvasculature as a result of microvascular obstruction [155]. Maximal hyperaemia is required to correctly assess CFR, as suboptimal microcirculatory vasodilatation result in underestimation of the severity of microvascular obstruction [156, 157]. CFR by thermodilution uses the micromanometer tip of the pressure wire as a thermistor to generate a thermodilution curve and to measure the velocity of the intracoronary delivered saline bolus [158, 159] (See **Appendix 9.3** for theory of CFR). In order to carry out measurements the pressure wire was placed at the site of balloon occlusion within the coronary artery. A 3-ml bolus of saline was then delivered in triplicate followed by the induction of maximal hyperemia by the rapid injection of 5ml of 0.3mg/ml adenosine solution. Measurements were then repeated again in triplicate (3ml Saline) during maximal hyperaemia [160, 161]. The pressure wire used was connected to a dedicated interface (RADI Analyzer, Radi Medical Systems) with integrated software for the analysis of the thermodilution curves and the automatic calculation of CFR. Administered adenosine is known to cause microvascular coronary dilation through the activation of an adenosine receptor on the cell membrane of coronary myocytes [162]. These receptors are coupled to Gi-proteins and activation of this pathway opens potassium channels, which hyperpolarizes the cell leading to relaxation [163]. Adenosine was chosen for these studies as it is regarded the clinical gold standard for the induction of

maximal hyperemia due to its rapid onset, short duration of action, high safety profile, and simplicity of use [155].

2.4.7 Intracoronary MSC delivery

The protocol used was adapted from previous protocols verified in the CRVB [164]. After two hours of reperfusion a 1.5 F proxis infusion catheter (Pro-great) was positioned at the site of prior balloon inflation using a using a 6 French JL 4.0 G-stage PTCA guide catheter. Simultaneously 5000IU of heparin was administered. All 16 ml of the cell suspension or saline was then infused via the catheter at a rate of 1ml/min with 2 minutes rest between each 1ml injection. Cells were infused over a total of 48 minutes. Angiography was performed at the midpoint of cell delivery to determine if a no-reflow phenomenon was occurring. If flow appeared to be diminished a longer time interval between cell injections was adopted.

2.4.8 Sacrifice and tissue collection

Pigs were sacrificed at either 24 hours or at 6 weeks post procedure. Initial induction of anaesthesia and ventilation followed the same protocol as the myocardial infarction model protocol (**Section 2.4.2**). However, in order to access the LAD a sheath left carotid access was used. In order to determine the patency in the LAD an angiograph was carried out. A repeat 64-slice contrast CT was then also performed to allow determination of infarct size at 24 hours and at 6 weeks. Animals were then sacrificed via intravenous administration of 5mg of pentobarbitone (Merial Animal Health Ltd, Essex, UK). To expose the heart, the thoracic cavity was then opened and the aorta clamped. A 50ml 4% ThioflavinS (w/v) solution was injected into the left ventricle and allowed to perfuse for 30

seconds. Following this 50ml of 1% methylene blue (w/v) in saline solution was injected into the left ventricle and again allowed to perfuse for 1-2 minutes. Heart was then excised, washed and weighed. The heart was sectioned from base to apex in 5mm transverse sections. Section were then incubated in the dark in a 2% (w/v) 2,3,5-triphenyltetrazolium chloride (TTC) (Sigma Aldrich, MO, USA) for 10 minutes at room temperature. TTC staining allows us to delineate the infarct region clearly in the heart sections. TTC was used to differentiate between metabolically active and inactive tissues. The white compound is enzymatically reduced to red TPF (1,3,5-triphenylformazan) in living tissues due to the activity of various dehydrogenases (enzymes important in oxidation of organic compounds and thus cellular metabolism), while it remains as white TTC in areas of cell death/necrosis since these enzymes have been either denatured or degraded. Images of heart sections were taken using a cannon EOS550D 18 megapixel camera. The ThioflavinS injected at the time of sacrifice allowed us to identify regions of microvascular obstruction (MVO) within the infarct region. When observed under a UV light the regions of MVO correlated to dark regions on the heart sections in which no ThioflavinS was able to penetrate. Images of MVO were captured in the dark under a UV light again using a cannon EOS550D 18 megapixel camera. Tissue samples for each heart section were then taken from three regions, the infarct zone (IZ), the border zone (BZ) and the remote zone (RZ). Samples were embedded in OCT cryomolds and placed directly onto dry ice for freezing, placed in cryotubes and snap frozen by liquid nitrogen or placed in 15ml falcons in PFA for paraffin embedding. OCT embedded and snap frozen samples were stored at -80°C until required for further analysis. Infarct area was planimeterized using Image J software (U.S. National Institutes of Health,

Maryland, USA). Gross hemorrhagic areas were also delineated using Image J and expressed as a percentage of total heart area.

2.5 Tissue sampling

2.5.1 Apoptosis and cell infiltration in border zone

Analysis of apoptosis within the border region of infarcted tissue was carried out using a terminal deoxynucleotidyl-mediated dUTP nick-end labelling (TUNEL) method according to the manufacturer's instructions (**See Appendix 9.9**) (*In Situ* Cell Death Detection Kit, Fluorescein, Roche Diagnostics). Briefly, 5µm thick OCT section were cut using a cryostat and sections were placed on superfrost slides, all sections were maintained at -20°C until analysis. Just prior to TUNEL staining sections were placed in room temperature for 30 minutes. Sections were then fixed with 4% PFA for 20 minutes at room temperature followed by 30 minute wash in PBS. Slides were incubated in 0.1% (v/v) TritonX, 0.1%(w/v) sodium citrate solution for 4 minutes at 4°C followed by two PBS washes. 50 µl of TUNEL reaction mixture was placed on each section and incubated in a humidified chamber for 60 minutes at 37°C. Again 3x PBS washes were carried out following TUNEL reagent incubation. The nuclei of cells were stained with a 1:2000 DAPI (v/v) (in dH₂O) solution. Slides were washed again in PBS before being mounted with antifade (Thermo) and coverslipped. The number of TUNEL positive cells was counted in 45 images (magnification: 60X) per animal, derived from BZ taken from a midventricular slices. Data was expressed as a percentage of TUNEL positive cells/DAPI positive cells. Number of DiI positive cells was also counted and expressed as a percentage of the total number DAPI positive cells.

2.5.2 Trichrome staining for analysis of microvascular plugging

Trichrome staining was performed on paraffin embedded sections. PFA fixed tissue samples were dehydrated using an automatic tissue processor (Histokinnet) before being embedded in paraffin matrix. Slides were deparaffinised, hydrated and fixed before being stained. To deparaffinise, slides are placed in a couplin jar and the following washes performed. Two washes in xylene for 3 minutes, a 3 minute incubation with a 1:1 xylene in 100% ethanol solution, two 3 minute incubations in 100% ethanol, a 3 minute incubation in 95% ethanol and a 3 minute wash in 75% ethanol followed by a 3 minute wash in 50% ethanol. Finally slides are placed under running tap water and kept in tap water until required for analysis. For Trichrome staining slides were first placed in a coplin jar containing Bouin's solution for 15 minutes at 56°C before being washed under running tap water. Slides remained under the tap until the water was free of yellow coloration. The slides were then immersed in Hematoxyline Z solution for 15 minutes and washed again under tap water for 15 minutes before being rinsed in distilled water. Sections were then stained with a Ponceau 2R/ Acid Fuchsin stain for 2 minutes and then dipped in distilled water to remove any residual stain. Slides were subsequently treated with phosphotungstic acid solution for 5 minutes and counter stained with Aniline blue for 3 minutes. For the second last step slides were immersed in 1% Acetic acid solution before a final rinse in distilled water. Slides were then dehydrated and mounted with DPX and coverslipped.

2.6 Analysis of Tissue Factor

2.6.1 Surface Tissue Factor expression by immunocytochemistry

MSC were seeded at a density of 1000-2000 cells in an 8 well glass Nunc chamber. Cells were allowed to adhere and proliferate for 2-3 days until approximately 60% confluency was reached. All cell types adhered to glass and visual analysis demonstrated that glass has no apparent effect on the cell viability. Media was then removed and the cell monolayer was washed in PBS before fixation with ice cold methanol for 5 minutes. Methanol fixation was used for cellular TF antigen expression analysis by immunostaining as PFA is known to reduce the antigenicity of cells and crosslinking can obstruct antibody binding. A permeabilization step was added for TF detection as previous work revealed that TF antibody staining in nonpermeabilised fibroblasts demonstrated staining only on the cell periphery[165]. Cells were washed again with PBS. Blocking buffer was then added to each well for 30 minutes in order to block any nonspecific antibody binding. The blocking solution consisted of 5% normal goat serum and 0.1% (v/v) TritonX in PBS. After blocking, cells were incubated with Tissue Factor primary antibody (Bioss, Woburn, MA 01801) or IgG control antibodies (Abcam, Cambridge, UK) at a dilution of 1:50 in blocking buffer at 4°C overnight. The next day cells were washed 3 times in PBS before the secondary antibody (goat anti-rabbit Alexa Fluor 488, 1:1000 Abcam, Cambridge, UK) was added. Cells were then incubated for 45 minutes with a goat-anti rabbit 488 antibody. Nuclei of cells were stained with a 1:2000 DAPI (v/v) solution for 5 minutes before being mounted with antifade and coverslipped. Tissue Factor immunostaining was analysed by confocal microscope (Nikon D-Eclipse confocal microscope system) and analysed using Nikon EZC1-3.30 software

2.6.2 Analysis of surface Tissue Factor expression by FACS

Porcine MSC and porcine fibroblasts were trypsinized and counted to a concentration of 1×10^6 cells. Cells were centrifuged and washed in PBS twice to ensure the adequate removal of serum. Cells were then incubated with a 1:100 dilution of Tissue factor antibody (Rabbit anti-tissue factor, Bioss, Woburn, MA 01801) in FACS buffer for 1 hour at 4°C in the dark. After primary antibody incubation cells were washed and centrifuged, before being incubated with a secondary antibody (goat anti-rabbit Alexa Fluor 488, 1:1000 Abcam, Cambridge, UK) at a concentration at a 1:1000 for 45 minutes at 4°C in the dark. IgG control incubations were carried out for each experiment (Abcam, Cambridge, UK). Tissue Factor expression was analysed on a FACS aria flow cytometer using BD FACSDiva™ software (Becton Dickinson, Franklin Lakes).

2.6.3 Assessment of Tissue factor Protein Expression by

Immunoblotting

MSC or porcine aortic fibroblasts were lysed using 1X lysis buffer (50 mM Tris HCL, 150 mM NaCl, 1% NP-40, 0.5% sodium deoxycholate, 0.1% sodium dodecyl sulphate (SDS), pH 8) containing 1X Complete Protease inhibitor cocktail (Roche). The protein concentration was assessed using a BCA Protein assay, and resolved by 12% SDS-PAGE. Following electrophoretic transfer onto nitrocellulose membranes, TF was detected by immunoblotting with 1:500 anti-TF rabbit polyclonal (Bioss, Woburn, MA 01801) and visualized by a 1:5000 dilution of a horse radish peroxidase-conjugated goat anti-rabbit IgG antibody (Jackson Laboratory) and chemiluminescence (Supersignal West Pico, Thermo

Scientific). TF was quantified by densitometric comparison with a 1:5000 dilution beta-actin loading controls (Sigma Aldrich, MO, USA)

2.6.4 Analysis of thrombin generation and coverage under physiological flow conditions [166, 167]

In vitro flow experiments were carried out to identify MSC contribution to thrombin generation and platelet adhesion. Initially, flow chambers were coated with collagen for 2 hours and then washed with PBS just prior to starting experiments. MSC and fibroblasts were trypsinized and counted to a concentration of 5×10^5 cells. Cells were labelled using DiI as previously described in section 1.3. Whole blood was collected in a 0.4% (w/v) sodium citrate and labelled with a 10 μ M quinacrine dihydrochloride (w/v) solution (Sigma) for 30 minutes at room temperature. The assembled flow chamber (Ibidi) (**Figure 2.1**) was then placed on the stage of an inverted confocal microscope. Whole blood; whole blood + MSC; whole blood, MSC + Heparin were perfused over the collagen-coated flow chamber at a controlled flow rate of 10dyn/cm² using a syringe pump and software (Ibidi, pump control software V1.3.4) Basal shear stress within the coronary circulation averaged 10dyn/cm² [168] and was therefore used at the shear flow rate for all *in vitro* flow studies.

Five images were captured every 5 minutes for a 15 minute time period. Thrombus coverage was calculated using NIS-elements BR software and expressed as average percentage of thrombus coverage.

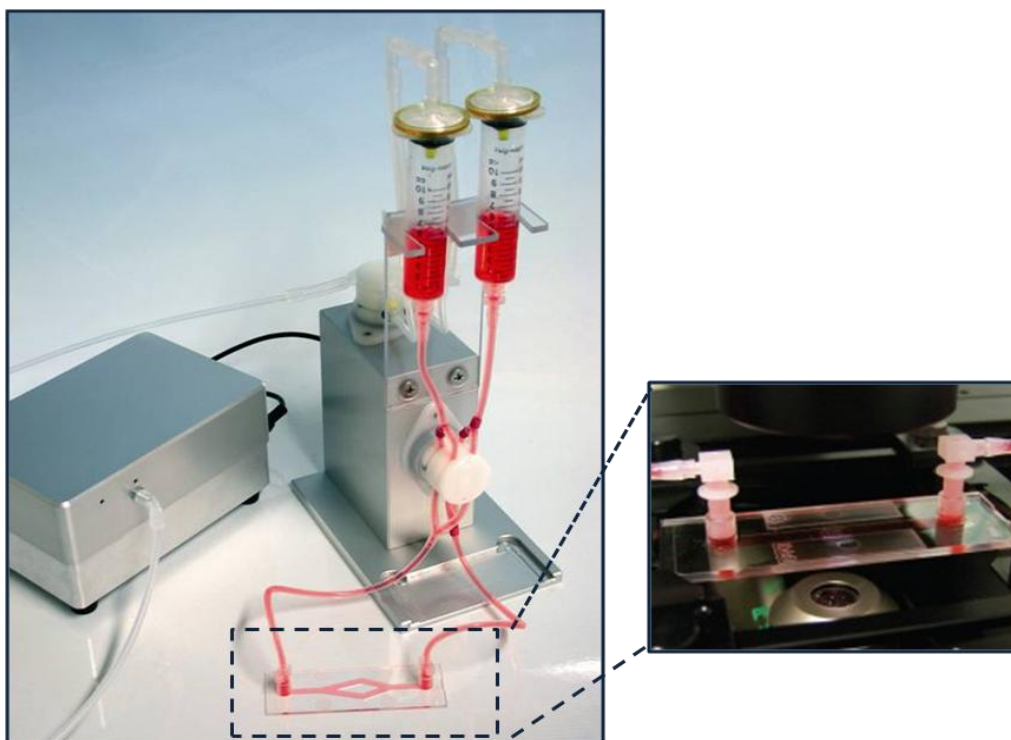


Figure 2.1 Ibidi Flow system

Figure adapted from Ibidi.com

2.6.5 Analysis of Tissue Factor activity

Tissue factor activity was quantified using a chromogenic activity assay (Actichrome[®] TF, American Diagnostica, Stamford, USA) (**Appendix 9.4**). The Actichrome TF assay measured the peptidyl activity of human tissue factor in cell lysates. MSC, FB, EC (2×10^5) were lysed by repeated freeze thaw cycles in recommended cell lysis buffer. The lysates were then mixed with human factor VIIa and human factor X and incubated at 37°C during which time the TF in the sample forms a complex with FVIIa which converts the human factor X to factor Xa. The amount of Xa generated was measured by its ability to cleave SPECTROZYME FXa, a highly specific chromogenic substrate for Xa, which was added to the reaction solution. The cleaved substrate released a para-nitroaniline (pNA) chromophore into the reaction solution and absorbance was

measured at 405nm wavelength using a plate reader. A standard curve was constructed by plotting the mean absorbance value measured by each TF standard against its corresponding concentration. The TF concentrations were then interpolated directly from the standard curve.

2.6.6 Thrombin generation

The TECHNOTHROMBIN® TGA assay is based on monitoring the fluorescence generated by thrombin cleavage of a fluorogenic substrate over time upon activation of the coagulation cascade by TF (**Appendix 9.5**). The fluorogenic substrates are designed with an amino acid that is cleavable by Thrombin and upon substrate cleavage a fluorescent dye is released and starts emitting a fluorescent signal. The changes in fluorescence over time allows for the calculation of the concentration of thrombin (nM) respective to the thrombin calibration curve over time. The reagents used in the assay did not contain TF but did contain concentrations of micelles of negatively charged phospholipids. Citrated plasma was re-calcified by Ca^{++} present in the substrate solution and TF bearing MSC were capable of triggering thrombin generation in plasma. AUC refers to the total concentration of thrombin generated over time. Technoclone software (Technoclone, GmbH) provided required only the addition of raw data to construct thrombin generation curves.

2.7 Analysis of secretome of porcine and human MSC

The secretome of human and porcine MSC was compared using a human antibody cytokine array kit (Quantibody® Human cytokine array 5, Raybiotech, Medical supply Co., LTD, Dublin). The protocol was performed according to

manufacturer's instructions (**Appendix 9.7**). Briefly, 5×10^5 human and porcine MSC were plated in a T25 flask. After 24 hrs cells had adhered and were approximately 80-90% confluent. Cells were washed three times with PBS to fully remove any residual serum. Cells were incubated with serum free α -MEM basal media for 48 hours. After 48 hours the media was collected, centrifuged and filtered through a $2\mu\text{m}$ filter to remove any remaining cells. Cytokine analysis was carried out using the antibody array kit. Basal media was used as a control and signal intensities were determined using ImageJ software. Data was represented as % of cytokines which refers to normalisation of results to positive control.

2.8 Sparcl1 study

2.8.1 Sparcl1 ELISA

Sparcl1 concentration in conditioned MSC media was measured using human Sparcl1 Elisa kit (Sino Biological Inc.). MSC were seeded at a concentration 1×10^5 MSC in a 24 well plate and allowed to adhere overnight. At 24 hrs media was changed and allowed to incubate for a further 48 hours. Media was collected and ELISA was carried out according to full manufacturer's protocol (**Appendix 9.6**). Briefly, capture antibody was added to 24-well plate and allowed to incubate overnight. The next day standards and samples were added to the plate and allowed to incubate at room temperature for two hours before adding detection antibody. Substrate was added and optical density of each well was analysed using a microplate reader set to 450nm. A standard curve was constructed by plotting the mean absorbance value measured by each Sparcl1 standard against its corresponding concentration. The Sparcl1 concentrations in samples were then interpolated directly from the standard curve.

2.8.2 Sparcl1 MI model

The MI model was similar to that used in the chronic MSC study, however, 10 μ g of reconstituted recombinant human Sparcl1 (R&D systems) was delivered via the coronary artery directly after the 120 minutes of reperfusion using the Progreat® delivery catheter.

2.8.3 Dose of SPARCL1

Dose of SPARCL1 was extrapolated from the MSC CM Elisa to match the 25x10⁶ MSC delivered in previous studies as this number of cell conferred functional benefits. (1ml of CM was collected from 1x10⁵ MSC – ~ 40ng extrapolated to the equivalent of 25x10⁶ MSC =10 μ g). Recombinant Sparcl1 was reconstituted in 8 ml of saline before delivery.

2.9 Statistics

2.9.1 Power calculation

The sample size for each experiment was estimated based on power analysis to detect a minimum 20% difference between mean in experimental and control groups with less than 15% variance within the means. The power of the test was set at probability (power) 0.95. The Type I error probability associated with the test was set at 0.05.

2.9.2 Analysis

All data are represented as mean \pm SEM. Difference between groups was analysed by unpaired Student t-test or multiple analysis of variance by ANOVA followed by Bonferroni's post-hoc testing. All statistics were carried out using

Graphpad Prism Version 4 (GraphPad Software, Inc., California, USA). *P<0.5

was considered significant, *p<0.05, **: p<0.01*** p<0.001.

Reagent	Volume (100ml)	Final Concentration
DMEM (LG)	87.5ml	
Dexamethasone 1mM	10 μ l*	100nM
Ascorbic acid 2-P 10mM	0.5ml	50 μ M
β glycerophosphate 1M	1ml	10mM
FBS**	10ml	10%
Penicillin/Streptomycin	1ml	100U/mL penicillin 100 μ g/mL streptomycin

Table 2.2 Osteogenic Media

Reagent	Volume (100ml)	Final Concentration
DMEM (HG)	87.6ml	
Dexamethasone 1mM	100 μ l	1 μ M
Insulin 1mg/ml	1ml	10 μ g/ml
Indomethacin 100mM	200 μ l	200 μ M
500mM MIX	100 μ l	500 μ M
Penicillin/Streptomycin	1ml	100U/mL penicillin 100 μ g/mL streptomycin
FBS	10ml	10%

Table 2.3 Apipogenic Induction Media

Reagent	Volume (100ml)	Final Concentration
DMEM (HG)	88ml	
Insulin 1mg/ml	1ml	10 μ g/ml
Penicillin/Streptomycin	1ml	100U/mL penicillin 100 μ g/mL streptomycin
FBS	10ml	10%

Table 2.4-Adipogenic Maintenance Media

Reagent	Volume (100ml)	Final Concentration
DMEM (HG)	95ml	
Dexamethasone 1mM	10µl*	100nM
Ascorbic acid 2-P: 5mg/ml	1ml	50µg/ml
L-Proline: 4mg/ml	1ml	40µg/ml
ITS+ supplement	1ml	6.25 µg/mL bovine insulin 6.25 µg/mL transferrin 6.25 µg/mL selenous acid 5.33 µg/mL linoleic acid 1.25 mg/mL BSA
Sodium pyruvate	1ml	1mM
Penicillin/Streptomycin	1ml	100U/mL penicillin 100µg/mL streptomycin

Table 2.5- Incomplete Chondrogenic medium

Complete Chondrogenic medium (CCM)

To 1ml of ICM add 0.5µl of TGFβ-3 to give a final concentration of 10ng/ml

Chapter 3

Porcine MSC isolation and cell delivery optimization in MI

3.1 Introduction

Before the benefit of any therapeutic agent can be established, efficacy must be first demonstrated in accurate and relevant models of the disease state in question. This chapter will begin to introduce the models and procedures used for all *in vivo* work described in this thesis and provide experimental reasoning as to why these models were chosen in relation to the delivery of MSC therapy.

The main objective of any pre-clinical research is to act as a bridge in translating basic science into clinical practice. Therefore, to accurately replicate the clinical scenario of acute MI experimentally, large animal models were used. In the area of cardiovascular research pigs are increasingly seen as superior to other large animal models such as dogs and primates [169]. The main advantage of using pigs is their close anatomical, physiological and immunological resemblance to that of human subjects [170]. Most importantly however, experimentally, it has been demonstrated that the porcine heart responds biochemically and metabolically in similar ways to that of human after the induction of MI [169]. Previously, the majority of early cardiovascular research was carried out on dogs, however, their extensive collateral circulation and more recent ethical limitations has decreased usage of this species [171, 172]

The age of the animal model used is an important experimental consideration. Due to the fast growth rate of domestic pigs and the holding facilities available, the pigs used in these studies are generally 3-5 months old. Studies confirm that this is sufficient age for fully developed central nervous system regulation of cardiovascular function [173]. For all *in vivo* experiments female Landrace pigs were used. Females were chosen primarily for ease of handling as male non

castrated landrace pigs tend to be more aggressive. The preclinical use of landrace pigs has been experimentally verified in other studies at the CRVB laboratory [94, 174] and due to local breeding suppliers, the use of Landrace was a convenient and inexpensive model to use.

The target artery selected for induction of MI and the position of the balloon occlusion catheter are also important experimental design considerations. In the majority of preclinical studies ischemia is induced through the occlusion of the LAD artery; however ischemia has also been induced via the circumflex artery [175, 176]. The LAD artery of a pig heart is anatomically similar to that of a human, therefore occlusion of the LAD in pigs creates an infarct that is similar in size and distribution to that of human presenting with a LAD infarct [177]. Circumflex occlusion would have yielded a much smaller infarct with greater difficulty in detecting small differences between groups. Additionally this approach may have required much greater sample sizes. The more proximal (closer to the origin) the occlusion in a coronary artery, the greater the territory damaged. A study which evaluated two occlusion positions and two times of occlusion recommended that a mid-LAD occlusion can fulfil most of the key criteria for a reproducible, low risk and minimally invasive experiential model of MI[178]. Proximal LAD occlusion led to increase mortality compared to that of mid-LAD occlusion and a 30 minute occlusion did not substantially affect cardiac function [178]. A 90 minute mid-LAD induced a significant infarct in a previously well-established model used and verified within the CRVB and was therefore used in all *in vivo* studies.

Restoration of blood flow to an artery post infarction can lead to what is known as ischemia/reperfusion (I/R) injury [179]. Oxygen free radicals released on the restoration of blood flow cause additional damage to the myocardium including myocardial haemorrhage, MVO and arrhythmias [179]. In clinical setting revascularization whether via thrombolytics or PCI is standard practice and therefore I/R injury is unavoidable. Using a model which represents I/R injury is clinically relevant and our studies therefore used a reperfusion model as opposed to an ischemia alone model. The I/R model used for these studies consisted of a 90 minute LAD occlusion followed by 120 minutes of reperfusion before therapy was delivered (**Figure 3.4**). This allowed comparative analysis with prior studies in our lab and studies reported in the literature.

Before beginning to test the effect of MSC *in vivo*, a reproducible porcine MSC cell culture that could be easily isolated and expanded from porcine bone marrow needed to be established. The isolated MSC from our in-house production protocols had to be capable of meeting the minimal criteria set by the International Society for Cellular Therapy, such as adherence to plastic, tri-lineage differentiation and specific surface marker expression before they could be defined as MSC and used for *in vivo* studies [70].

MSC cell numbers, routes and models used in pre-clinical research for the treatment of ischemic heart disease has varied significantly (**Table 3.1**). Therefore the main aims of this study were to firstly isolate and characterise our in house derived MSC and then to identify and optimise an MSC cell dose and delivery strategy that was reproducible and safe when delivered in the established acute porcine MI protocol. The protocol used was designed based on the concepts

described with the aim to represent a clinical MI scenario as accurately as possible.

Cell number 10 ⁶	Route	Time after MI	Animal	Type of infarction	Model	Follow up Weeks	Author
2	IC	1 h	Pig	LAD	I/R	4	Valina[133]
5	IC	28d	Pig	LAD	No I/R	4	Yang [134]
5	IC	28d	Pig	LAD	I/R	4	Yang[135]
7.1	TE	16d	Pig	LAD	I/R	1.5	Gyongyosi[180]
10	IC	3d	Pig	LAD	I/R	4	Lim [131]
10	IC	1 h	Pig	LAD	I/R	13	Jiang [181]
17	TE	14d	Pig	LCX	No I/R	4	Schneider[182]
50	Trans	1 h	Pig	LAD	I/R	4	Wang[183]
50	IC	20m	Pig	LAD	I/R	2	Llano[184]
50	IC/TE/IV	15 m	Pig	LAD	No I/R	6	Freyman[119]
80	TE	28d	Pig	LAD	No I/R	4	Li
60	TE	14d	Pig	LAD	I/R	2-4	Shake[80]
75	TE	3d	Pig	LAD	I/F	2-8	Hatzistergos[122]
100	TE/IC	7d	Dog	LAD	I/R	2	Perin[185]
100	Surgical	28d	Pig	LAD	No I/R	4	Tomita[186]
100	IC	5d	Pig	LAD	I/R	4–8	Qi [187]
200	TE	3d	Pig	LAD	I/R	1-8	Amado[188]
200	IC	84d	Pig	LAD	I/R	12	Queved[82]o
200	TE	2d	Pig	LAD	I/R	8	Schuleri[189]
320	IV	1 h	Pig	LAD	I/R	13	Price [190]
39-370	IV	1 h	Pig	LAD	I/R	12	Halkos [191]
24-440	TE	3d	Pig	LAD	I/R	8–12	Hashemi[125]
23-440	Surgical	1 h	Sheep	LAD	No I/R	4–8	Hamamoto [192]
1000	IC	7d	Pig	LAD	I/R	6	Qian [193]

Table 3-1 Pre-clinical MSC cell studies

Preclinical cell therapy studies in large animals with acute MI and chronic ischemic cardiomyopathy.

IC, Intracoronary injection, IV, intravenous injection, TE, Transendocardial injection, I/R, Ischemia Reperfusion, d, Day, h, Hour, m, minute, LAD, Left Anterior Descending Artery, LCX, Left Circumflex

3.2 Results

3.2.1 Isolation and expansion of porcine MSC

MSC were easily isolated and expanded from the iliac crest from our in-house pigs (**Figure. 3.1 A,B**). On average 15-30ml of bone marrow was collected and at 10 days approximately $6-10 \times 10^6$ MSC were present in culture. For *in vivo* experiments approximately 30-40 days was required from initial isolation allowing for approximately 4 population doublings and 100×10^6 MSC. Isolated pMSC were capable of adhering to plastic when maintained in standard culture conditions and microscopic examination of isolated cells revealed a homogenous fibroblastoid spindle like shaped MSC population. (**Figure. 3.1 B, 3.3 A**).

3.2.2 MSC differentiation and surface marker expression

Culture expanded MSC were analysed more extensively according to their relative expression of mesenchymal markers. Flow cytometric analysis showed that the pMSC populations were positive for the characteristic MSC markers CD90, CD29, CD105 but lacked the expression of myeloid CD11b and CD14 markers (**Figure 3.2 A-G**). Culturing of MSC in differentiation promoting conditions revealed that the isolated pMSC were capable of differentiating along all three lineages. Control cells were stained with the corresponding dyes. (**Figure. 3.3 A-D**)

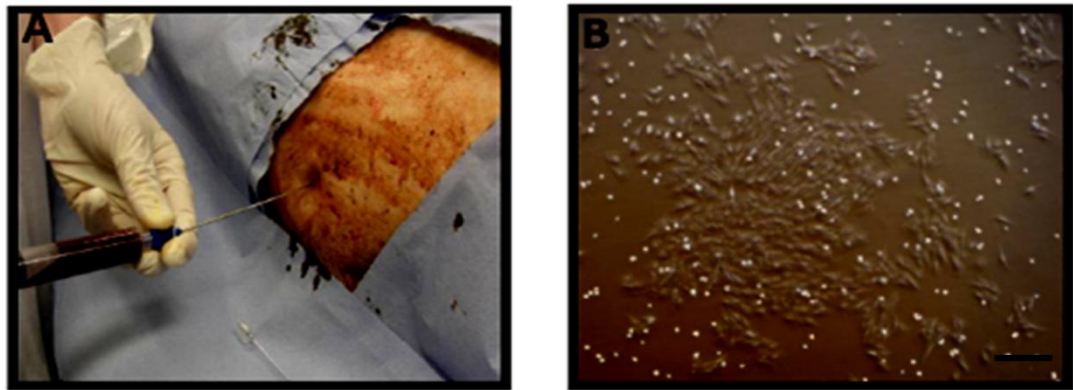


Figure 3.1 Porcine MSC Isolation

A. Porcine MSC were isolated from bone marrow extracted from the Iliac crest and were expanded in culture **B.** Light Microscopic image of plastic adherent pMSC at P0 in culture. pMSC at P0 are initially capable of forming colonies within culture conditions. Scale bar represents 200µm.

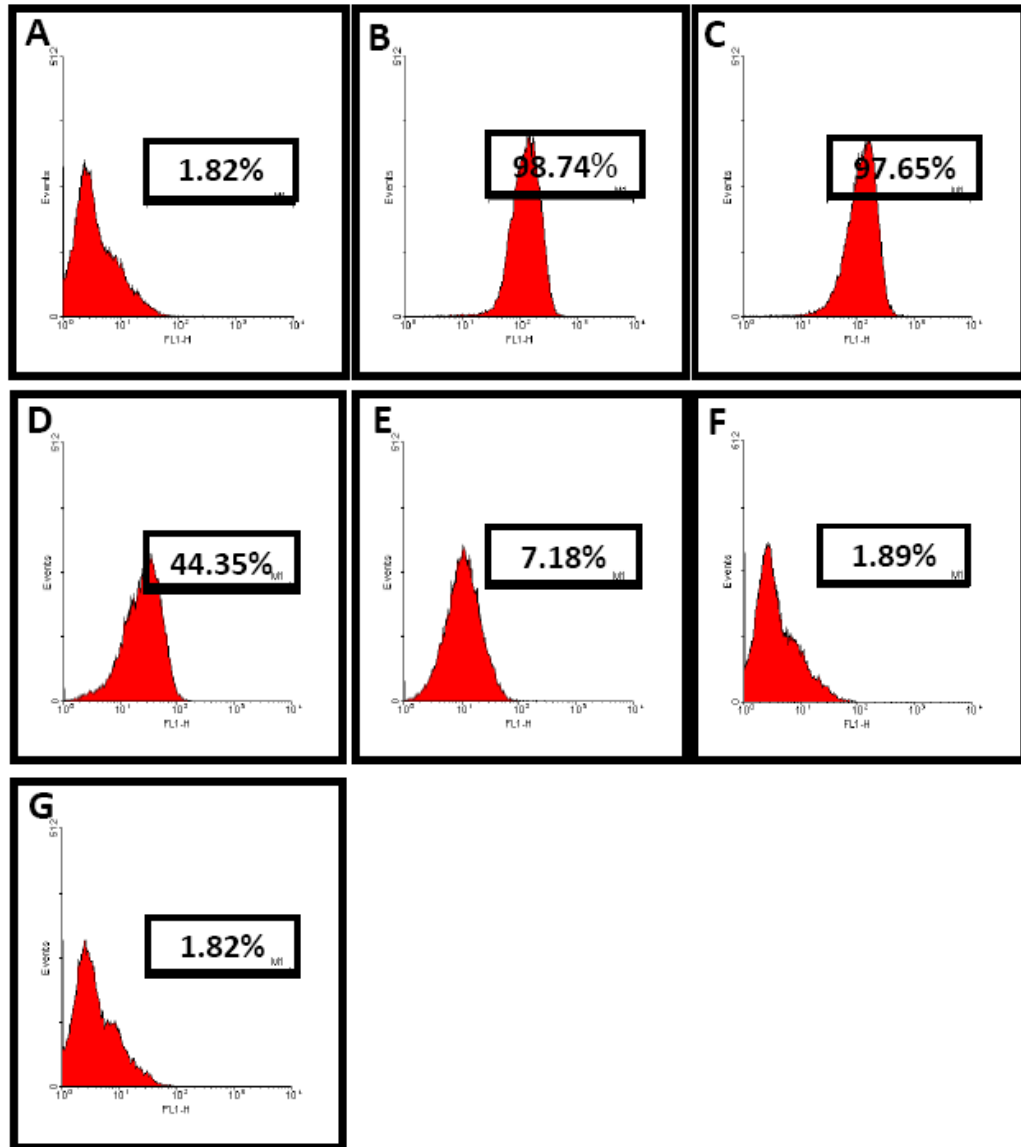


Figure 3.2 MSC surface marker expression.

pMSC were characterised by their surface marker expression. MSC were positive **A**. Isotype **B**. CD29 **C**. CD90 **D**. CD105 and negative for **E**. CD14, **f**. CD11b. **A and G**. Isotype and Unstained respectively (n>3)

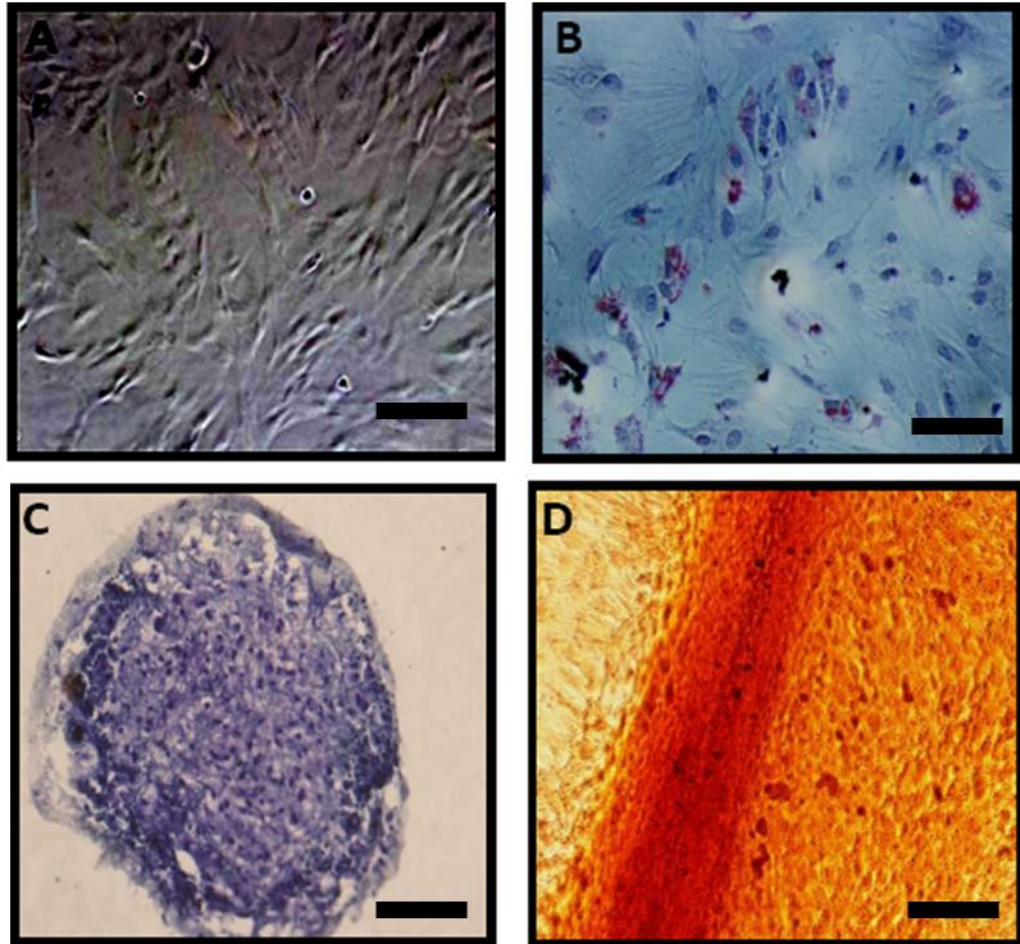


Figure 3.3 Porcine MSC are capable of tri-lineage differentiation

pMSC were characterised by ability to differentiate into adipocytes, chondrocytes, and osteocytes. **A.** MSC control **B.** Adipocytes stained with oil red O, **C.** chondrocytes stained with alcian blue and **D.** osteocytes stained with alizarin red. Scale bar represent 100µm (n>3)

3.2.3 Efficiency of DiI cell labelling and viability of MSC

In order to track MSC within the myocardium post-delivery, MSC were stained using the lipophilic membrane stain DiI. Flow cytometric analysis revealed a high percentage of DiI positive staining indicating efficient uptake with over 99% of MSC staining positive after 20 minute incubation with the DiI solution (**Figure 3.5 A**). In addition, fluorescence microscopy analysis revealed uniformly vibrant staining MSC after incubation with DiI solution (**Figure 3.5 B**). To determine if DiI had an effect on cell viability and to ensure delivered MSC were viable and there was no loss during cell preparation DiI labelled MSC were counterstained with 7AAD (**Figure 3.5 C**). Flow cytometric analysis confirmed that DiI labelling had no effect on the viability of MSC *in vitro*. In addition, labelling efficiency of MSC is maintained after transfer *in vivo* up to 24 hours after MSC administration (**Figure 3.5 D**).

3.2.4 Initial dosing studies

A 90 minute proximal LAD occlusion resulted in an anterolateral infarct of approximately 50% of left ventricle. (**Figure 3.6, A-B**) **Figure 3.6 C** illustrates a typical LV cross-section outlining infarct by TTC staining. In order to determine the optimal MSC dose tolerated by our pigs initial dosing studies were carried out according to **Table 3.2**. Delivery of 100×10^6 MSC at high flow rates of 20ml/min resulted in 100% pig mortality and post mortem analysis revealed that severe tissue extravasation was the casual factor (**Figure 3.7**). Subsequently, lower doses MSC were delivered at lower flow rates, 30×10^6 delivered at lower flow rate of 2ml/min was tolerated until the last injection at which point the VF occurred and defibrillation strategies failed to resuscitate the animal. The concentration of cells per injection also had an impact on pig mortality, delivery

of MSC at a low flow rates but at concentrations higher than 25×10^6 resulted again in fibrillation and animal mortality. Subsequent dosing studies used significantly lower cell numbers at lower delivery flow rates with the additional intervals of 2 minutes between each injection. 15×10^6 MSC were well tolerated at low flow rates and so the dose was then increased to 25×10^6 which could also be delivered with no significant adverse events occurring. 25×10^6 MSC delivered at 2 ml/min at a concentration of 1.5×10^6 with a 2 minutes interval between each injection was the optimum tolerated dose of MSC when delivered via the coronary artery. However, no re-flow directly after MSC administration within the coronary artery was observed by angiography. (Figure 3.8 A-C)

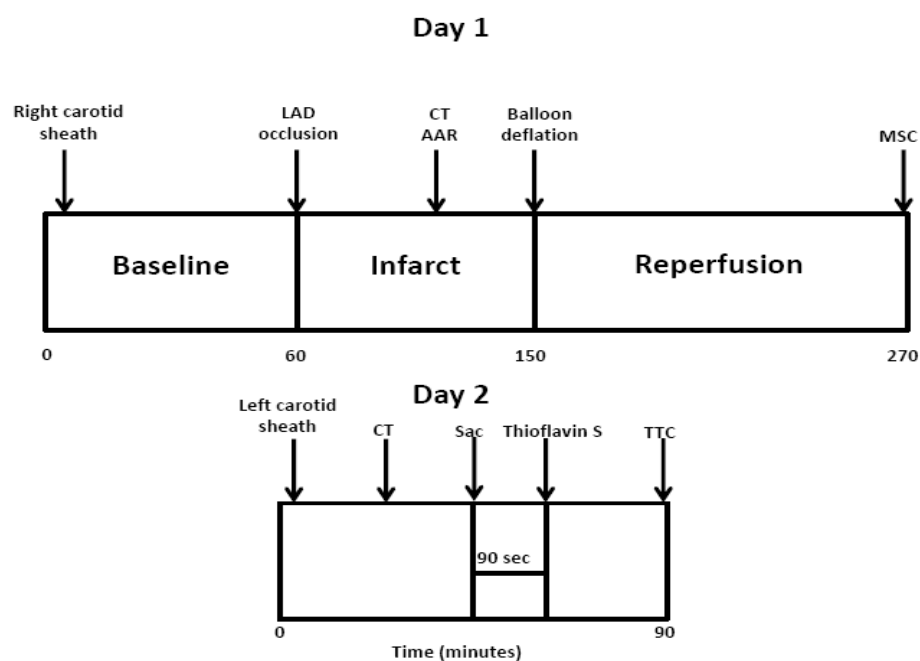


Figure 3.4 Infarct and MSC delivery protocol

Protocol included a 90 minute mid LAD occlusion followed by 120 minutes of reperfusion before cell therapy was delivered. 24 hours after initial procedure the animal was sacrificed and heart was explanted and stained to identify region of infarct

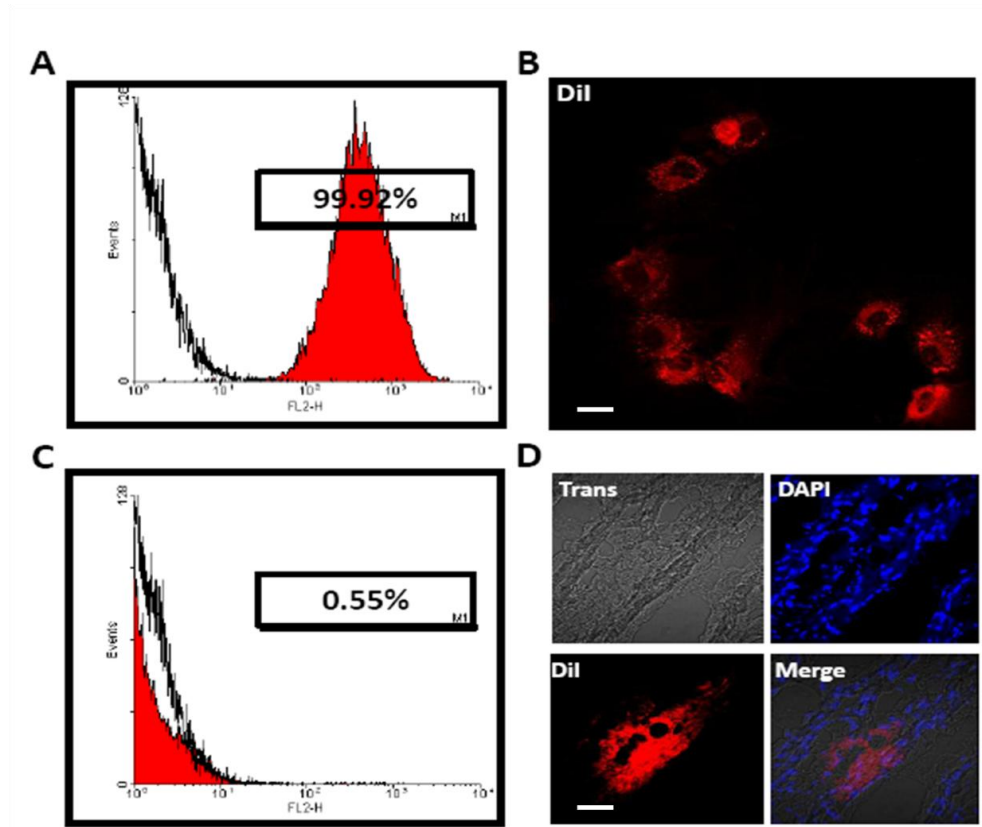


Figure 3.5 MSC DiI labelling

pMSC were labelled with DiI in order to track their infiltration *in vivo*. **A.** Post DiI staining, 99.92% of MSC stained positive for DiI as analysed by FACS. **B.** Immunofluorescence analysis of DiI stained MSC revealed that DiI labelled cells displayed diffuse whole cell labelling **C.** DiI labelling had no effect on cell viability as evident by 7AAD staining as analysed by FACS. **D.** OCT section of the Border Zone of the infarct region revealed the presence of DiI labelled MSC 24 hours post infusion. The *in vivo* delivery of labelled cells had no effect on the DiI labelling efficiency and MSC were readily observed within the myocardium. Scale bars represent B.50 μ m D.100 μ m (n>3)

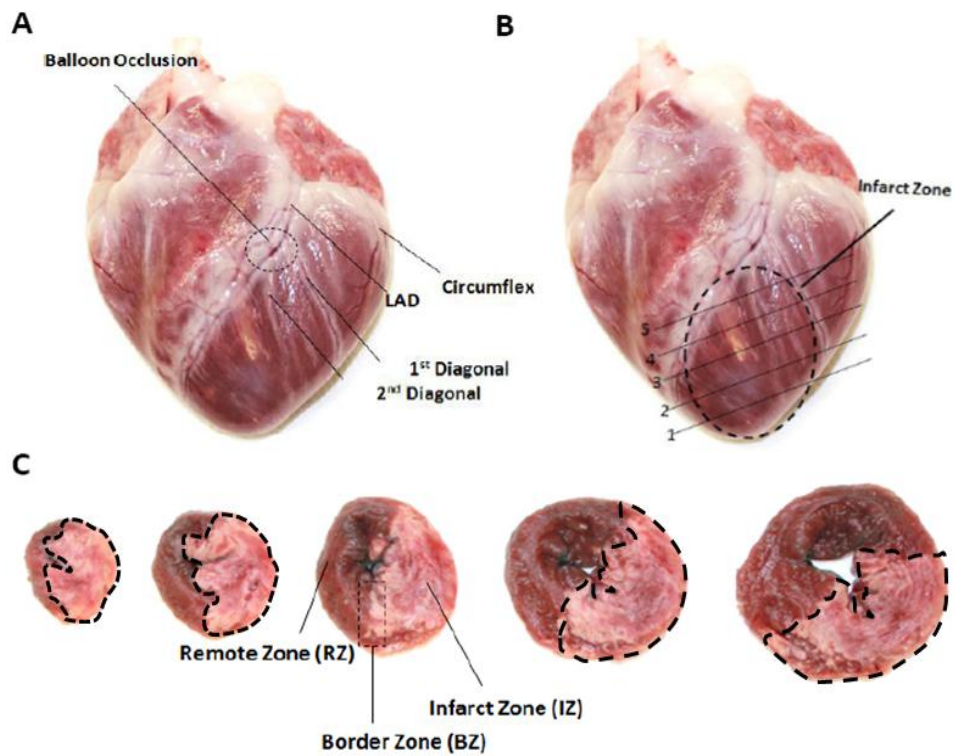


Figure 3.6 Macroscopic images of infarcted porcine heart

A. Macroscopic image depicting balloon positioning during infarct induction. **B.** Image displaying the typical region affected by balloon occlusion which corresponds to the sampled region. Explanted hearts were typically cut into 5, 0.5-1cm cross section from apex to base. **C.** A typical LV cross-sectional slice. The non-infarcted myocardium (RZ) on the left stains red with TTC while the infarcted myocardium (IZ) on the right does not stain with TTC and remains pale. TTC= triphenyltetrazolium chloride. Explanted hearts typically weighed 200-250g. The infarcted region following a mid LAD infarct affected approximately 50% of the total LV area as displayed above.

Cell No 10 ⁶	Flow rate	Inject	Cells/ml	Total Injection Time	Outcome
100	20ml/min	1	10x10 ⁶	30 seconds	Fibrillation, Death, Tissue extravasation
30	2ml/min	10	1.5x10 ⁶	30 minutes 1min injection 2min recovery	Tolerated 9 Injections, fibrillation after 10 th injection, Death
25	2ml/min	5	2.5x10 ⁶	13 minutes 1min injection 2min recovery	Fibrillation after 3 rd injection, Death
9	2ml/min	3	1.5x10 ⁶	7 minutes 1min injection 2min recovery	Pig Survived
15	2ml/min	5	1.5x10 ⁶	13 minutes 1min injection 2min recovery	Pig Survived
25	2ml/min	8	1.5x10 ⁶	24 minutes 1min injection 2min recovery	Pig Survived

Table 3.2 MSC Dosing study

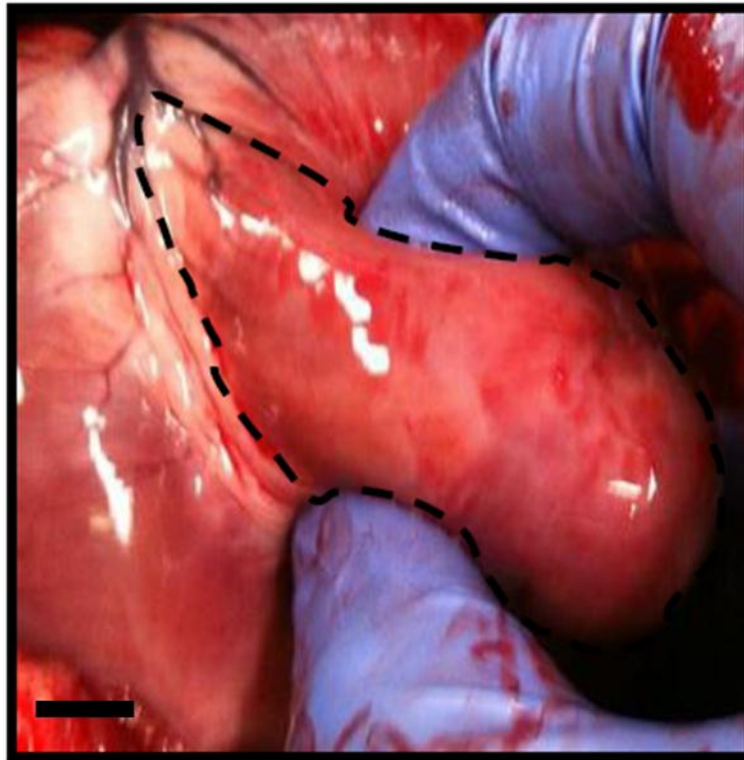


Figure 3.7 MSC tissue extravasation

Post mortem image illustrating MSC infiltration out into the extravascular tissue at the MSC infusion site post-delivery of 100×10^6 MSC in one bolus injection at a delivery rate of 20ml/min. Scale bar represents 1cm

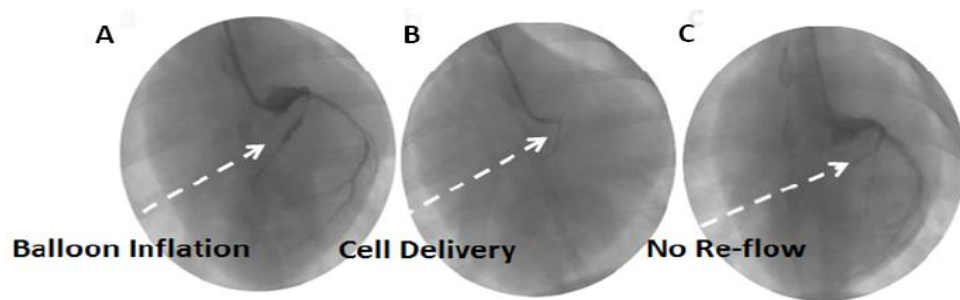


Figure 3.8 *Angiography at MI, during MSC delivery and post MSC delivery*

A. Representative image illustrating position of balloon inflation and no re-flow beyond balloon. **B.** Image illustrating positioning of catheter during MSC delivery.

C. Representative image showing no re-flow within the LAD post MSC administration

3.3 Discussion

This initial study demonstrated the feasibility of isolating MSC from porcine BM. Isolated MSC were expandable to high cell numbers, while maintaining the MSC characteristics as described by the ISCT. This study also highlighted the maximum cell dose that could be safely tolerated from a mortality and arrhythmia perspective when cells were delivered via the coronary artery in an acute MI model.

Due to the heterogeneous nature of MSC a single definite MSC marker has yet to be identified. All of the antigens recommended by the ISCT can also be expressed by other cells and without a distinct marker it remains difficult to definitely identify our cells as MSC although they are as well characterised as any MSC used in pre-clinical studies in the literature. However, for these studies, having two other reproducible characterizing criteria such as tri-lineage cell differentiation and adherence to plastic allowed us to define our cells as MSC.

The advantages of DiI labelling over other cell labelling strategies were its ease of application, the quality of staining, its low cell toxicity and lack of known immunogenicity. DiI which is a lipophilic carbocyanine has an extremely high extinction coefficient and diffuses laterally within the membrane resulting in whole cell staining. A study comparing the labelling efficiency of bone marrow stromal cells with three cell tracing dyes BrdU, FISH and DiI confirmed that DiI in addition to having the highest labelling efficiency also retains its high labelling efficiency after two subcultures, thus, allowing for longer *in vivo* tracking capability [194].

Initial dosing studies used a cell number of 100 million MSC, as per **Table 3.1**. The number of MSC used in numerous pre-clinical studies has varied substantially. No study has to date addressed the question of the optimal therapeutic MSC dose when delivered via the coronary artery. The phase I/II POSEIDON trial carried out by Hare *et al* begun to address this by comparing three different doses of MSC when delivered by transendocardial IM injection. In this study 20, 100 and 200 million MSC were delivered in patients with ischemic cardiomyopathy. CT analysis at 30 days post MSC injection revealed an inverse dose response in which the low dose concentration of 20 million MSC produced the greatest reductions in LV volumes and the greatest increases in EF [118]. This concept of lower cell dosing having improved therapeutic benefit over higher doses was also demonstrated in a pre-clinical study in which pre-cursor MSC were delivered in a sheep model of coronary ligation. Increasing doses of 25, 75, 250 and 450 million MSC were injected into the myocardium. Echocardiography at 4 and 8 weeks illustrated that the lower doses of 25 and 75 million significantly improved infarct expansion and increased left ventricular end diastolic volumes and left ventricular end systolic volumes (LVEDV and LVESV) [195].

To date most cell therapy studies within the cardiac field have assumed that the higher the dose of cells the more efficacious the treatment and a number of small studies although not in relation to MSC have supported this concept. In a mononuclear bone marrow stem cell trial, 100 million and 10 million cells were delivered via the coronary artery after acute MI. Follow up at 3 months demonstrated improved regional myocardial function in a dose dependent manner [196].

Determining an optimal MSC dose is important in order to maximize the benefit of MSC as a therapy. Future studies should aim to establish this by carrying out extensive pre-clinical large animal studies using a wide range of MSC doses. A previous MSC study has delivered up to 60 billion MSC via the coronary artery in a porcine acute MI model and no adverse events were reported [197]. This study however used MSC that were only cultured for 10 days with no cell characterisation or differentiation analysis. Due to the short period of cell expansion it could be possible that the cells used in this study were more similar to bone marrow MNCs. The lack of specific methodologies from these studies leaves it unclear as what the optimal MSC dose really is.

Freyman *et al* demonstrated that IC delivery of MSC after infarction resulted in decreased distal blood flow [119]. In a follow on study members of the same group proposed that delivery of a single, continuous infusion at increased flow rate decreased mortality and preserved blood flow [138]. Delivery of MSC using the same methods in our initial dosing studies resulted in tissue extravasation of cells. The main differences between Wilensky's and this current study include, increased cell number from 50 million MSC to 100 million, increased LAD occlusion time and reperfusion time (20 vs. 120 minutes) in our study. Although these differences may not explain the cause of tissue extravasation it may explain the reductions in flow observed and arrhythmias observed in our studies.

Similar to other IC MSC delivery studies [198-200] this study has highlighted that, by delivering 25×10^6 MSC via the coronary artery, although no major adverse events such as mortality occurred, a reduction in coronary flow could still be observed after cell delivery. At present no study has provided a mechanistic

reason for the reduction of flow associated with microvascular plugging other than the large MSC cell size and high cell numbers. Therefore further studies over the remainder of this thesis will provide mechanistic insight into the possible cause of adverse events associated with IC MSC delivery in the setting of M

Chapter 4

Identifying the *in vitro* procoagulant nature of Mesenchymal Stem Cells

4.1 Introduction

Within the cardiac repair/regenerative medicine field a number of adverse events have been associated with the delivery of MSC via the coronary artery in animal models of MI. Observed events include, intravascular cell aggregation, significant reductions in arterial flow [201], microvascular obstruction, ST elevation and the presence of microinfarcts [136, 137]. Although these events have illustrated the possible risks associated with this type of cell delivery many mechanistic questions remain unanswered such as the proximate cause of diminished microvascular flow and the likelihood that MSC are contributing to MVO.

MSC cell size has been suggested to be one of the key factors in these events [119, 137]. Cultured MSC are typically reported to be 10-30 μm in diameter which may [136, 202-205] explain the evident lodging of MSC within small diameter capillaries (10-15 μm) in organs such as the lungs and liver. This concept is partially supported by an experiment in which systemic delivery of MSC in conjunction with the nitric oxide donor vasodilator sodium nitroprusside could in part counteract cell lodging within the lung, liver, kidney and spleen [206]. Fisher *et al* designed a study based on the hypothesis of cell size which aimed at comparing the first pass distribution of four labelled cell types after systemic delivery [202]. MSC (18 μm), multipotent adult progenitor cells (MAPCs-16 μm), bone marrow mononuclear cells (BMNMC-7 μm) and neural stem cells (NCS-16 μm) were infused intravenously in a rat animal model. In agreement with the nitroprusside study there was a 30-fold increase in lung passage for the smaller BMMNC when compared to the other larger cell types. This suggests there may be a size threshold above which cells contribute to MVO. Surprisingly however, they also found a significant 2-fold increase in first passage

for MAPCs and NCSs when compared to MSC, even though their cell sizes were relatively comparable. Blocking of cell surface adhesion receptors such as P-selectin or VCAM-1 did not enhance pulmonary MSC passage. Based on these findings Fisher suggested that factors other than cell size and the expression of surface adhesion molecules were responsible for cell lodging post delivery. [202].

The pre-clinical findings mentioned above [202, 207] along with our own observations underscore our hypothesis that MSC may in fact be promoting a prothrombotic state upon exposure to blood. Accordingly, we decided to investigate whether therapeutic MSC may have surface expression of TF, a key initiator of the soluble coagulation cascade (**Figure. 1.8**) and whether this expression profile could have functional consequences for thrombosis *in vitro*.

4.2 Results

4.2.1 MSC expressed significant surface TF

To assess whether prothrombotic activity was innate to the cultured MSC population under investigation, TF expression by porcine MSC, FB and EC was determined using immunofluorescence, flow cytometry and immunoblotting. Significant TF immunostaining was detected in MSC and FB but was near absent in EC (**Figure 4.1**). Surface TF expression of FB and MSC was also confirmed by flow cytometry which showed that MSC TF levels were higher than that of FB, 20.7% vs. 12% respectively (**Figure 4.2**). Western blot analysis confirmed these surface expression data in that MSC expressed approximately 2-fold more TF protein compared to FB (**Figure 4.3**).

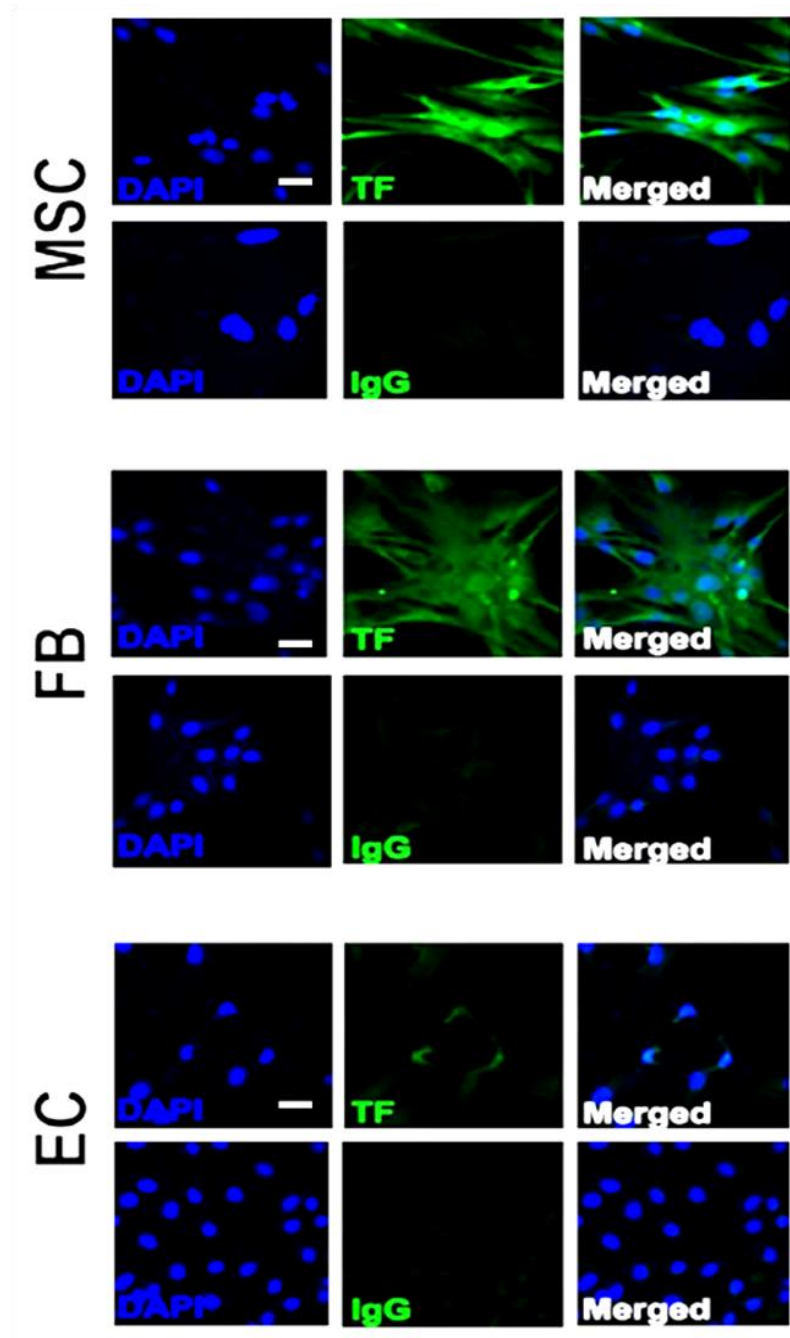


Figure 4.1 MSC expression of TF by immunocytochemistry

Cultured Mesenchymal Stem cell (MSC), Fibroblasts (FB) and endothelial cells (EC) were immunostained for TF (Green) and isotype controls respectively. MSC and FB displayed the presence of both surface and nuclear expression of TF; EC however displayed negligible amounts of TF. To highlight the nuclei, cells were counter-stained with DAPI. 60X images were captured using Nikon D-Eclipse confocal microscope system. Scale bars represent 10 μ m (n=3)

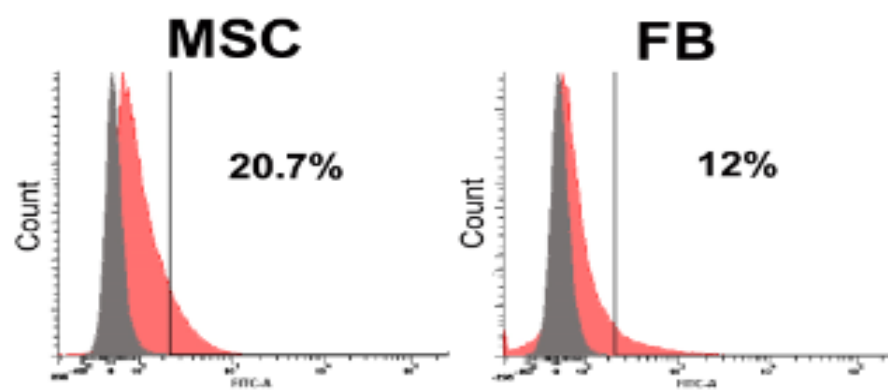


Figure 4.2 MSC express surface TF

Flow cytometric analyses showing that cultured MSC and FB stained positive for TF (Red overlay), surface TF was more highly expressed on MSC than on FB (20.7% vs. 12% respectively)(n=3)

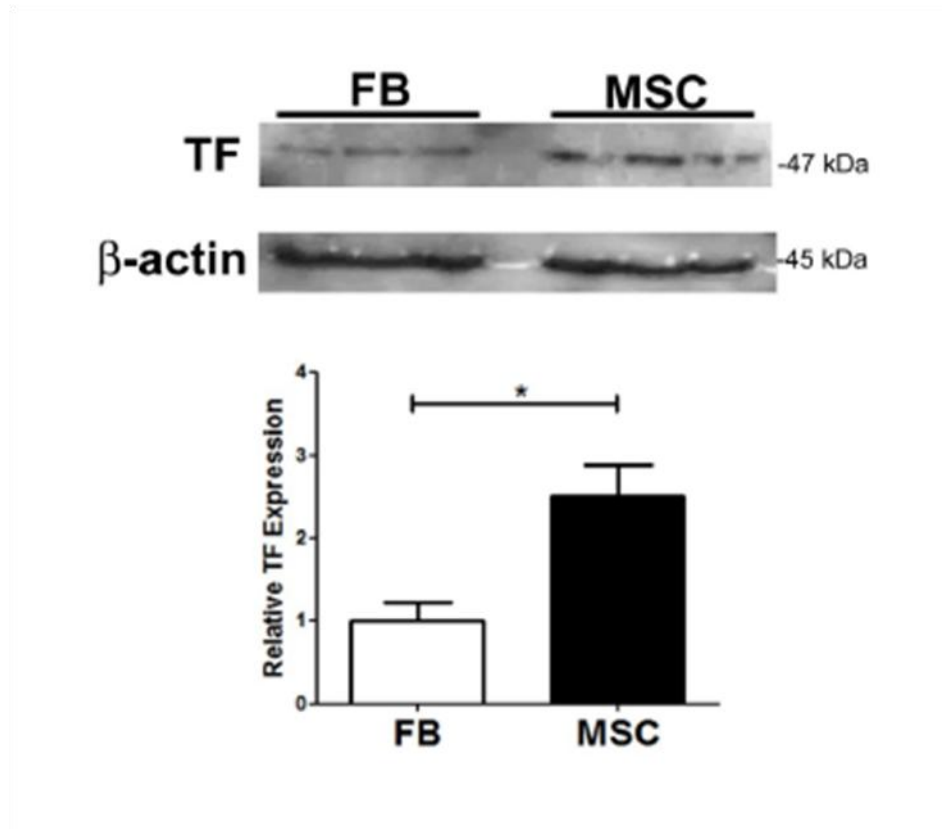


Figure 4.3 *MSC express TF*

Immunoblot of TF expression and β -actin by MSC and FB. Quantification of relative expression of TF by MSC and FB cells lysates corrected for β -actin loading, showing a significant increase in the relative expression in MSC compared to FB. *: $p < 0.05$ (n=3 samples)

4.2.2 TF expressed by MSC was catalytically active and supported thrombin generation *in vitro*

To identify if the TF expressed was biologically active, the TF catalytic activity of MSC, FB and EC was analysed by chromogenic TF activity assay. In MSC, TF activity was significantly greater than that for both FB and EC (**Figure 4.4**). To determine if MSC, due to high TF activity, were also capable of supporting thrombin generation, a fluorogenic substrate assay was used to measure levels of thrombin. Thrombin generation was significantly elevated in the presence of MSC compared to platelet poor plasma and MSC + heparin controls (**Figure 4.5**).

4.2.3 MSC augment thrombus build-up under flow conditions

The capacity of innate procoagulant activity observed in MSC to influence platelet thrombus deposition on collagen at arterial shear rates [208] was also assessed by an *in vitro* flow system designed to model the initiation of arterial thrombosis in response to endothelial damage. In comparison to whole blood only the presence of MSC significantly increased thrombus deposition on collagen. Importantly, it was also observed that when heparin an antithrombin agent was added along with MSC, thrombus deposition was reduced to similar levels as seen with unheparinized whole blood controls (**Figure 4.6 A, B**). An equivalent augmentation in thrombus coverage was observed in human blood supplemented with human MSC, which was also abrogated by heparin (**Figure 4.6 C**).

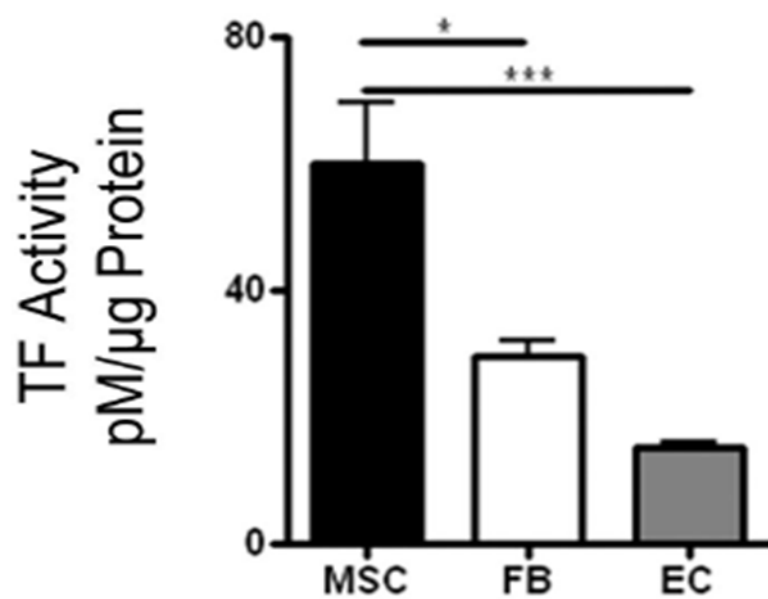


Figure 4.4 MSCs express active TF

Quantification of TF activity of MSC, FB and EC cells lysates as assessed using a chromogenic substrate (ACTICHROME®). MSC TF activity is significantly higher when compared to both FB and EC (n=3) (*:p<0.05, *** p<0.001)

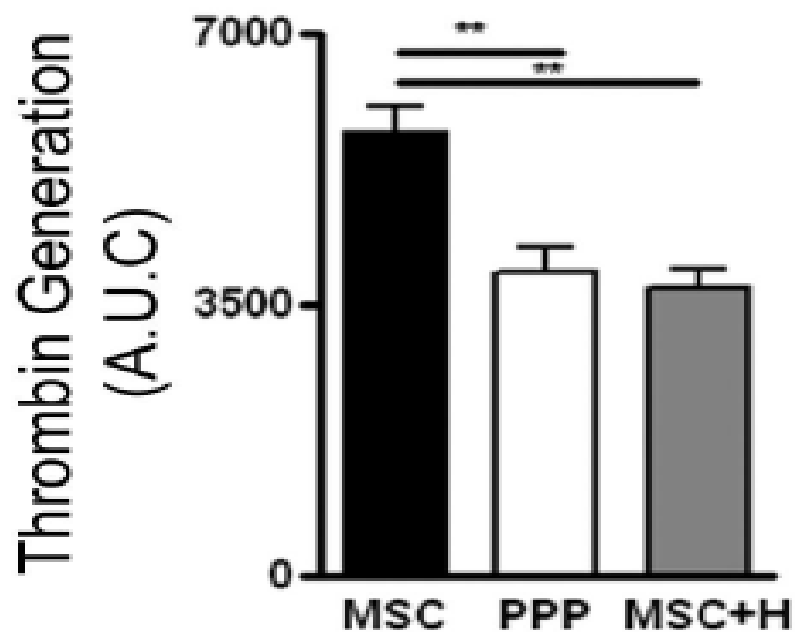


Figure 4.5 MSC are capable of inducing thrombin generation in vitro

Thrombin generation was measured at 37°C in platelet poor plasma alone or supplemented with MSC in the presence or absence of heparin by use of the Techonothrombin® TGA assay. Area under curve (AUC) refers to the amount of thrombin generated over time. MSC potential for thrombin generation was abrogated by the addition of heparin (n=3)(**: p<0.01)

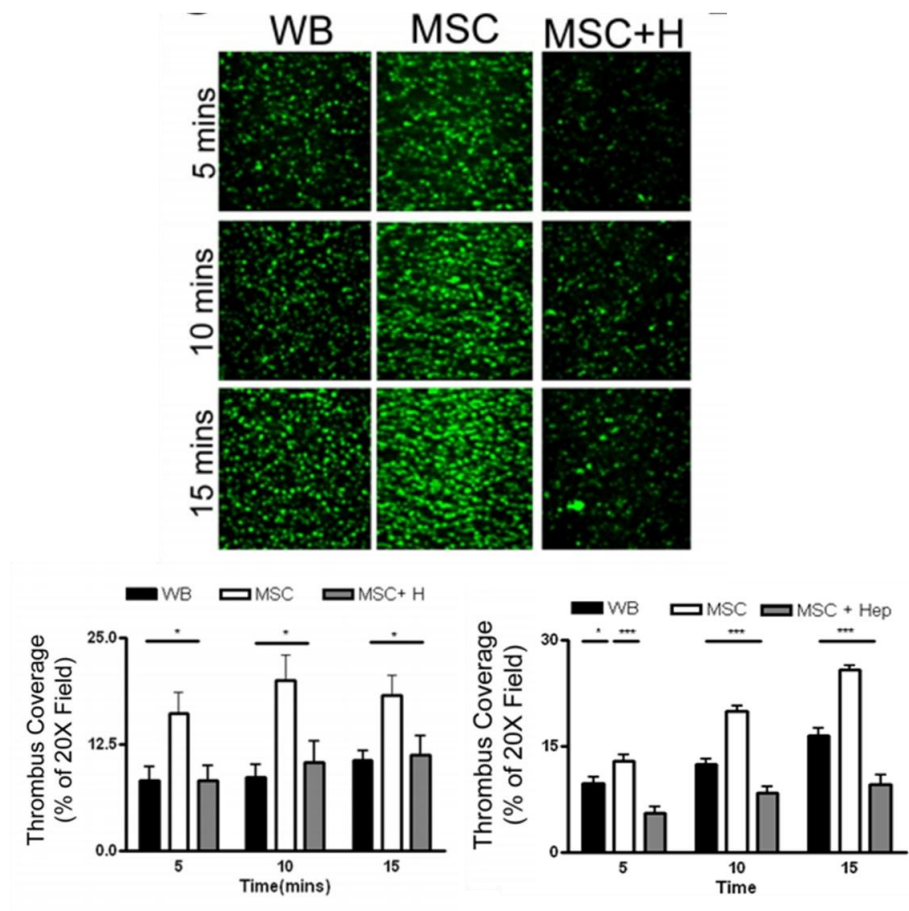


Figure 4.6 MSC potentiate thrombus build-up on collagen during ex-vivo flow at arterial shear

A. Whole blood labelled with mepacrine (Green) was perfused at a shear stress of 10 dyn/cm² over collagen in absence or presence of MSC and heparin. Representative images of thrombus deposition (x20 magnification) B, Quantification of thrombus coverage using pig MSC and pig blood C. Quantification of thrombus coverage using human MSC and human blood shows significant enhancement of thrombus coverage in the presence of MSC, which was inhibited by 25 U/ml heparin (n=3) (*p<.0.05, **: p<0.01, *** p<0.001,)

4.3 Discussion

A possible candidate protein that is known to cause reductions in coronary flow associated with microvascular obstruction is the prothrombotic protein TF [209, 210]. Due to our *in vivo* observations (**Figure 3.8**) that MSC delivery was causing a reduction in coronary blood flow it was reasonable to speculate the MSC could be expressing TF. Since our identification of the expression of TF by MSC, other groups have also identified the same phenomenon. Stephenne *et al* demonstrated that cells of mesenchymal lineages such as BM-MSC, hepatocytes, fibroblast, myofibroblasts and adult liver derived mesenchymal progenitor cells (ALPCs) all have pronounced procoagulant activity (PCA) [211]. Clotting time of whole blood with the addition of BM-MSC, hepatocytes, fibroblast, myofibroblasts and ALPCs as analysed by Rotational thromboelastometry (ROTEM), was decreased by up to 90% when compared to the control cell bone marrow- hematopoietic stem cell BM-HSCs. This PCA was associated with TF expression and similar to our data only negligible amounts of TF were associated with ECs. ECs for the most part do not express TF as EC within the vasculature are in constant contact with blood and therefore require high degree anticoagulant activity [212]. Following the evaluation of this PCA Stephenne and co-authors determined whether this activity could be modulated. Supplementary data suggested that heparin was capable of abrogating the PCA of BM-MSC and fibroblasts however both heparin and bivaluridin were required to completely abrogate PCA of hALPCs [211]. This study highlighted also that the source of MSC isolation appeared to have an effect on the cells PCA. MSC isolated from different sources had varying expression levels of TF and this suggests that TF may be responsible for diverse biological functions depending on the MSC niche.

TFs involvement in thrombus build up under flow conditions is associated with the initial interactions between von willebrand factor (VWF) and collagen (**Figure 4.7**). High shear exposes binding sites for platelet GPIb α and VWF which results in loss of platelet velocity and facilitates platelet tethering and rolling on the collagen matrix[213]. Stable binding and platelet arrest is mediated through activation of GPIIbIIIa [213]. Thrombus growth is propagated through platelet/platelet interactions which are mediated by the binding of fibrinogen, fibrin and VWF to activated GPIIbIIIa and the binding of GP1b α (**Figure 4.7**). In parallel to this, TF by means of activation of extrinsic coagulation pathway is further activated by GPIIbIIIa mediated platelet aggregation via the production of thrombin [213] (**Figure 4.7**).

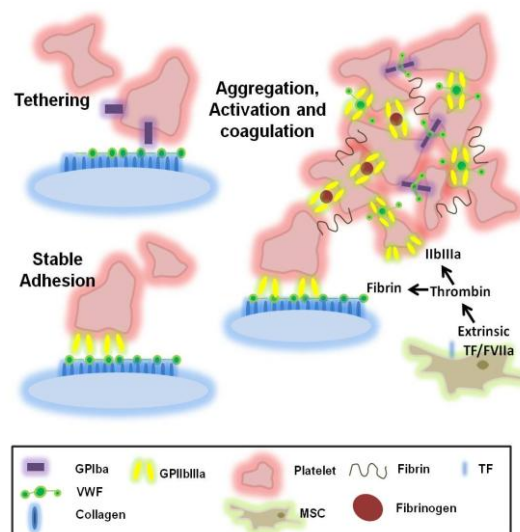


Figure 4.7 TF role in thrombus build up on collagen during ex-vivo flow at arterial shear

Collagen binds von Willebrand factor (VWF), which promotes platelet adhesion and activation through the glycoprotein Iba (GPIb α). Rolling platelets adhere and spread on the collagen matrix via the interaction of GPIIbIIIa. Thrombus aggregation and growth is caused by platelet/platelet interaction which is mediated by the binding of fibrinogen, fibrin and VWF to activated GPIIbIIIa and the binding of GP1b α . TF through the activation of the extrinsic coagulation pathway produces thrombin which further activates GPIIbIIIa propagating further thrombus formation

Recently it has been suggested that the expression of TF by MSC may be due to cell culturing and expansion [214, 215]. A study carried out by Tatsumi *et al* showed that adipose derived MSC (ADSCs) were associated with high TF expression [215]. Intravenous administration of cultured ADSC in mice lead to 85% mortality due primarily to pulmonary embolism. Interestingly however, this did not occur after infusion of uncultured adipose derived cells. Upon further analysis it was identified that uncultured ADSC did not express TF, however, both TF and expression and coagulation were increased after expansion in culture. This finding was corroborated by Moll *et al* who wanted to ascertain if human MSC are compatible with human blood [214]. Here it was illustrated that human BM-MSC of low passage displayed only weak PCA which could be increased significantly by passaging. PCA was correlated with TF expression and this was confirmed by demonstrating that the PCA effect could be abrogated by blocking the TF pathway. Due to the extensive expansion of our MSC required for our *in vivo* studies cells were expanded up to P8 and it is therefore plausible the events that we have observed are due to cell culturing. Additional studies are required to definitely determine the effect of culture on MSC in particular in relation to expression of TF. Casual factors within the culture environment that result in this increase in TF expression still need to be further explored. TF induction could be due to various *ex vivo* factors such as, biological aging, culture additives such as calf serum, passaging protocols or freeze-thawing.

The procoagulant activity of our MSC may also be caused in part, by expression of other surface molecules. Moll *et al* in addition to the expression TF also demonstrated that MSC expressed Collagen I and fibronectin [214]. Collagen I is responsible for platelet adhesion and activation and may have been a contributing

factor to the platelet thrombus formation observed in our studies. Further experiments would be required to fully elucidate these factors.

As we cannot identify MSC *in vivo* without culturing we cannot definitely say that MSC do not express TF under normal physiological conditions within the body. The ability to increase TF expression suggests that TF may in fact be responsible for some of MSCs biological functions. TF has multiple biological functions *in vivo*, in addition to it being an activator of blood coagulation it is also recognised as an important signalling receptor. TF is capable of activating signalling cascades involved in cell proliferation, cell migration and cell survival such as the mitogen-activated protein kinase and the phosphoinositide 3-kinase/AKT pathways [216]. MSC are mobilised and found within the circulation during injury [217-219]. For this to occur MSC are unlikely to express TF, however, it is conceivable that MSC, upon reaching the site of injury may up-regulate TF, which activates signalling required for various reparative biological functions.

Subsequent studies aimed to determine if TF expression could have functional consequences when delivered in a porcine model of acute MI *in vivo*. Since elevated TF levels may be associated with hypercoagulability and thrombosis [145], we hypothesized that MSC, through the expression of TF could give rise to intravascular thrombosis when administered by an intracoronary route in an *in vivo* porcine model of myocardial ischemia. Subsequent studies also aimed at identifying if by using an adjunctive therapeutic approach we could abrogate thrombotic events associated with MSC delivery thus facilitating safer cell administration.

Chapter 5

The acute effect of intracoronary delivery of TF expressing MSC in a porcine model of MI

5.1 Introduction

Identifying the presence of TF on MSC and confirming it was catalytically active and thrombogenic *in vitro* provides a biologically plausible mechanism whereby MSC may promote reductions in coronary blood flow and MVO during MSC IC delivery[220]. Based on the findings from *in vitro studies* (Section 4), we aimed to identify *in vivo* the effect of TF bearing MSC after IC delivery with specific focus on abrogating TF effects using an antithrombin strategy.

The term ‘No-reflow’ refers to the reduction in blood flow within the coronary arteries despite being supplied by an ostensibly patent artery following percutaneous revascularization of ischemic myocardium [221]. The principal cause of no-reflow is MVO which is caused by vasoconstrictions and microvascular thrombus within the microvessel bed (microvessels $\leq 200\ \mu\text{m}$ in diameter) of the myocardium [222]. No-reflow is reported to occur in approximately 5-50% [223, 224] of MI patients, depending on the study, despite successful opening of the culprit lesion. No-reflow is considered an adverse event as it is associated with poor prognostic outcomes such as increased mortality, increased risk of arrhythmias, adverse LV remodelling and increased incidence of heart failure [225]. Over the past decade, advancements in diagnostic modalities used for assessing coronary flow have been made including coronary flow reserve, contrast echo perfusion, PET and MRI are now being used in clinical practice [226]. To accurately assess if our MSC were causing a reduction in coronary flow after administration coronary flow reserve (CFR) measurements as the gold standard were utilised.

As a reduction in CFR may be a manifestation of MVO, it can also be speculated that administering exogenously additional cells which expresses TF into a post MI microcirculatory environment would further exacerbate the degree of MVO that occurs post MI. A small study in which MSC were delivered via the coronary artery in a sheep model of MI did reveal the presence of cells that were ‘consistent in size and morphology of MSC’ occluding microvessels within the infarct region [227]. Therefore, in order to assess the microscopic effect of TF bearing MSC delivery post MI extensive histological and immunohistological analysis were also performed ex-vivo 24 hours after cell delivery.

From a clinical perspective it is also important to assess if MSC are improving heart function. In order to assess heart function the following *in vivo* studies utilised multi-detector computed tomography (MDCT) analysis at 24 hours post MSC delivery.

As global functional improvements, measured by CT, may not be observable within only 24 hours of cell delivery, as evident in previous studies carried out in the CRBV [94], looking at the effects of MSC delivery at a cellular level may reveal more of the acute benefits associated with delivery of this cell. There is ever increasing evidence that improved cardiac function is associated with the reversal of cellular apoptosis linked to the secretion of paracrine factors such as VEGF, FGF-2, HGF and IGF after the delivery of MSC *in vivo* [95-97, 228]. Within our own lab, the paracrine beneficial effect of EPC condition media has been associated with the secretion of the cytokine IGF-1 [94, 229]. Delivery of a low dose IGF-1 in a porcine model of MI was associated with a significant reduction in apoptosis within the border zone at 24 hours and consequently a

significant improvement in global heart function at 2 months [94]. Based on findings from the studies carried out by the CRVB and findings from others that suggest that MSC secrete a similar array of cytokines[95-97] the following *in vivo* studies were performed to assess the acute anti-apoptotic effect of MSC post MI.

5.2 Results

5.2.1 MSC administration was associated with intramyocardial haemorrhage and reduced coronary flow reserve.

Having established that MSC exhibit robust PCA and prothombotic potential *in vitro*, the relationship between MSC delivery and microvascular flow *in vivo* was examined. Preliminary experiments identified 25×10^6 MSC as the maximum cell number that could be safely infused via a porcine coronary artery without causing arrhythmias or intramyocardial oedema. Additional heparin + saline controls are not required for the following experiments as heparin is routinely delivered via the coronary prior to cell delivery, therefore it can be assumed that additional heparin added to saline would have no additional effect of the functional outcome of the study. and Macroscopic analysis of explanted hearts 24 hours post MI and MSC administration showed significant areas of haemorrhage in the myocardium (**Figure 5.1 A, B**). In contrast, when MSC were co-administered with an anti-thrombin (heparin), hemorrhagic areas were reduced to levels equivalent to those observed with saline treatment alone (**Figure 5.1 A, B**). Measurements of CFR were obtained both pre and post IC delivery of 25×10^6 MSC post MI. MSC administration resulted in a significant reduction in CFR compared to saline alone. This reduction in flow was again improved significantly by the co-administration of heparin with MSC (**Figure 5.2**).

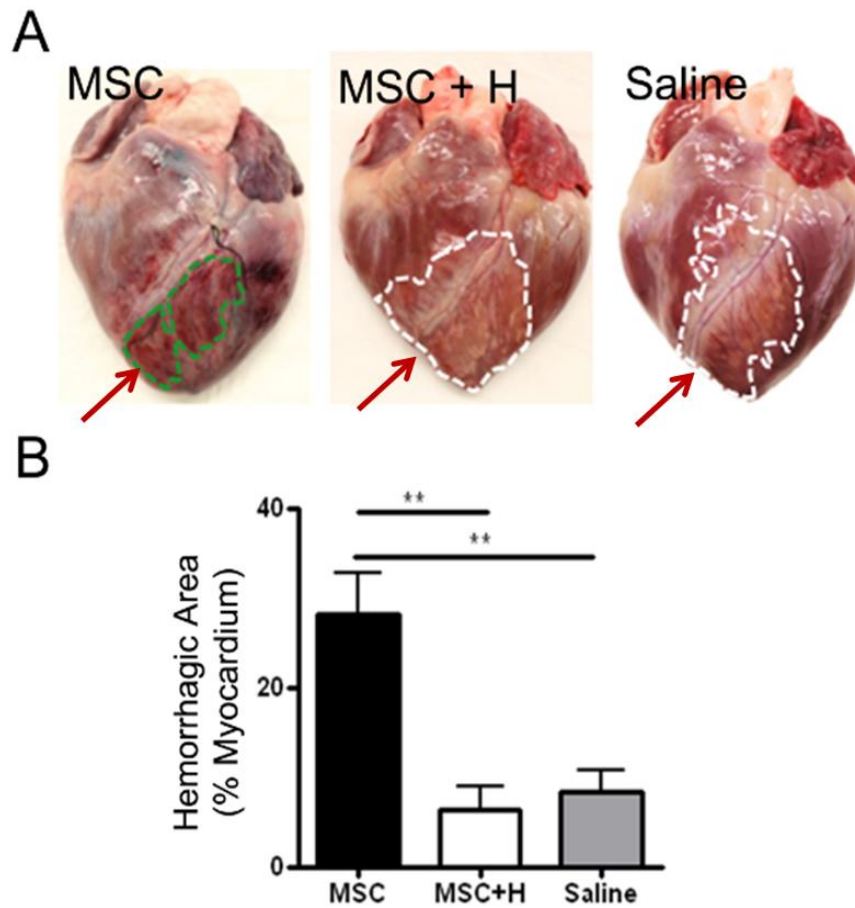


Figure 5.1 *MSC delivery increases myocardial haemorrhage at 24 hours post intracoronary administration in a porcine model of acute MI*

A. Macroscopic images of hearts post MI with infarct territory (white dashed lines) and haemorrhaged areas (green dashed lines) indicated. (n=6) **B.** Quantification of hemorrhagic areas expressed as a percentage of the myocardium are shown. Heparin co-administration with MSC significantly abrogates myocardial haemorrhage. (n=6) (**: $p < 0.01$)

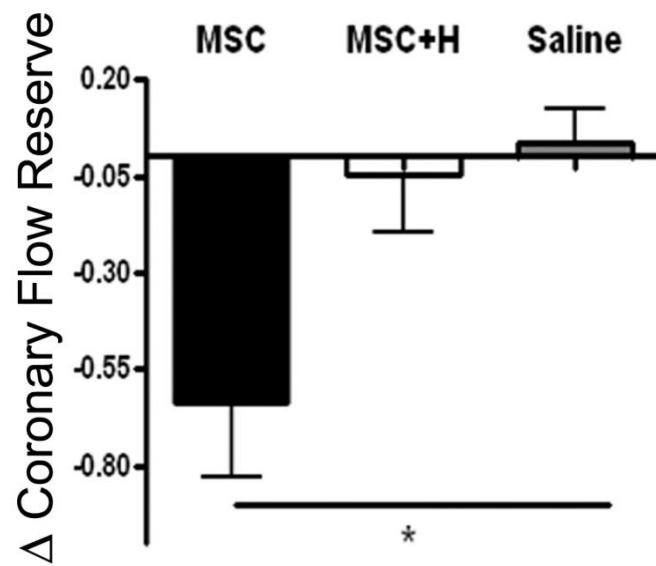


Figure 5.2. MSC delivery reduces coronary flow reserve 24 hours post intracoronary administration in a porcine model of acute MI

Quantification illustrating the changes in coronary blood flow as analysed by CFR within the LAD artery before and after the delivery of 25×10^6 MSC in the presence and absence of heparin and saline control alone. Delivery of MSC without heparin caused a significant reduction in coronary blood flow when delivered in an acute MI setting, whereas delivering MSC in the presence of heparin did not affect coronary blood flow and flow remains similar to that of when saline alone was administered. ($n \geq 8$) (*: $p < 0.05$)

5.2.2 Intracoronary MSC administration was associated with *in situ* microvascular thrombosis and ameliorated by heparin co-administration

To examine the mechanism of MSC-induced reduction in CFR and whether MSC actively participated in microvascular thrombosis, histological evaluation of the microvasculature in the infarcted myocardium was carried out. Occluded microvessels were visualised by Masson Trichrome staining (**Figure 5.3 A**). Quantification of the number of occluded vessels (normalised to total vessel number) revealed a significant increase in the number of occluded microvessels (≤ 200 μm diameter) in the MSC treated group when compared to both the MSC + Heparin and saline treated group (**Figure 5.3 B**). To further elucidate the participation of TF positive MSC in microvascular thrombosis (MVT) multicolour confocal microscopy was utilized to co-localize DiI-labelled MSC with TF, von Willebrand factor and platelet antigen-positive in areas of microvascular thrombosis. Immunofluorescence imaging within the infarct regions showed co-localization of fluorescent DiI signal (red-used to track delivered MSC) with the platelet antigen CD61, indicating the presence of MSC in platelet rich thrombus. Moreover, VWF and TF, implicated in situ arterial thrombosis, co-localized with labelled MSC in regions of microvascular obstruction suggesting TF rich MSC were also likely implicated in de novo thrombosis generation *in vivo* (**Figure 5.4**).

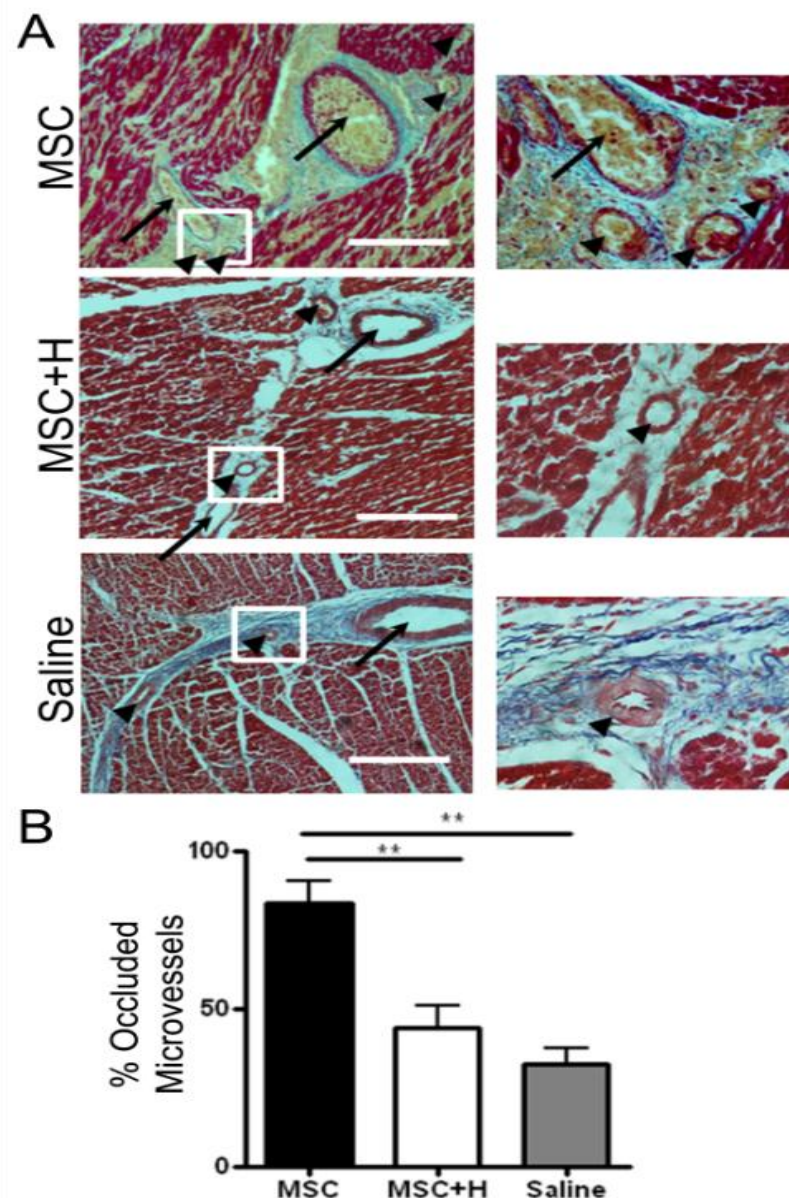


Figure 5.3 MSC promote microvascular thrombus formation in vivo post MI

A. Representative images of infarct zone stained with trichrome reveal occluded, thrombus filled microvessels (black arrows) 24 hours post MSC delivery. White inset shows occluded microvessels at high magnification. **B.** Quantification of occluded microvessels in the infarct zone expressed as a percentage of the total microvessels evaluated per HPF showing a significant reduction in the percentage of in microvessel occlusion associated with heparin co-administration with MSC or control saline treatment. Scale bars represent 200 μ m. (~750 microvessels ranging from 20-200 μ m analysed.) (*:p<0.05, **:p<0.01) (n \geq 5)

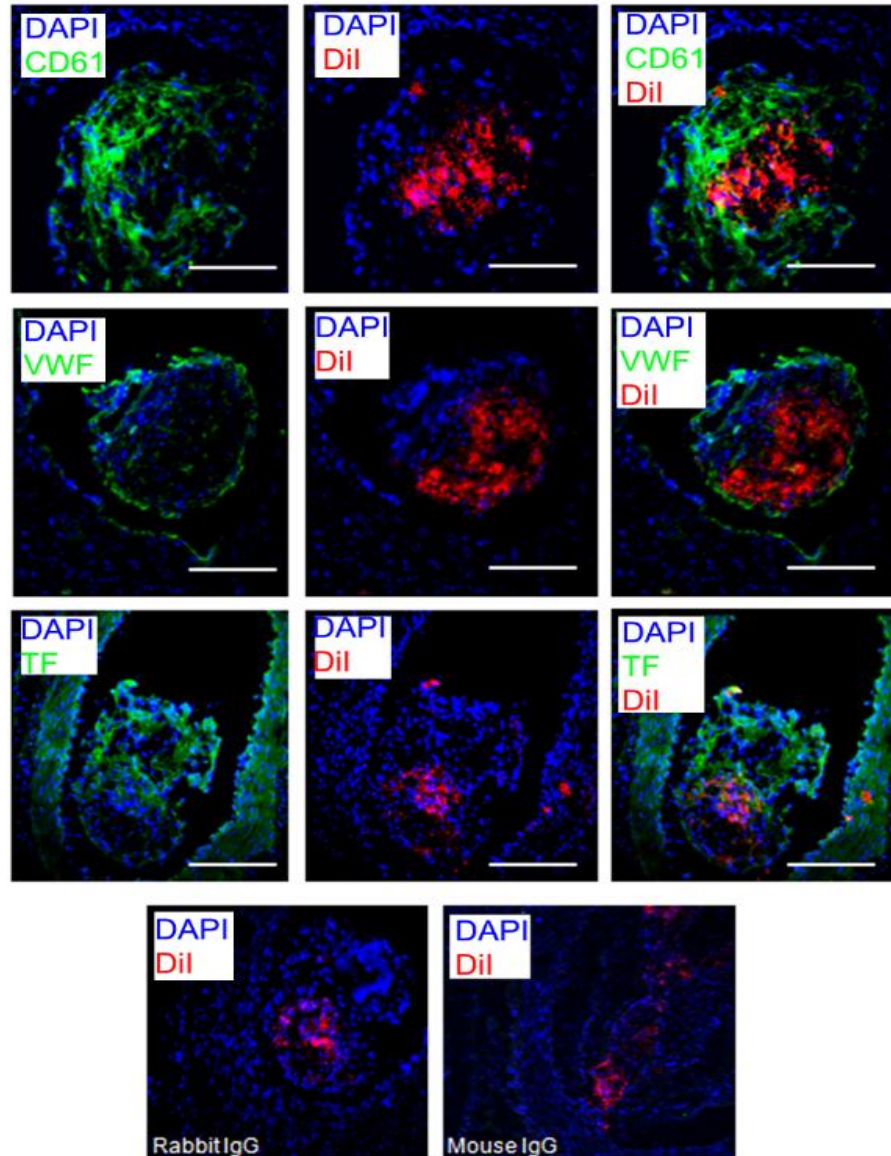


Figure 5.4 MSC are associated with in situ microvascular thrombosis post MI
Representative immunofluorescent images of MSC related microvessel thrombus formation *in vivo* shows co-localization of MSC (red) with the platelet marker CD61 (Green), the initiator of arterial thrombosis VWF (green) and TF (green). Nuclei counterstained on each image with DAPI (blue). IgG control images for rabbit and mouse primary antibodies used are also shown. Scale bars represent 200µm

5.2.2.1 Heparin enhanced MSC delivery to the infarct territory and decreased apoptosis

Since heparin co-administration with MSC ameliorated associated side effects including CFR reduction, microvascular obstruction and thrombosis, the effect of heparin on improving MSC delivery efficiency was determined. 24 hours after MSC delivery, the percentage of DiI positive cells within the border zone was quantified. The percentage of MSC (over total nucleated cells) within the infarct border zone (BZ) was significantly increased with the addition of heparin (**Figure 5.5 A, B**). The cytoprotective efficacy of MSC administration with respect to cardiomyocyte apoptosis within the BZ, was assessed by TUNEL staining. Apoptotic signal was significantly decreased with MSC treatment compared to saline and there was no significant difference between the two MSC groups with or without heparin co-administration signifying that heparin administration had no adverse effect on MSC therapeutic outcome (**Figure 5.5 C, D**).

5.2.3 MSC delivery has no effect on acute infarct size or on acute hemodynamic function

MSC delivery in the presence or absence of heparin did not have an effect on acute infarct size as analysed by TTC and CT when compared to saline controls 24 hours after cell administration (**Figure 5.6 A, B, C, D**). In addition MSC also had no effect on the cardiac function parameters analysed by CT at 24 hours post cell administration. Functional parameters analysed included End-Systolic Volume (ESV), End-Diastolic Volume (EDV), Ejection Fraction (EF), Cardiac Output (CO) or Stroke Volume (SV).(**Figure 5.7 A-E**)

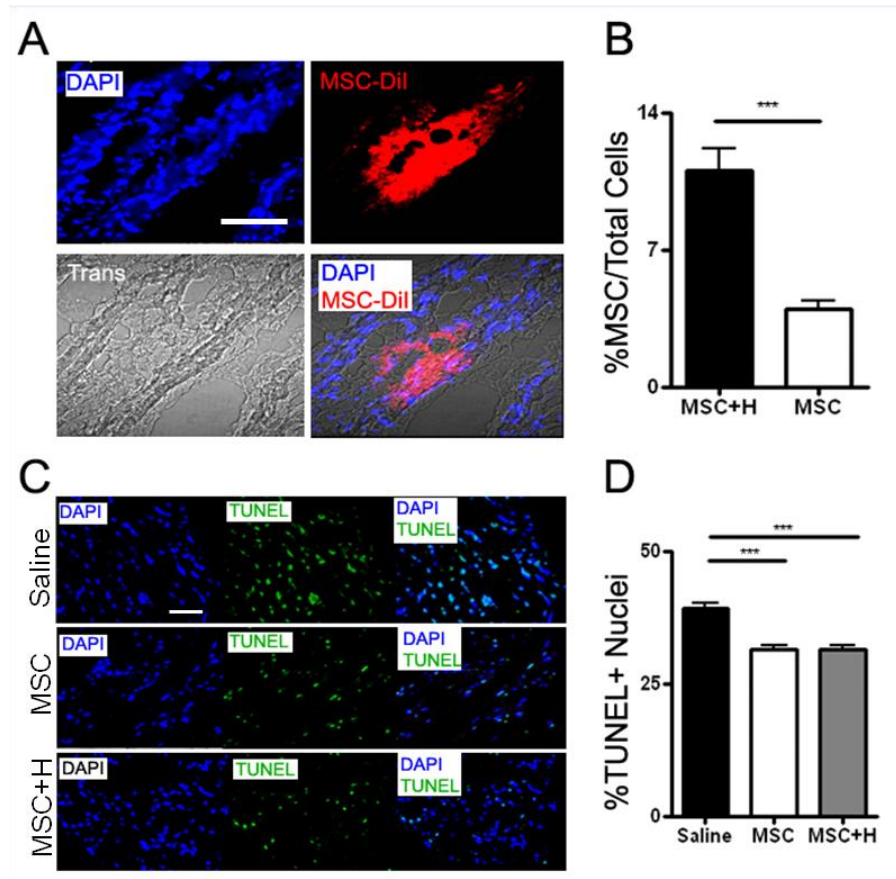


Figure 5.5 Heparin increases MSC infiltration in infarct border zone and decreases apoptosis post MI

A. Representative image of DiI (Red) stained MSC in infarct border zone (IBZ). Nuclei counterstained on each image with DAPI (Blue), translucent light microscope image (trans) within cardiac muscle. **B.** Quantification of MSC infiltration 24 hours post MSC delivery, heparin significantly increased the number of MSC within the border zone compared to MSC treatment alone. **C.** Representative images of TUNEL staining of IBZ sections from saline- and MSC-treated animals. Nuclei were stained in blue with DAPI. Apoptotic cells are TUNEL positive (Green). **D.** Quantification of apoptotic cells in the IBZ by determining the percentage of apoptotic cells. MSC lowered IBZ apoptosis compared to saline controls and this was unchanged by heparin (DAPI and TUNEL positive) of total cells (DAPI positive). Approximately 25,000 nuclei were counted (n=6) Scale bars represent 100µm

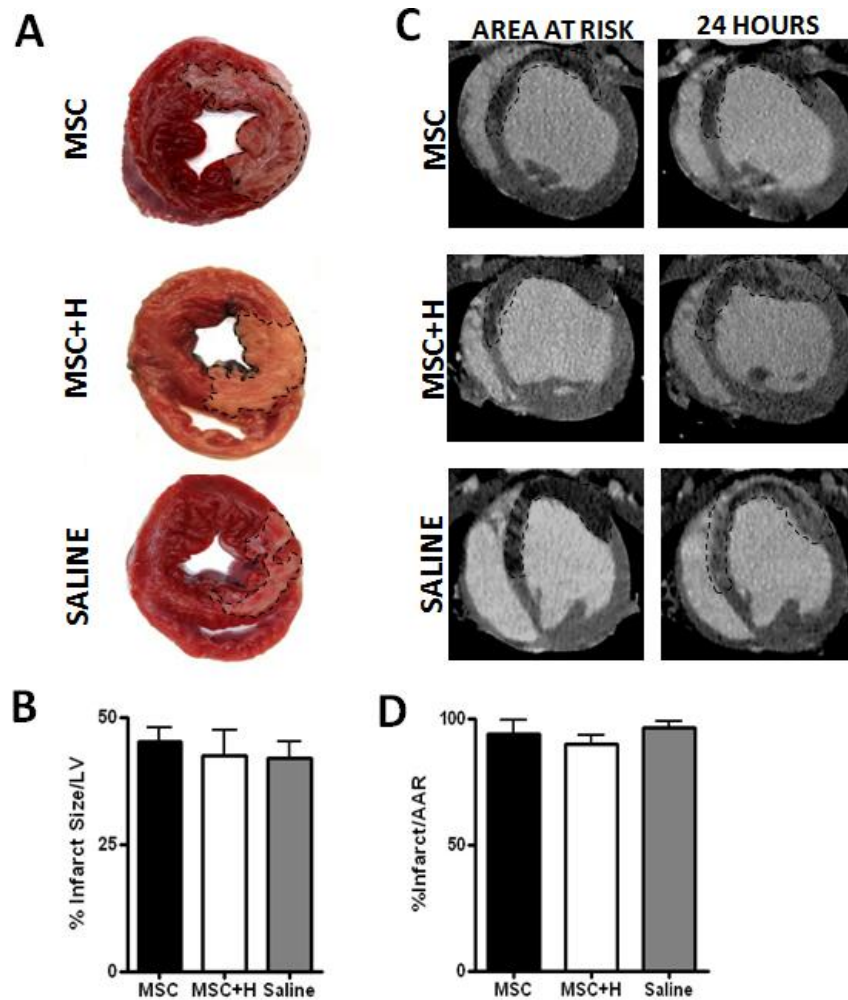


Figure 5.6 Acutely MSC delivery has no impact on acute infarct size post MI
A. Macroscopic images of triphenyltetrazoliumchloride-stained transverse heart sections from saline-treated and MSC treated pigs. Broken lines delineate the area of infarction. **B.** Quantification of the percentage of infarct area relative to LV. **C.** Representative CT images of infarcted regions 24 hours post MSC delivery. Arrowheads indicated the regions of infarct. **D.** Quantification of the percentage of infarct area relative to area at risk assessed by CT. ($n \geq 6$)

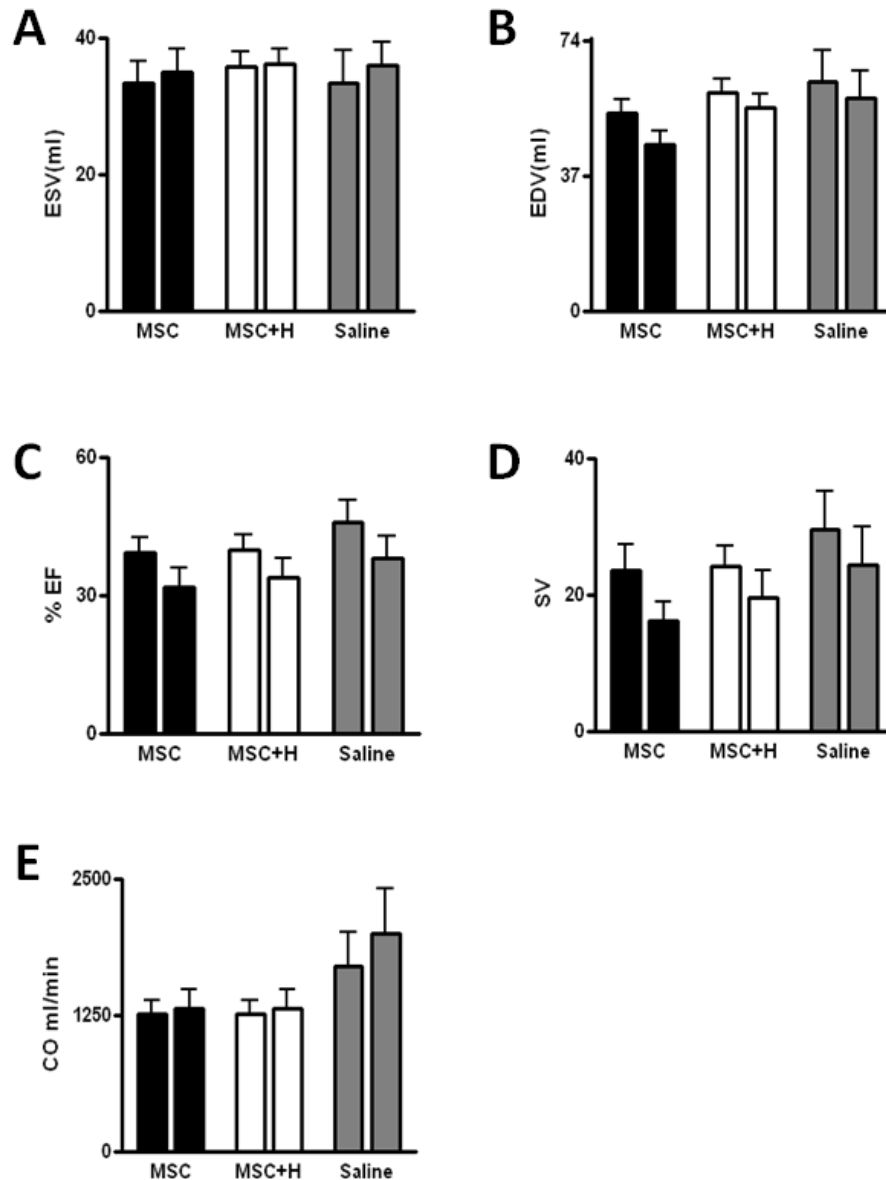


Figure 5.7 Acutely MSC delivery has no impact on cardiac function post MI

MSC delivery had no effect on acute cardiac functional parameters as analysed by CT 24 hours after cell delivery. Parameters assessed included **A.** End diastolic volume (EDV), **B.** End systolic volume (ESV), **C.** ejection fraction (EF), **D.** stroke volume (SV) or **E.** cardiac output (CO) at 24 hours as analyzed by CT. Left columns show heart function at baseline and right at 24 hours post MSC therapy. (n≥6)

5.3 Discussion

The work in the current section characterizes the TF-dependent prothrombotic activity innate to MSC in the context of *in vivo* arterial thrombosis. Here we demonstrate that TF-mediated *in situ* thrombosis is most likely responsible for MSC induced microvascular obstruction in the setting of MSC therapy post MI. Moreover, we show that co-administration of an anti-thrombin agent significantly ameliorates these adverse events associated with MSC delivery providing a viable and safe means of MSC-based cell therapy *via* the intracoronary route.

5.3.1 Mechanisms of Tissue Factor induced adverse events post MSC delivery

Emerging studies of MSC from other sources and species demonstrate varying levels of expression of TF by MSC and allude to the procoagulant nature of MSC [211, 214, 230]. Cellular TF is known to be expressed in three forms, as surface, encrypted and as an intracellular protein [231, 232]. TF containing microparticles are also known to be released from cells [233]. Therefore it is conceivable that delivered MSC may potentially disseminate procoagulant activity through not only cellular TF but through the release of coagulant TF positive microparticles. [143] Within the vasculature TF may trigger *in situ* microvascular thrombosis through platelet activation and aggregation. Platelets express PAR-1 and PAR-4 receptors and thrombin activation of either is sufficient to initiate aggregation. In addition to PAR activation, VWF through its interaction with platelets plays an integral part in the initiation of arterial thrombus formation [234]. Our experiments have provided the first demonstration of the co-localisation of VWF with platelets and TF on MSC within a thrombus post IC MSC delivery.

TF also plays a role in driving the coagulation-inflammation cycle in which thrombin generation, also via PAR-1 and PAR-4 lead to G protein and NF- κ B mediated expression of P-selectin, E-selectin, VCAM1 and ICAM1. Induction of these adhesion molecules enhances leukocyte migration and activation within the infarcted region [235]. Also indirectly, TF, through the production of fibrin increase local proinflammatory activation of endothelial cells and increases their expression of adhesion molecules.[236-238]. Fibrin degradation also acts as a chemoattractant for neutrophils which release proteolytic enzymes and oxygen free radicals which further exacerbate myocardial injury after MI [239]. Soluble murine TF (sTF1-219) has also been shown to increase IL-6 secretion which is accompanied by fibrin overproduction and platelet aggregation. TF driving the coagulation-inflammation circuit induces further cardiovascular complication including arrhythmias [240] and hypertension [241]. Evidence also suggests that cardiac exposure to exogenous TF can lead to pump dysfunction through the induction of cardiac hypertrophy [242]. Co-culturing of MSC with activated lymphocytes increases MSC prothrombotic properties by increasing surface expression of TF [214]. Although this has not been confirmed *in vivo* it can be speculated that delivering MSC into an infarcted area where MSC are likely to encounter activated lymphocytes may further increase the adverse thrombotic effect of MSC.

Activation of PAR-1 via thrombin can also contribute to microvascular flow reductions giving rise to local vasoconstriction [243]. Other than coagulation TF plays a role in other cellular processes such as cell migration and proliferation and thus it is conceivable that TF may also contribute to some of the beneficial paracrine effects seen following MSC administration [244]. A study investigating

the effect of TF on cardiomyocyte proliferation and growth demonstrated that when rat H9c2 cardiomyocytes were exposed to increasing concentrations of recombinant TF there was a significant effect on cell proliferation and apoptosis [242]. Lower concentrations of TF increased cell proliferation but intermediate concentrations only induced proliferation after short term exposure and caused apoptosis on prolonged exposure. The highest dose of TF induced H9c2 cardiomyocytes apoptosis as measured by both capase-3 activity and p53 nuclear localisation [242]. This study supports the hypothesis that TF may be beneficial to cardiac repair in smaller doses but may be detrimental in higher doses and provides insight into our study, in that although we were increasing the number of MSC within the myocardium there was no additional benefit with regard decreases in apoptosis. It may be also possible that the prothrombotic nature of MSC is required for some of MSC paracrine effect observed *in vivo*, for example, when MSC come in contact with activated platelets they secrete fibrinolytic enzymes and display ECM remodelling activity [245].

5.3.2 Heparin effect on MSC procoagulative activity

Whether heparin interacts directly and functionally with TF remains controversial, but its anti-coagulant activity is considered predominantly to involve allosteric modification of anti-thrombin III which in turn binds to and inactivates thrombin[246]. Accordingly, unfractionated heparin has been the standard of adjunctive antithrombin therapy during PCI for more than three decades [247] and is used to counteract acute thrombogenicity arising from mechanical plaque disruption along with ongoing thromboembolic events that may be potentiated by either guide wire or device placement in the artery [248]. The introduction of prothrombotic cells, such as TF-expressing MSC, into in ischemic zone, may thus

potentially aggravate an already unstable environment during PCI which is frequently complicated by no reflow following device deployment alone. Adjunctive unfractionated heparin therapy during MSC co-administration was chosen here because this strategy fits with existing clinical practice and anti-thrombin targeting heparin includes a broad range of binding partners such as ATIII, Factor X as well as thrombin itself [247]. Our data confirms that such an approach successfully counteracts all prothrombotic and procoagulant activities caused by intracoronary transferred MSC in the setting of acute MI.

In other cardiac cell therapy investigations, heparin has been thought to influence the engraftment of bone marrow derived mononuclear cell populations through disruption of the SDF-1/CXCR4 ligand/receptor axis in mice [249]. These investigators and others [211] have suggested the use of the direct thrombin inhibitor bivalirudin to obviate any concerns on heparin's impact on stem cell mobilization or delivery in cardiac repair. In contrast to this however, recent findings published by members of the same group illustrated that heparin dose-dependently increased HGF levels which they suggest subsequently dose-dependently increased the mobilisation of a subset of mesenchymal cell known as cMABS or circulating mesoangioblasts [250]. Further studies will be needed to test this later hypothesis with a broader spectrum of antithrombotic agents including direct thrombin inhibitors, anti-coagulants and novel platelet inhibitors on the prothrombotic activity of MSC post intracoronary administration. Indeed, in trials assessing antithrombotic agents for protection against post-PCI microvascular dysfunction, bivalirudin and the GPIIb/IIIa antagonist eptifibatide were shown to synergistically improve coronary flow reserve and myocardial perfusion [251]. When cancer cell lines (pancreatic cell line BxPC-3, MDA-MB-

231 breast cancer cell line, LoVo colocalcarinoma cell line, SKOV-3 ovarian cancer cell line, malignant melanoma cell line) are cultured with heparin it has been shown that heparin down regulates TF through regulation of NF- κ B [252]. Pre-treatment or culturing of MSC with heparin with adjunctive bolus treatment may thus be an additional option to reduce potential adverse procoagulant activity associated with cultured MSC. Another agent that may be applicable to prevent TF related adverse event which is already being used in cardiovascular medicine is amiodarone. Breitenstein *et al* hypothesised that the beneficial effect attributed to amiodarone may not be solely due to their electrophysical properties but also to other mechanisms such as prevention of thrombus formation. To test this theory Breitenstein investigated whether amiodarone effects TF expression and found that amiodarone showed downregulation of both TF surface expression and TF activity on vascular cells [253]. Co-administering MSC with amiodarone could circumvent the bleeding risks with other anti coagulants and should be explored in future experiments.

5.3.3 Tissue Factor induced Microvascular Obstruction

In human subjects, the presence of microvascular obstruction detected within the infarct zone by MRI is associated with more severe infarctions, impaired LV remodelling and less downstream functional recovery compared to those without [254, 255] Recently, a reduction in flow (as assessed by angiographic Thrombolytics In Myocardial Infarction (TIMI) grading) was detected after intracoronary cell delivery of a mesenchymal precursor Stro3+ cell isolate and it was suggested that a reduction in flow was associated solely with high cell numbers [256]. Our hypothesis that TF associated with MSC may be responsible for CFR reduction *in vivo* is supported by other studies in which IC injection of

recombinant TF leads to vasoconstriction and flow impairment providing a causal mechanistic relationship between TF antigen presentation and the reduction in CFR associated with MSC delivery[209]. In our experiments we determined the contribution of delivered MSC to microvascular thrombosis within the infarct territory using confocal microscopic analysis. Here we showed co-localization of DiI-labelled MSC and platelet-rich thrombus as well as MSC and TF coexpression within microvascular luminal thrombi providing evidence of an *in vivo* association between MSC delivery, TF associated prothrombotic blood components and thrombotically occluded microvessels.

In conclusion, this *in vivo* study has identified that MSC prothrombotic activity as defined *in vitro* is associated with a loss in CFR and *in situ* MSC-derived microvascular thrombosis when MSC are administered into the porcine coronary circulation post MI. Co-administration of heparin successfully ameliorates all of these side effects of MSC delivery. These findings highlight that the management of possible prothrombotic side effects of MSC should be a significant consideration during future investigative and clinical trials of MSC administration especially via the intracoronary route.

Chapter 6

Long term cardiac functional benefit of MSC when delivered in the presence of heparin

6.1 Introduction

Ischemia triggers a cascade of cellular and biochemical processes that drive functional and structural changes to the myocardium known as remodelling [28]. The compensatory ‘reparative’ processes that occur in response to MI include, scar formation, infarct expansion, ventricular dilatation, fibrosis and myocyte hypertrophy of the non-infarcted myocardium [257]. Alterations to left ventricle chamber architecture is characteristic of ventricular remodelling and result in changes to ventricle shape from the normal elliptical shape to a more spherical shape (**Figure 1.4**) [258]. These alterations result in enlargement of the heart and increased LV chamber dimensions which subsequently lead to functional deterioration of the myocardium, decreasing the hearts ability to pump adequately and ending in HF. The extent of remodelling that occurs correlates closely with the degree of initial myocardial damage and is consistently associated with poorer outcomes [258].

For any therapy to be translatable to a clinical scenario there must be observable long term health benefits. Pre-clinically MSC have demonstrated the potential to facilitate long term cardiac repair and regeneration [259]. The main aim of these experiments however, was to evaluate the long term benefits of MSC therapy and in particular to illustrate that delivering MSC in the presence of heparin had no adverse effect on the therapeutic outcomes associated with MSC delivery with regard to functional cardiac improvements. In order to do this, parameters of LV remodelling such as LVEF, EDV, ESV, wall motion, infarct size and collagen deposition were analysed 6 weeks after the delivery of 25×10^6 MSC in the presence of heparin in a porcine model of acute MI and compared to control, saline treated animals (**Figure 6.1**).

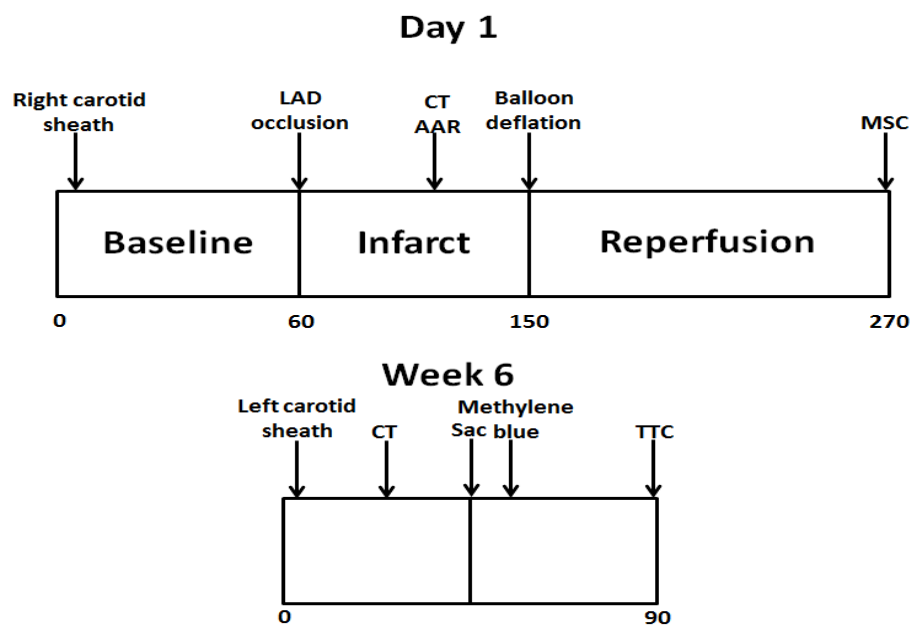


Figure 6.1 Chronic MI model

At 6 weeks post initial procedure animals underwent a similar procedure to that of the acute study at 24 hours. CT scan was obtained in order to assess functional improvements at 6 weeks before the animal was sacrificed.

6.2 Results

6.2.1 Chronic effect of heparin assisted intracoronary MSC

delivery on chronic infarct size and global ventricular remodelling

The therapeutic efficacy of heparin-assisted intracoronary MSC delivery was assessed at 6 weeks post MI. MSC treatment significantly reduced infarct scar size in animals when compared to saline treatment alone (**Figure 6.2**). Additional parameters of chronic remodelling, including global left ventricular End-Systolic Volume (ESV), Left Ventricular End-Diastolic Volume (EDV), and left ventricular Ejection Fraction (EF) were determined by 64-slice CT. MSC delivery was associated with a ~ 20% relative improvement EF over saline treated group (**Figure 6.3**). MSC therapy significantly decreased EDV and ESV compared to saline treatment providing further evidence for sustained beneficial effects on LV remodelling after MI. (**Figure 6.4**)

6.2.2 MSC delivery in the presence of heparin improved cardiac wall motion at 6 week s.

Using General Electric (GE) CT CardioIQ software infarct wall motion was determined at 6 weeks post infarct in the MSC and the saline treated animals. The infarct territory was used for quantitative analysis. At 6 weeks post MI, there was a significant increase in infarct-related wall motion in the MSC group versus saline control group (**Figure 6.5**).

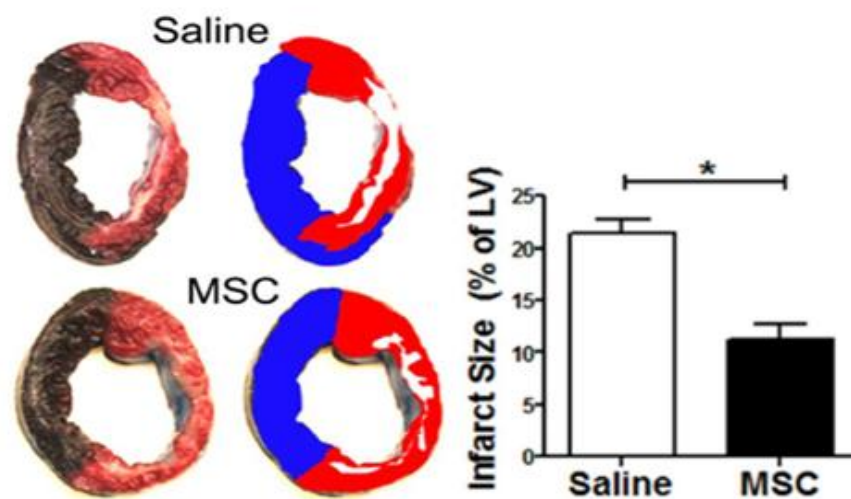


Figure 6.2 MSC therapy reduces infarct size at 6 weeks post MI.

Representative macroscopic images of TTC-stained sections of hearts six weeks post MI treated with saline or MSC. Methylene blue dye exclusion was used to highlight the area at risk of infarction. The remote territory is highlighted as blue, the area at risk, red and the infarct territory is highlighted as white. B: Quantification of the infarct area represented in A. (n=6) (*p<0.05).

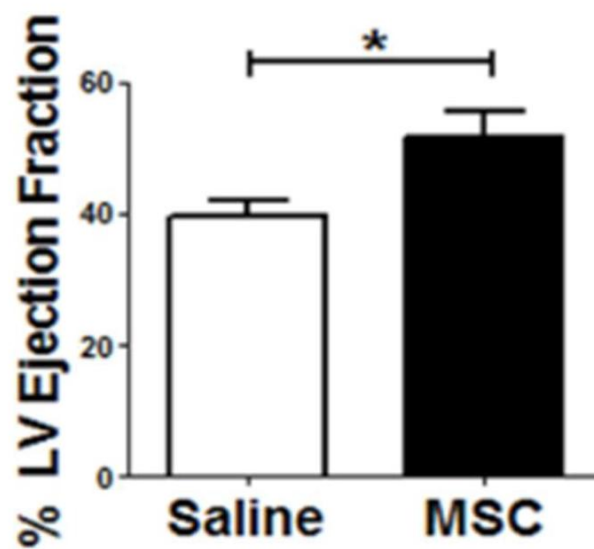


Figure 6.3 MSC therapy significantly improves Left ventricular ejection fraction at 6 weeks post MI

Evaluation of left ventricular function by CT showing that MSC delivery significantly increased the ejection fraction compared with saline treatment alone (n=6) (*p<0.05).

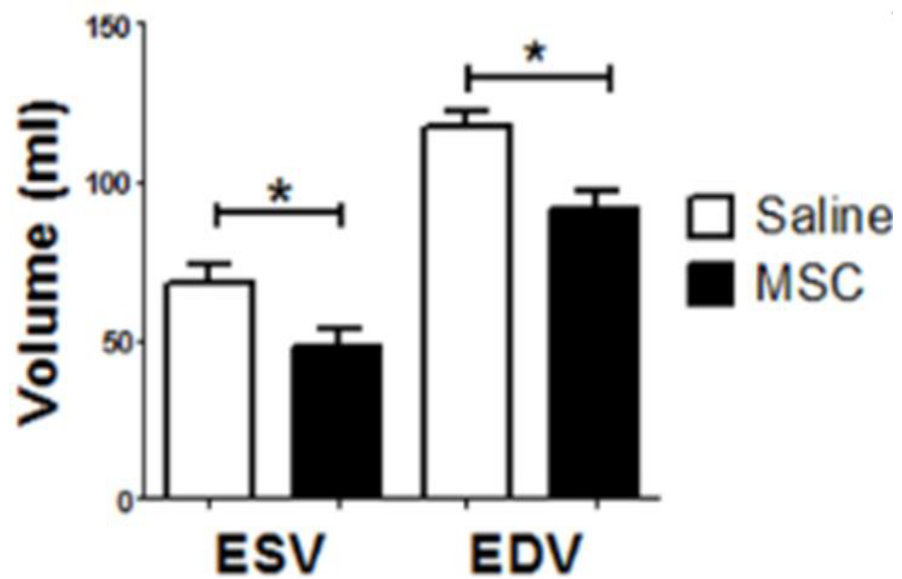
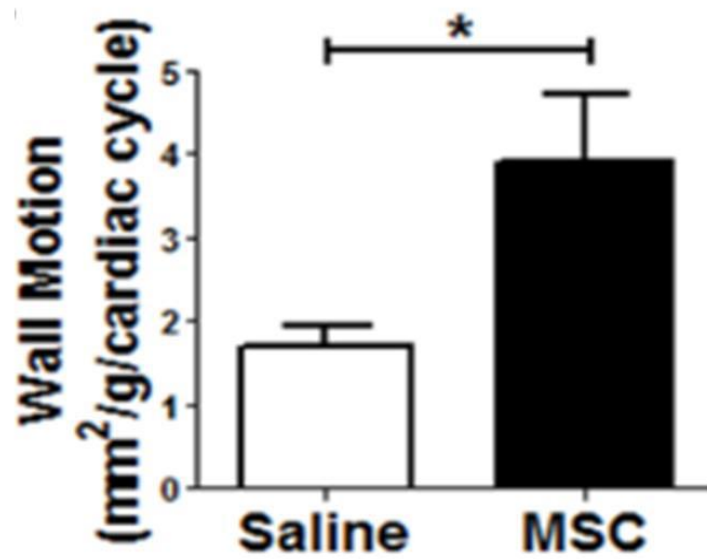


Figure 6.4 MSC therapy significantly improves left ventricular volumes at 6 weeks post MI

Evaluation of end systolic (ESV) and end diastolic volume (EDV) showing a significant reduction in both LV volumes associated with MSC delivery over saline delivery alone. (n=6) (*p<0.05).



6.5 MSC therapy significantly improves wall motion at 6 weeks post MI

MSC delivery improves in left ventricular wall motion (inmm²/g/cardiac cycle) when compared to Saline treatment alone(*:p<0.05)(n=6)

6.2.3 MSC delivery decreased infarct fibrosis

Picrosirius Red staining of the infarct related region revealed decreased collagen deposition in the MSC treated group when compared to saline treated groups. This provides supportive evidence of decreased histological scar formation at 6 weeks post MSC administration (**Figure 6.6**).

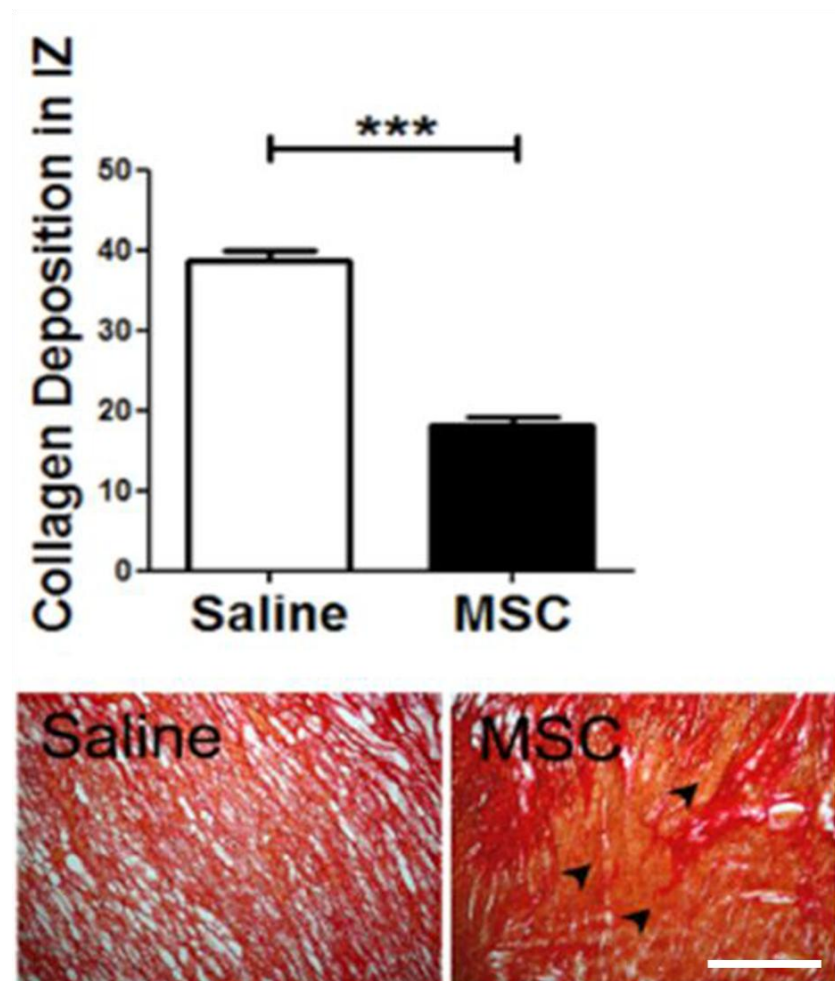


Figure 6.6 MSC delivery is associated with decreased collagen deposition at 6 weeks post MI

Representative image depicting picrosirius red staining of the infarct zone showing a significant reduction in collagen deposition in MSC-treated animals compared with saline six weeks post MI (***: $p < 0.0001$) arrowheads indicate areas of myocardial preservation evident in the MSC group. (n=6) Scale bar represents 200 μ m

6.3 Discussion

The main necessity of this study was to demonstrate the long term efficacy of heparin assisted MSC delivery. Herein it is demonstrated that MSC in the presence of heparin confers structural and functional benefits in both the regional and global myocardium at 6 week post MI.

As mentioned in the previous chapter there has been a number of issues surrounding the use of heparin during cell therapy administration. The use of heparin has been implicated in decreasing the ability of cells to home and migrate within the myocardium [260]. Heparin has been suggested to disrupt the CXCR4/SDF axis which has been demonstrated to impair the functional capacity of cells such as BM-MNC used in cardiovascular repair [249, 260]. The main paper supporting this concept was published by Seeger *et al* in 2012 [249]. Here it was demonstrated that heparin profoundly and dose dependently prevented SDF-1 induced BM-MNC migration [249]. The study revealed that if BM-MNC were pre-treated with heparin there was a significant reduction in the homing ability of injected cells in a mouse ear wound model. From these results Seeger *et al* concluded that bivalirudin should be used instead of heparin during the delivery of BM-MNC in clinical studies [249]. Due to these findings, the pre-treatment of BM-MNCs with heparin has been used to explain to the negative results obtained in the TIME trial, in which, no significant clinical benefits were observed after BM-MNC administration in patients [261]. The SWISS-AMI trial which also evaluated the effect of BM-MNC post MI also showed no statistical significance between BM-MNC treated and control treated groups in relational to functional cardiac improvements [262]. Here investigators did not use heparin during cell administration suggesting that the lack of efficacy of BM-MNC observed in the

TIME trial was not necessarily due to the pre-treatment of BM-MNCs with heparin [262]. Our MSC study provides additional evidence that heparin does not impact MSCs regenerative capability by showing delivering MSC in the presence of heparin improved functional cardiac parameters at 6 week post MI. Nevertheless, although our data speaks against a negative heparin effect on MSC, additional studies in other models may be required comparing MSC delivery in both the presence and absence of heparin to fully confirm our data. In this current study MSC delivery was associated with the preservation of left ventricular EF in treated animals. EF relates to the volume of blood that is pumped by the left ventricle during each cardiac cycle and its preservation is considered a major determinant of patient prognosis and quality of life [257]. A reduction in EF is frequently accompanied by LV dilatation, an increase in systolic and diastolic volumes and an increase in the occurrence of lethal ventricular arrhythmias [263]. As can be seen from this study and corroborated by others, EF is directly linked to infarct size. Here we report a significant reduction in infarct scar size as well as a correlative reduction in EF at 6 weeks post MSC administration. Experimentally it has been shown in large animal models that infarct scar size can be reduced as early as 3 days and sustained out to 90 days post MSC delivery [82, 264]. Hare *et al* carried out a long term allogeneic MSC study in a large animal model of MI and in agreement with findings in our study, reductions in infarct size associated with MSC delivery correlated closely with both reduction in ESV and EDV [264]. In addition, Hare demonstrated that MSC delivery not only improved LV chamber volumes but also showed that the heart architecture in MSC treated animals had a less altered configuration which was ascribed to the observable salvation in cardiac pump function [264].

MSC have been shown to be beneficial at each stage of the repair and remodelling process post MI and although the exact mechanisms by which MSC delivery exert their therapeutic benefit is not fully understood a number of possible mechanisms have been proposed (**Section 1.3**). Taking all possible mechanisms of actions related to MSC repair and regeneration into account it becomes clear that MSC do not work by acting on one repair pathway alone but multiple pathways are modulated to produce the overall repair and regeneration effect that has been observed within the MSC field. The following chapter we will begin to move away from the idea of direct cell therapy and begin to address indirect paracrine mechanisms of repair.

Chapter 7

MSC secreted paracrine factors and their role in cardiac repair

7.1 Introduction

The field of cell therapy has begun to move in new directions. As more is understood about the mechanisms of MSC benefit it is becoming more apparent that their main action may be through the secretion of paracrine factors [91] which act on other cells to elicit repair. This chapter will begin to explore some of these secreted factors implicated in the post injury repair response.

Recent data presented as an abstract [265] has identified a promising therapeutic MSC secreted factor known as SPARC-like protein 1 (SPARCL1, Hevin, SC1 and Mast9). SPARCL1 is a member of the SPARC gene family of extracellular matrix glycoproteins. Extracellular matrix proteins are primarily expressed during development, during growth, in response to injury and are found in abundance in adult cells in which there is continued turnover, such as bone [266].

SPARCL1 is thought to be involved in cell migration, is localised in high endothelial venules where it is proposed to be involved in cell adhesion and facilitate lymphocyte transendothelial migration [267]. SPARCL1 has also been implicated in modulation of extracellular matrix synthesis and assembly and the deletion of SPARCL1 in a dermal wound mouse model resulted in microscopic and macroscopic alteration to dermal collagen and decorin assembly [268]

SPARCL1 has an amino acid sequence that is approximately 50% homologous to that of SPARC and shares an identical C terminal domain, including a Ca^{2+} binding domain and a follistatin-like domain (**Figure 7.1**) [269]. SPARC regulates the production of ECM proteins and influences activity of growth factors such as PDGF, VEGF and FGF [266]. One of the main papers that prompted further research into the cardiac repair capabilities of SPARC and

SPARC like proteins was published in 2009 by Schellings *et al* [270]. This study set out to establish if SPARC played a role in infarct healing and ECM maturation after MI. This group utilised SPARC-null mice and interestingly, the SPARC-null mice exhibited a fourfold increase in mortality due to increased cardiac rupture after MI induction when compared to wild type mice. In addition, over expression of SPARC in wild type mice showed signs of improved collagen maturation and prevented cardiac wall expansion and subsequently cardiac dysfunction after MI [270].

1	MKTGLFFLCLLGTAATAIPTNARLLSDHSPKTAETVAPDNTAIPSLRAEAEENEKETAVST	60	Q14515	SPRL1_HUMAN
1	-----	0	P09486	SPRC_HUMAN
61	EDDSHHKAEKSSVLKSKEESHEQSAEQGKSSSQELGLKDQEDSDGHLVNLVYAPTEGTL	120	Q14515	SPRL1_HUMAN
1	-----	0	P09486	SPRC_HUMAN
121	DIKEDMSEFQEKKLSNTIDFLAPGVSSFTDSNQESITKREENEQEPNYSHHQLNRSSK	180	Q14515	SPRL1_HUMAN
1	-----	0	P09486	SPRC_HUMAN
181	HSQGLRDQGNQEPDNISNGEEEEKEPGEVGTNDNQERKTELPREHANSKQEDNTQS	240	Q14515	SPRL1_HUMAN
1	-----	0	P09486	SPRC_HUMAN
241	DDILEESDQPTQVSKMQEDEFDQGNQEQEDNSNAEMEEENASNVNKHQETEWQSQEGKT	300	Q14515	SPRL1_HUMAN
1	-----	0	P09486	SPRC_HUMAN
301	GLEAISNHKEITEKTVEALLMEPTDDGNITPRNHGVDDDDGDDGGDGPRLSASDD	360	Q14515	SPRL1_HUMAN
1	-----MRAWI	5	P09486	SPRC_HUMAN
	:			
361	YFIPSQAFLEAERAQSIAYHLKIEEQREKVHENE-NIGITEPGEHQEAKGAENSSNEET	419	Q14515	SPRL1_HUMAN
6	FFLLCL----AGRALAPQQEALPDETEVVEETVAEVTESVGVANFV--QV-EVGEFDDG	58	P09486	SPRC_HUMAN
	:*: . * * : : : : * * . : : . * . : . : . : :			
420	SSEGNMRVHAVDSCMSFQCKRGHICKADQGGKPHCVCDPVTCP--TKPLDQVCIDNQIT	478	Q14515	SPRL1_HUMAN
59	AEETEEVVAENPCQNHCKHGGKVCLENNITMCVCQDPTSCPAPIGEFEKVCSDNKT	118	P09486	SPRC_HUMAN
	:. * : . * * : * ..:***:***: * : . * *****:*** :***:***:			
479	YASSCHLFATKCRLEGTKKGHLQLDYFGACKSIPTCTDFEVIQFPLMRDNLKNILMQ	538	Q14515	SPRL1_HUMAN
119	FDSSCHFFATKCTLEGTKKGHLHLDYIGPKYIPCLDSELTEFPLMRDNLKNVLT	178	P09486	SPRC_HUMAN
	: ****:***** *****:***: * * * * * : *****:***: *			
539	YEANSEHAGYLNEKQRNKVKKIYLDKRLLAGDHPIDLLRDFKGNVHYVYFVHWQFSE	598	Q14515	SPRL1_HUMAN
179	YERDED--NNLITEKQKLRVKKIHENEKRLAGDHPVELLARDFEKNVYMYIFFVHWQFGQ	237	P09486	SPRC_HUMAN
	** :. : * * * : ****: **** *****:*** ****:***:*****:.			
599	LDQHPMDRVLIHSELAPLRASLVPMHCITRFFEECDPNKDKHITLKEWGHCFGIKEEDI	658	Q14515	SPRL1_HUMAN
238	LDQHPIDGYLSHTLAFRLAPLIFMEHCITRFFETCDLNDKYLALDEWAGCFGIKQKDI	297	P09486	SPRC_HUMAN
	*****: * * :***** * :***** ***** * : : : : * * . * * : : * *			
659	DENLLF 664 Q14515 SPRL1_HUMAN			
298	DKDLVI 303 P09486 SPRC_HUMAN			
	* : : : :			

Figure 7.1 SPARC and SPARCL1 homology.

SPARCL1 shares approximately 50% of its amino acid sequence with that of SPARC. This allows us to postulate similar functions to both proteins.

Prior work has established through conditioned media experiments that MSC secrete a SPARC-like protein SPARCL1 [265]. Following this discovery, in order to determine if SPARCL1 is cytoprotective, *in vitro* assays using neonatal rat cardiomyocytes exposed to hypoxic conditions were carried out. Following the addition of varying concentrations of recombinant SPARCL1 cell viability, cytotoxicity, caspase activity and gene expression were analysed [265]. SPARCL1 treatment resulted in a significant increase of cell viability and a decrease in apoptosis. These observations were confirmed by gene and protein expression which demonstrated elevated expression of anti apoptotic genes Bcl-2, and reduction of anti fibrotic genes, Col1 and Col3 [265]. SPARCL1 protein also exhibited pro-angiogenic properties by increasing tubular and capillary formation in an *in vivo* matrigel angiogenesis assay [265].

Based on this *in vitro* cytoprotective data [265] and previous published data that SPARCL1 modulates ECM [268] it was hypothesised that SPARCL1 would influence tissue regeneration, remodelling and repair post MI. SPARCL1 was also selected as a paracrine factor that may exhibit both the acute prototypical paracrine factor that may exhibit both the acute cytoprotective and chronic matrix remodelling as seen in chapters 4-6. Therefore the therapeutic effect of recombinant SPARCL1 was evaluated when delivered in a chronic model of MI. 6 weeks after the delivery of the protein cardiac functional parameter including, EDV, ESV, EF, CO and SV were examined by CT. In addition to this *in vivo* work, further analysis of MSC conditioned media was carried out in order to detect other factors secreted by MSC that may potentially augment cardiac repair and regeneration.

7.2 Results

7.2.1 MSC secrete SPARCL1

Analysis of MSC conditioned media collected at 48 hours by ELISA revealed that MSC abundantly secrete SPARCL1. Endothelial cells secreted negligible amounts of SPARCL1, similar in concentration to that of control basal media. (**Figure 7.2**)

7.2.2 SPARCL1 has no effect on cardiac functional parameters.

Delivery of 10µg of recombinant human SPARCL1 via the coronary artery in an acute porcine model of MI had no significant effect on cardiac functional parameters at 6 weeks post-delivery. Functional analysis was carried out by CT and included measurements of End Systolic Volume (ESV), End Diastolic Volume (EDV), Stroke Volume (SV), Cardiac Output (CO) and Ejection Fraction (EF). (**Figure 7.3**)

7.2.3 MSC secrete a wide array of paracrine factors.

Conditioned media analysis using RayBiotech® cytokine array assay revealed a large spectrum of cytokines secreted by both porcine MSC and human MSC. Conditioned media was collected at 48 hours and α -MEM basal media was used as a negative control. Signal intensities were determined using ImageJ software and expressed relative to positive controls provided by manufacturer (**Figure 7.4, 7.5, 7.6, 7.7 and 7.8**). Eighty different cytokines were examined of which 14 were identifiable in MSC conditioned media and are shown in Figure 7.4

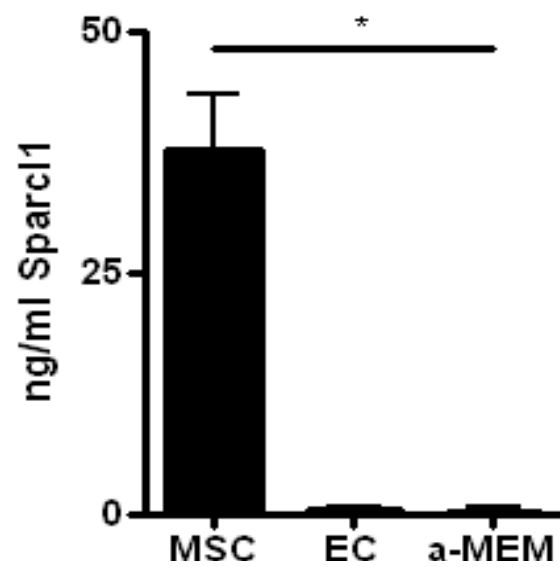


Figure 7.2 MSC expression of SPARCL1

Conditioned media from MSC and EC was collected after 48 hours in culture. MSC released significantly higher levels of SPARCL1 into media that of ECs (Control Cells). α -MEM basal media was used as a negative control. (n=3)

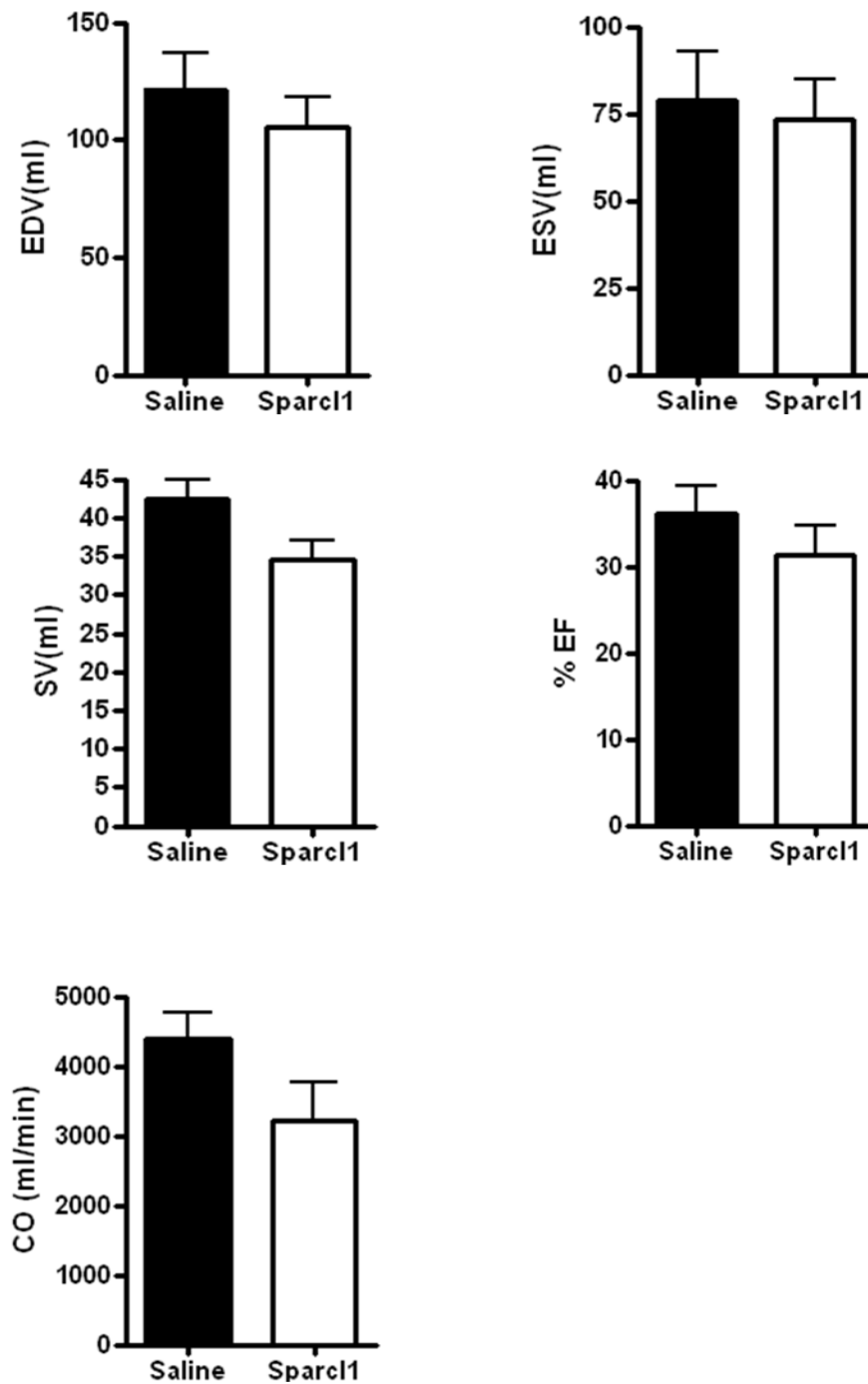


Figure 7.3 CT functional cardiac analysis 6 weeks post SPARCL1 delivery

Analysis of the effect of SPARCL1 on cardiac functional parameters was carried out 6 week post-delivery of 10 μ g of recombinant SPARCL1 by CT when compared to saline treated controls alone. No functional benefit was observed with regards EF, ESV, EDV, SV and CO. (n=4)

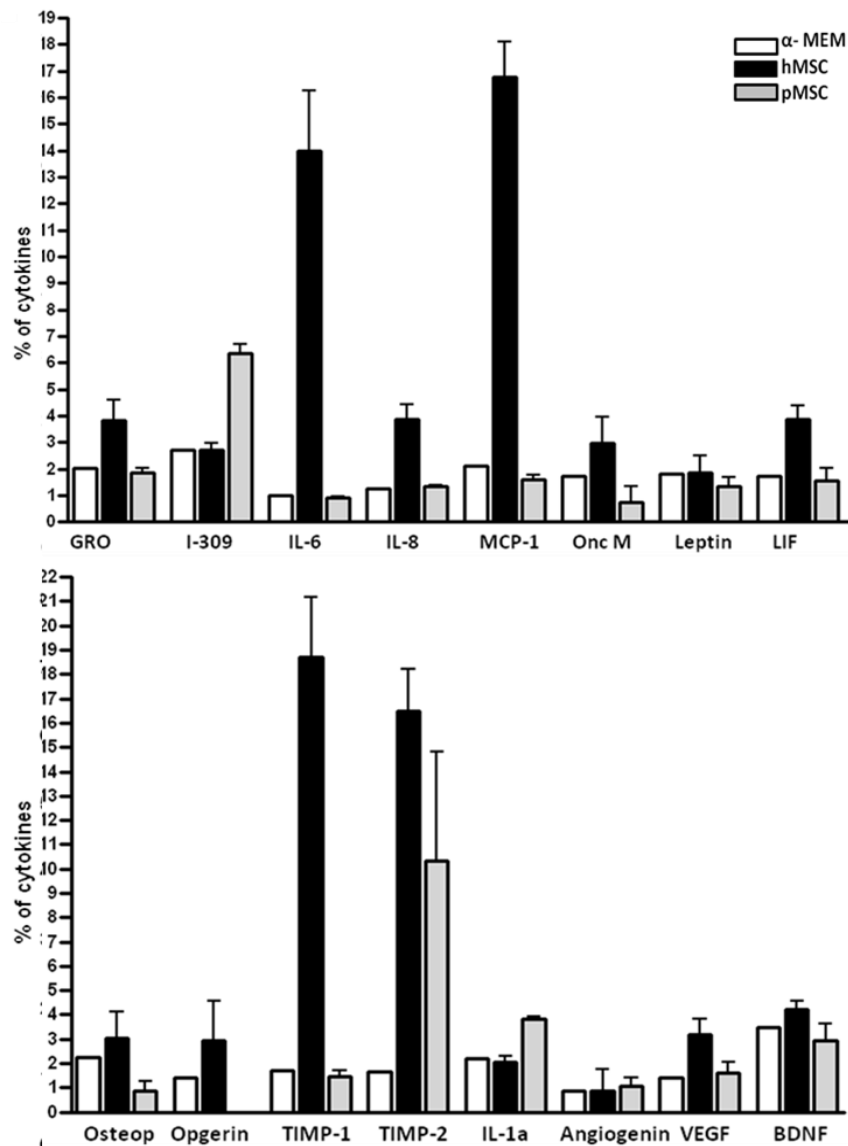


Figure 7.4. MSC cytokine analysis

Conditioned media of both porcine and human MSC. After 48 hours, conditioned media was collect from pMSC and hMSC cell cultures. MSC demonstrated a diverse secretory profile. α -MEM was used as a negative control. Cytokine and chemokine secreted included **GRO**-CXCL1, **I-309**-CCL1, **IL-6**-Interlukin 6, **IL-8**-Interlukin 8, **MCP-1**-Monocyte chemotactic protein 1, **OncM** -Oncostain M, **LIF**-Leukemia inhibitory factor, **Osteop**-Osteopontin, **Opgerin**-Osteoprotegerin, **TIMP**- Tissue Inhibitors of Metalloproteinases, **IL-1a**-Interleukin1a, **VEGF**-Vascular Endothelial Growth Factor, **BDNF**- Brain-derived Neurotrophic Factor. (n=2) All values are normalised to the provided positive control.

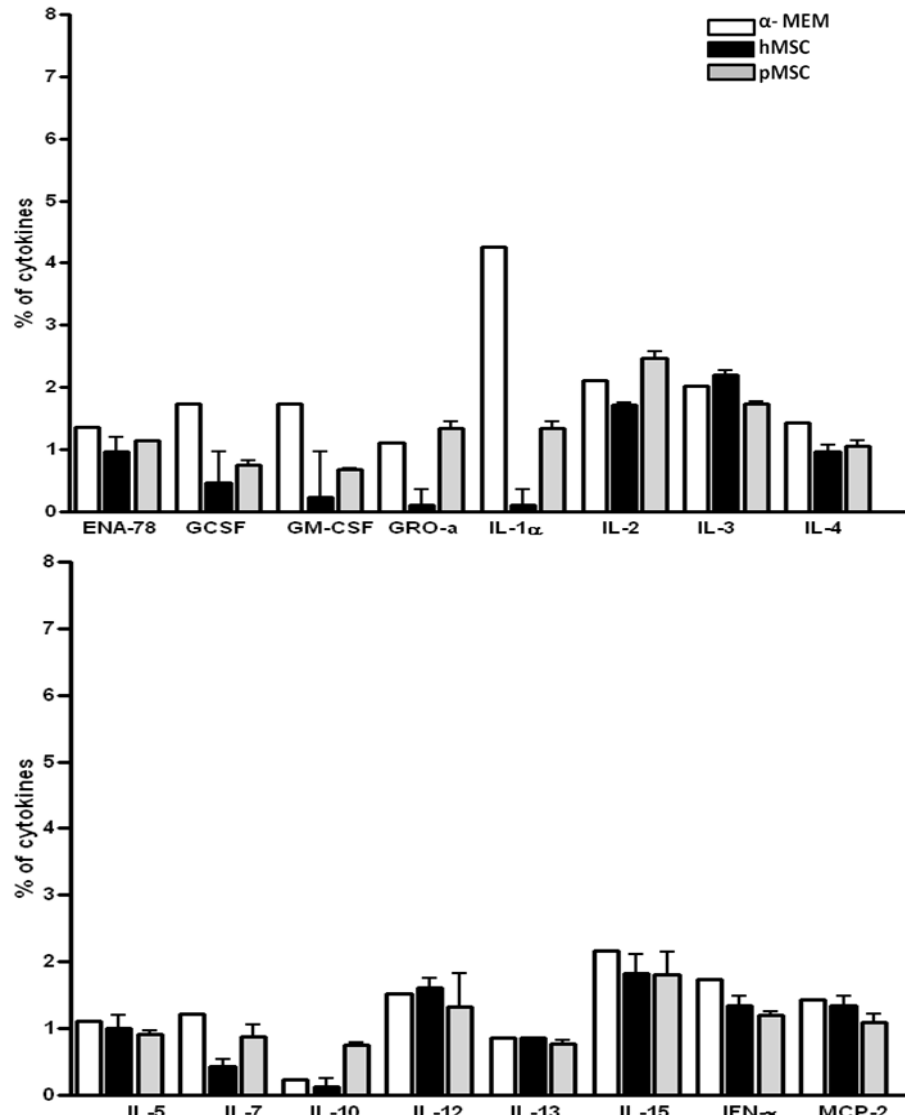


Figure 7.5. MSC cytokine analysis

ENA-78- C-X-C motif chemokine 5, **GCSF**- Granulocyte colony-stimulating factor, **GM-CSF**- Granulocyte-macrophage colony-stimulating factor, **GRO-α**- C-X-C motif ligand 1, **IL-1α**-Interleukin 1α, **IL-2**- Interleukin 2, **IL-3**- Interleukin, **IL-4**-Interleukin 4, **IL-5**- Interleukin 5, **IL-7**- Interleukin 7, **IL-10**- Interleukin 10, **IL-12**- Interleukin 12, **IL-13**- Interleukin 13, **IL-15**- Interleukin 15, **IFN-γ**- Interferon gamma, **MCP-2**- Monocyte chemotactic protein 2, (n=2) All values are normalised to the provided positive control.

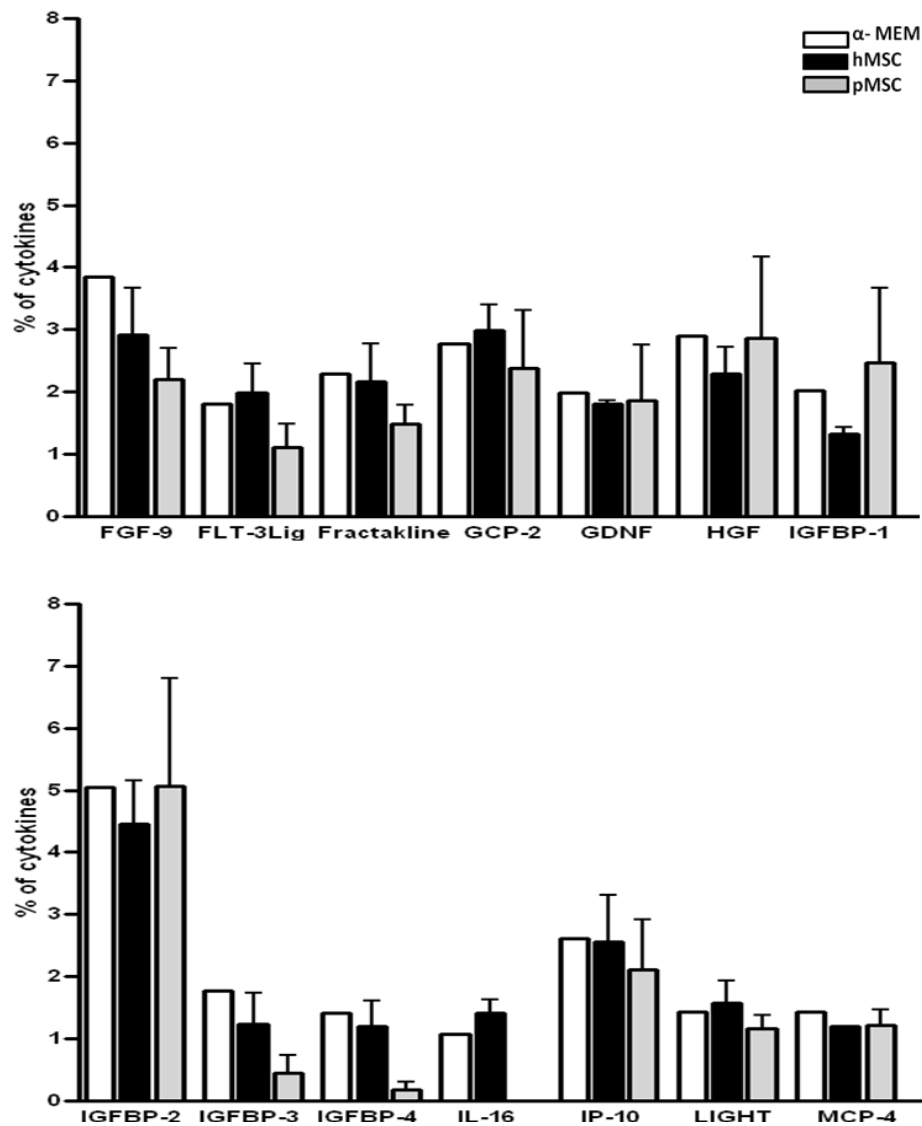


Figure 7.6. MSC cytokine analysis

FGF-9- Fibroblast growth factor 9, **FLT-3Lig**- Fms-related tyrosine kinase 3 ligand, **GCP-2**- Human granulocyte chemotactic protein-2, **GDNF**- Glial cell-derived neurotrophic factor, **HGF**- Hepatocyte growth factor, **IGFBP-1**- Insulin-like growth factor-binding protein 1, **IGFBP-2**- Insulin-like growth factor-binding protein 2, **IGFBP-3**- Insulin-like growth factor-binding protein 3, **IGFBP-4**- Insulin-like growth factor-binding protein 4, **IL-16**-Interlukin16, **IP-10**- C-X-C motif chemokine 10, **LIGHT**- Lymphotoxins, inducible expression, competes with HSV glycoprotein D for HVEM, **MCP-4**- Monocyte chemotactic protein-4. (n=2) All values are normalised to the provided positive control.

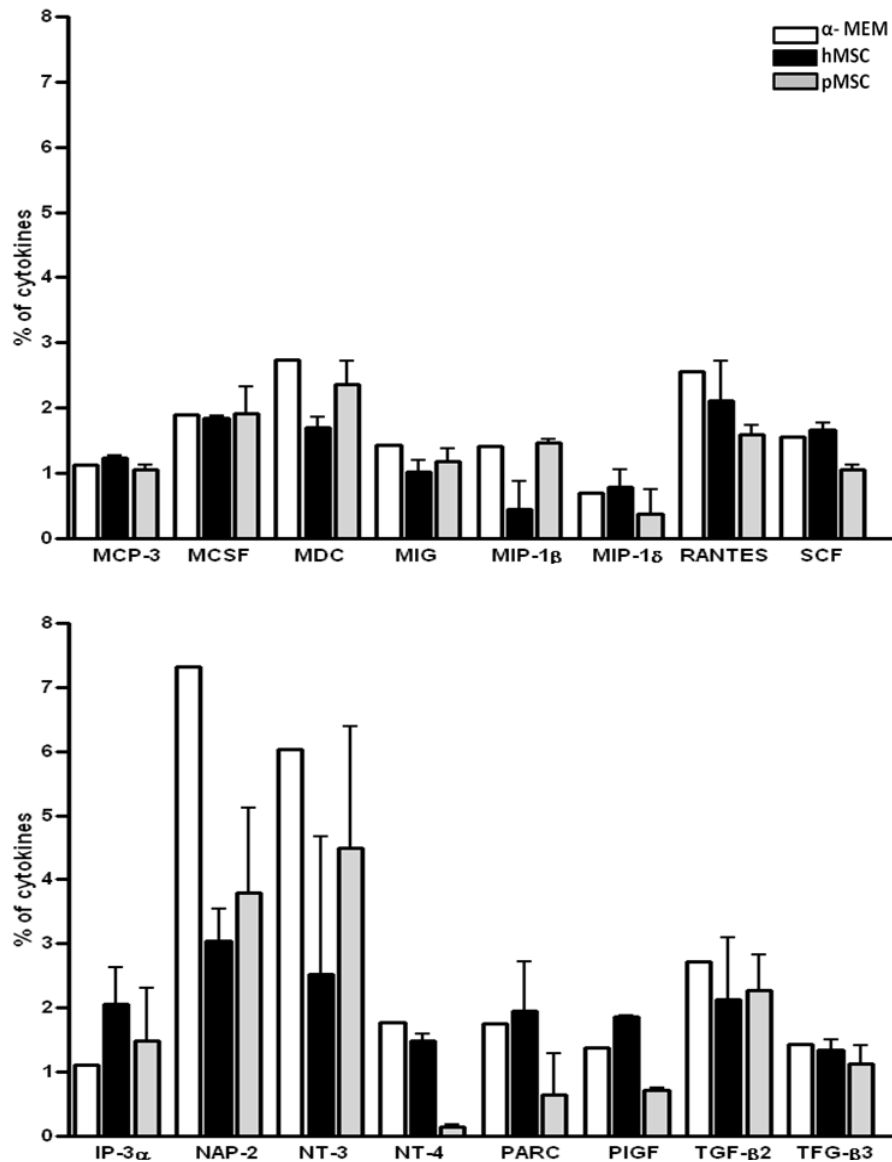


Figure 7.7. MSC cytokine analysis

MCP-3-Monocyte chemotactic protein 3, **MCSF**-Macrophage colony-stimulating factor, **MDC**-Macrophage-derived chemokine, **MIG**-C-X-C motif ligand 9, **MIP-1 β** -Macrophage inflammatory protein-1 β , **RANTES**-C-C motif ligand 5, **SCF**- Stem Cell Factor, **IP-3 α** -Macrophage inflammatory protein 3 α , **NAP-2**-Neutrophil-activating protein-2, **NT-3**-Neurotrophin-3, **NT-4**-Neurotrophin-4, **PARC**- Pulmonary and activation-regulated chemokine, **PIGF**-Placental growth factor, **TGF- β 2**- Transforming growth factor-beta 2, **TGF- β 3**-Transforming growth factor-beta 3. (n=2) All values are normalised to the provided positive control.

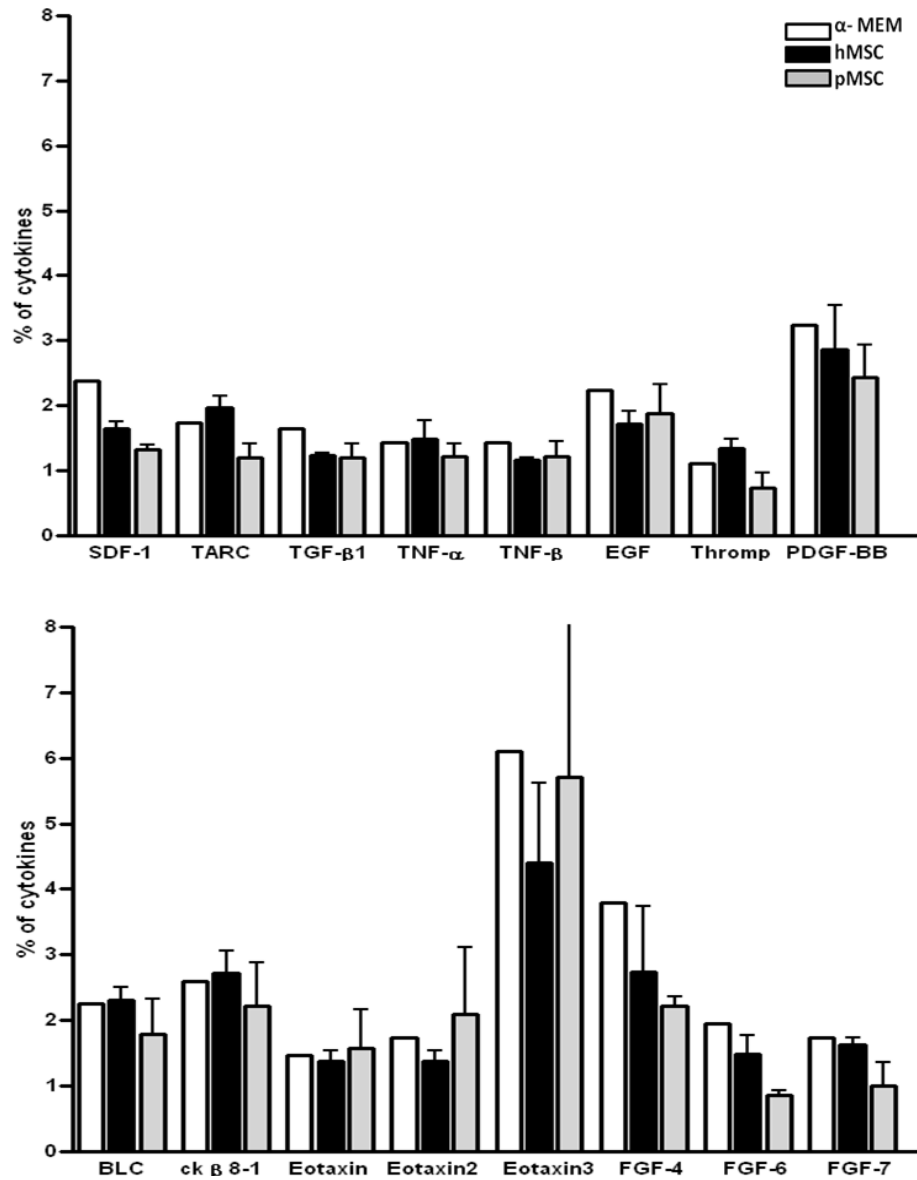


Figure 7.8. MSC cytokine analysis

SDF-1- Stromal cell-derived factor 1, **TARC**- C-C motif ligand 17, **TGF-β2**- Transforming growth factor-beta 3, **TNF-α**- Tumor necrosis factor-α, **EGF**- Epidermal growth factor, **Thromp**- Thrombopoietin, **PDGF-BB**-Platelet-derived growth factor, **BLC**- B-lymphocyte chemoattractant, **CK β 8-1**- Macrophage Inflammatory Protein 3, **FGF-4**- Fibroblast growth factor-4, **FGF-6**-Fibroblast growth factor-6, **FGF-7**- Fibroblast growth factor. (n=2) All values are normalised to the provided positive control.

7.3 Discussion

This section has begun to explore the wide variety of factors secreted by MSC, in particular it has highlighted the secretion of SPARCL1. To date no published work has shown the release of SPARCL1 by MSC. Before undertaking this study it was hypothesised that delivery of SPARCL1 would infer cardiac functional benefits post MI. Despite the promising unpublished *in vitro* data, chronic analysis of animals 6 weeks after delivery of 10µg of recombinant Sparcl1 protein, showed no functional cardiac improvements. It can also be concluded that the delivery of 10µg of SPARCL1 had no adverse effects on cardiac performance and no adverse events were noted during or after its delivery.

Chaurasia *et al* described how SPARCL1 plays a pivotal role in corneal wound healing and that SPARCL1 may be a novel therapeutic worth pursuing past initial pre-clinical studies [271]. Corneal wound healing is similar to that of infarct healing that occurs post MI in so far as damage to the cornea causes an initial acute response including cellular apoptosis, the release of local pro-inflammatory cytokines such as IL-1, TGF-β and PDGF, cell clearance and the activation of, and migration of myofibroblasts to the site of injury [271]. These events result in wound contraction, ECM disorganisation, adverse remodelling and scar formation. Chaurasia *et al* demonstrated how the exogenous topical application of recombinant SPARCL1 to the damaged corneas protected cells from undergoing apoptotic cell death, decreased inflammatory events such as MMP activity, reduced αSMA positive cells in the region and decreased fibrosis and irregular ECM production [271]. The repair process here is mechanistically similar to that required for MI repair however, our SPARCL1 study failed to demonstrate any positive results in the heart.

There are a number of possible reasons as to why SPARCL1 had no therapeutic effect on MI repair in this study. Firstly, the timing of drug delivery may not be optimal, as SPARCL1 is an ECM modulating factor and has been shown to regulate collagen assembly [268]. The delivery of SPARCL1 may thus be more beneficial at later time points in the repair process, possibly after the initial acute injury response has completed and during the remodelling phase. Secondly, the dose of SPARCL1 delivered may not be adequate to elicit functional improvements. Although we extrapolated from our *in vitro* data to match an equivalent dose to that of the MSC dose that was administered in previous studies this SPARCL1 dose may not be sufficient. From the successful Chaurasia study much higher doses of SPARCL1 were applied, 100µg of recombinant SPARCL1 was applied for 3 days at 24 hours intervals [271]. Additional dose ranging studies may be required to identify if increased amounts of SPARCL1 would infer additional functional improvements. Thirdly, the method of delivery of the protein may not be appropriate. Again referencing the study carried out by Chaurasia *et al* topical application of recombinant SPARCL1 was capable of improving corneal repair suggesting that maybe alternative delivery strategies may need to be utilised to obtain the optimal benefit of *in vivo* administration of SPARCL1. For instance, as SPARCL1 works predominantly on matrix then ECM slow release strategies for SPARCL1 delivery may be appropriate. Other strategies may involve protein PEGylation, drug encapsulation and drug delivery from drug eluting stents or hydrogels with slow release profiles.

In addition to identifying the expression of SPARCL1 this study has also elucidated other factors that are secreted by MSC. The study compared conditioned media of porcine and human MSC. Results show a disparity in

concentration of factors secreted by MSCs from different species and this may be real or in part attributed to the use of a human cytokine array. Antibodies may not be as specific for porcine proteins as they would be for humans. The cytokine array used was capable of identifying 70 cytokine and chemokines of which ~20% were identified to be secreted by MSC in the current study. The paracrine factors identified have been implicated in numerous cellular processes that may potentially be involved in cardiac repair. Of those identified within the conditioned media there is an overall suggestion these factors may be involved cell migration and tissue remodelling due to the presence of cytokines such as MCP-1, GRO, TIMP1, TIMP2, IL-8 and IL-10. Factors known to be associated with angiogenesis were not present in high concentrations in the current conditioned media study, although there was a slight increase in the concentration of VEGF. High levels of cytoprotective cytokines such as VEGF, IGF-1, bFGF and SDF have been present in previously reported MSC conditioned media experiments, especially after exposure to hypoxia. As *in vitro* culture environment plays a significant role in the factors released by stem cells it is therefore difficult to find coherence between studies, however there are a number of putative cytokines that are reported within the literature.

One of the most significantly secreted cytokines by MSC in the current study was the TIMPs. TIMPs are associated with influencing ECM ventricular remodelling post MI, their absence post MI has been linked to accelerated remodelling in both TIMP1 and TIMP2 deficient mice [272, 273]. To date no study has looked at the benefits of delivering recombinant TIMP1 or TIMP2, however, a recent abstract showed the benefits of continuous delivery of recombinant TIMP3 by a degradable hyaluronic acid based hydrogel [274]. Delivery of TIMP3, 14 days

after MI in a large animal model prevented adverse inflammatory events and progression of LV dysfunction [274]. Novel anti fibrotic agents such as TIMPs released by MSC may be promising future therapeutics for MI remodelling as stand-alone agents and may warrant further research. GRO, also known as CXCL1 and secreted by MSC has been shown to play a pro-inflammatory role post myocardial infarction due to its potent chemokine effect on neutrophils. GRO levels are increased post MI [275] and this GRO secreted by MSCs is of unclear significance in terms of additional therapeutic benefit. Another MSC secreted cytokine identified was IL-10 is a known anti-inflammatory cytokine that has been shown to be therapeutically beneficial post MI. Delivery of recombinant IL-10 attenuated both inflammation and myocardial remodelling in a mouse model of MI [276]. High levels of the pro-inflammatory cytokine IL-6 also released by MSC has been shown to increase inflammation, increase left ventricle adverse remodelling and to increase the incidence of HF. However, it is debatable whether IL-6 may be of benefit post MI, the receptor for IL-6, known as gp130, activation of gp130 is cardioprotective. Therefore high levels of IL-6 which activate gp130 should be beneficial as opposed to being disadvantageous. This illustrates the difficulty in determining the mechanisms of a single factor in the context of multiple proteins secreted by MSC.

Although this study has identified an array of factors, it is difficult to establish if MSC would have the same cytokine and chemokine profile when delivered into post ischemic environment of the myocardium. Further *in vitro* studies beyond the scope of this PhD thesis are required to fully allude the significance of these findings. Repair post MI is a highly dynamic process which involves multiple cytokines, proteins, molecules and cells being activated and deactivated in a

temporal and spatial continuum. The major challenge in the paracrine field therefore is in determining when and how much of what factor is required in order to be beneficial.

Experiments in this chapter primarily focused on SPARCL1, a relatively novel cytokine whose mechanism of action remain considerably unknown but showed promise both *in vitro* and *in vivo* in small animal studies. Further work should involve higher SPARCL1 dosing, varying time points after MI and delivery through a variety of performance enhancing strategies including local and slow release agents. With regard to MSC secretory profile, it may be useful to focus on classes of factors that affect early, midterm and late events post MI.

Chapter 8

Discussion and Future Directions

8.1 Discussion

8.1.1 Optimising MSC delivery

Initial dosing studies identified that 25×10^6 MSC to be the optimal dose of MSC that could be administered via the coronary artery in the absence of heparin without any major adverse events, such as death or ventricular arrhythmias occurring. In the porcine model this represents approximately 1×10^6 MSC/kg and was used in all following *in vivo* studies. Both preclinical and clinical studies have shown recently that the delivery of lower cell numbers in the range of 20 - 25×10^6 have a greater therapeutic effect than that of higher cell numbers [118, 192, 214]. Our current study corroborates these findings by illustrating that 25×10^6 MSC resulted in significant cardiac functional improvements at 6 weeks post MI. Although it has not been explored, delivery of higher cell numbers could be causing additional injury that is negating the positive effect of MSC therapy. Additional injury could be caused by the presence of more TF within the vasculature, triggering increases thrombus formation resulting in more severe MVO. More advanced imaging technologies such as 3D microvessel reconstruction by CT may allow researchers determine more accurately the fate of MSC within the cardiac microvasculature, including the evaluation of microvascular presence of MSC over time.

8.1.2 Safety concerns surrounding MSC therapy

Despite no major adverse events occurring, delivery of 25×10^6 MSC did result in significant reductions in coronary flow as measured by CFR after their administration. This reduction in flow post MSC therapy has been prevalent finding in the field since the first MSC studies *in vivo* [277]. Reductions in

coronary flow as a result of downstream occlusion within the microvascular bed is an indicator of poor prognostic outcome in patients being associated with increased incidence of HF and mortality [221]. Reductions in coronary flow and MVO occur post MI in the absence of cell therapy but administration of cells in the acute phase exacerbate this pathology. A large meta-analysis looking at 52 pre-clinical MSC studies raised safety concerns regarding MSC therapy. Although this study suggested that there was no significant increase in animal mortality after cell administration, ~60% of the preclinical studies determined the presence of safety issues after cell delivery [277]. In agreement, human trials have not reported increased mortality after cell delivery but laboratory investigations on MSC surface characteristics have suggested caution is warranted in the clinical use of MSC. For these reasons, the investigators of the TAC-HFT trial which reported one-year follow up data [278], chose to avoid intracoronary delivery when recently testing MSC treatment in ischemic cardiomyopathy patients. Our data would suggest that when using MSC for clinical practice heparin therapy may be useful in avoiding adverse MSC related events.

Although microvascular obstruction and reductions in coronary flow have been highlighted in the majority of studies, no study to date has investigated the causal mechanism surrounding MSCs effect on the microvasculature post MI. Our study has demonstrated for the first time that one mechanism responsible for MSC causing adverse events is due to surface expression of TF, which is the most potent propagator of coagulation. Not only has this study shown that MSC expresses TF but that the TF present is catalytically active and because of this MSC are capable of supporting thrombus formation and induce thrombin generation *in vitro*. As well as providing mechanistic evidence this study has also

provided a clinically applicable strategy for preventing microvascular occlusion, decreasing myocardial haemorrhage and reduction in coronary flow associated with MSC delivery. Herein it has been established that pre-treating the MSC with heparin can abrogate the pro-thrombotic effect of MSC both *in vitro* but most importantly *in vivo*. As mentioned, untreated MSC caused significant reductions in coronary flow after the delivery of 25×10^6 cells via the coronary artery. This reduction in flow was associated with downstream microvascular obstruction, which was illustrated in this current study by being able to identify labelled MSC expressing TF coupled with platelet aggregation and VWF expression within occluded vessels 24 hours after cell delivery (**Figure 5.4**). A paper published by Moll *et al* [214] suggests that cultured MSC due to their expression of TF triggered what the authors termed an instant blood-mediated immune reaction (IBMIR). The degree of this response Moll suggests is dependent on cell dose, cell passage and cell donor. Results following the intravenous administration of MSC revealed that MSC trigger a weak IBMIR response. This study was conducted on 44 patients who received 69 infusions of $1-3 \times 10^6/\text{kg}$ of MSC for the treatment of life threatening conditions such as graft vs. host disease. Analysis of serum samples at 24 hours found a 15% platelet count drop after administration and a five-fold increase in both the coagulation marker TAT and the complement activation marker C3a. *In vitro* Moll used a Chlander blood loop model to further investigate MSC compatibility with blood and observed that higher MSC doses corresponding to $1-3 \times 10^6/\text{kg}$ recipient weight resulted in faster and more prominent clotting in comparison to a dose equivalent of $0.2-0.5 \times 10^6/\text{kg}$ recipient. This higher dose is the same as the dose used in our *in vivo* studies however delivering the cell locally via the coronary artery rather than systemically may

intensify the responses observed in Moll's *in vivo* study. This again highlights the need for definitive MSC dosing studies and underlines the need for more extensive analysis of what may be occurring *in vivo* post MSC administration.

8.1.3 The effect of heparin on MSC

In other cardiac cell therapy investigations, heparin has been thought to influence the engraftment of bone marrow derived mononuclear cell populations through disruption of the SDF-1/CXCR4 ligand/receptor axis in a *in vitro* cell migration assay and in a mouse ear-wound model [279]. These investigators and others [211] have suggested the use of the direct thrombin inhibitor bivalirudin to obviate any concerns on heparins impact on stem cell mobilization or delivery in cardiac repair. From the data presented in this current study, heparin improves MSC infiltration into the infarct zone suggesting that heparin impairment of the SDF-1/CXCR4 system does not impact MSC uptake in this context. Moreover, heparin-assisted MSC delivery improved LV remodelling and function six weeks post MI. *In vitro*, it has also been demonstrated that heparin has no effect on MSC proliferation or differentiation [280].

Since management of thrombosis remains a key priority in the treatment of cardiac patients, further studies are required using a broader spectrum of anti-thrombotic agents including direct thrombin inhibitors, anti-coagulants and novel platelet inhibitors on the prothrombotic activity of MSC post intracoronary administration. Other drugs that may prevent MSC prothrombic activity include thrombin inhibitor melagatran [281], specific TF inhibitors [214] and activated protein C [282].

8.1.4 The role of MSC associated TF

This study has raised a number of questions surrounding the role of TF in relation to MSC. Further studies are required to establish if TF expression is due to culture expansion of cells or whether MSC express TF intrinsically. Previously it has been shown the higher the number of passages the cell has undergone the higher the expression level of TF [214]. It is not unreasonable to propose that the *in vitro* handling of MSC may be having a significant impact on their innate *in vivo* characteristics. Chemicals such as trypsin, FBS and washing buffers used in protocols such as passaging and cryopreservation may be influencing the function of MSC. Modifying culturing protocols could limit MSC TF expression without having to pre-treat with adjunctive drugs and may be advantageous. If cell culture is an influential factor minimal *in vitro* expansion of cells should be utilised and this could be achieved through increasing volume of bone marrow at initial aspiration, by using autologous cells and by using lower cell numbers. MSC cell sorting of TF positive and negative MSC and comparing their *in vitro* and *in vivo* behaviour may be a study that would provide significant insight as the role of TF with regard the therapeutic benefit of MSC cell therapy. Further in depth analysis as to what is causing TF expression is required.

8.1.5 Clinical implications

In the cardiac repair cell therapy field, there are number of on-going trials featuring MSC delivery through an intracoronary route such as WJ-MSC-AMI [283], SEED-MSC (NCT 01392105), and AMICI (NCT01781390) for acute MI. The management of possible prothrombotic side effects of MSC should therefore be a consideration during investigative and clinical MSC administration in a cardiovascular setting where augmented thrombogenicity may be potentially an

unheralded problem. Other trials targeting chronic myocardial ischemia such as POSEIDON [118] and PROMETHEUS utilize an intramyocardial delivery strategy which presumably may not give rise to this microvascular complication. Intramyocardial platelet activation has deleterious thrombotic and microembolic consequences of cardiac ischemia [284, 285] and has been effectively mitigated by glycoprotein IIb/IIIa targeting as shown for example, in the PROTECT TIMI-30 trial [251]. As a potential causative agent of platelet activation when delivered in the coronary vascular system, therapeutic use of MSC may thus require additional attention to anti-platelet treatment. Thus management of possible prothrombotic side effects of MSC should be a strong consideration during future investigative and clinical MSC administration especially via the intracoronary route.

The safety concerns associated with cell delivery into the ischemic myocardium that have been highlighted in this thesis are critical to patient safety and the safeguarding of positive outcomes of major efforts in cardiac cell therapy investigations, particularly in the light of large scale trials such as BAMI recently supported by European Commission Seventh Framework Programme FP7. The use of anti-coagulants for the administration of cells via the coronary route may be imperative to prevent the occurrence of adverse events illustrated in this setting.

8.2 Future Directions

Since their discovery, MSC when used in animal models for the treatment of MI have been shown to differentiate into new cardiomyocytes, promote local cardiac regeneration/repair, reverse cardiomyocyte death, and modulate adverse cardiac remodelling. Based on these promising findings clinical trials using MSC for cardiac repair have been initiated. Early clinical studies met safety endpoints and did show encouraging results such as improved EF [197, 286], a reduction in LV chamber size[197], decrease in ventricular arrhythmias and overall improvements in health [286]. These encouraging phase I studies prompted further new phase II clinical trials but unfortunately these clinical trials have not lived up to the early promises. The following discussion will describe possible ways in which MSCs and their by-products may be manipulated to increase their therapeutic benefit both in relation to the data obtained in this thesis and in the broader MSC field.

The disparity between results obtained in pre-clinical and clinical MSC studies may occur primarily due to study heterogeneity within the field. From a pre-clinical stand point and as can be seen from **table 3.1** there is little coherence between MSC pre-clinical studies. This heterogeneity prevents researchers from identifying the optimal therapeutic platform by which MSC exert their repair effect. Despite this, clinical trials are being undertaken based on variable pre-clinical results and it is now becoming apparent from larger MSC trials that results are modest and contradictory. Pre-clinical studies are ultimately undertaken to try and optimise a therapy before going to a clinical trial. They set out to determine early safety, feasibility, and efficacy of a therapy. In the field of cell therapy however, there are more fundamental issues related to the use of cells

including, optimal cell number, methods of delivery, timing of delivery and adequacy of efficacy end point analysis.

To decipher this preclinical complexity Spoel *et al* carried out a meta-analysis of 52 published pre-clinical studies involving stem cells therapy in large animal (N=888) experiments of ischemic heart disease [277]. The main finding of the paper was that cell therapy (includes all cells types delivered pre-clinically) improves LVEF by approximately 7.5% and that this increase is due primarily to a decrease in ESV [277]. Further cell specific analysis concluded that MSC as opposed to other cells provides the most therapeutic benefit when used to treat an LAD infarction or chronic total occlusion models. High cell numbers of more than 10^7 delivered one week post MI also had the most beneficial effect on LVEF [277]. Notably, animal species and route of delivery had no effect on therapeutic outcomes [277]. Although this meta-analysis study highlights some important points it does not negate the need for consensus in pre-clinical studies. The European Society of Cardiology set in place a task force to investigate the role of stem cell therapy in the treatment of cardiovascular disease and to suggest what further clinical studies were needed in the field. In 2006 the main consensus of the task force was that a dose optimisation study at different time points and via different routes would be of great scientific interest. However they also suggested that this would “take the best part of a century” and that a more pragmatic approach to demonstrating clinical efficacy was needed [287]. Despite these suggestions, not having established adequate pre-clinical data has prevented progression in this field and ultimately the efficacy of stem cells in human subjects remains unresolved. Even with complete optimisation of a cell therapy

translating to the clinic will pose its own problems. With pre-clinical studies, researchers in order to achieve reproducibility will use animal populations with minimal amounts of variability. Animals will be of similar age, usually young, usually of the same sex and species and with no comorbidities. This differs substantially from patient populations presenting at clinic even though they are required to meet inclusion criteria. To overcome this pre-clinical work should be carried out on varying animal populations, with a variety of ages and sex mixes. In addition, clinical trials must be large enough to overcome population variance in order to achieve statistical significance. Recent trials such as the BAMI (NCT01569178) trial which is a multinational, multicenter, randomised open-label, controlled, parallel-group phase III study has aimed to demonstrate that a single intracoronary infusion of autologous bone marrow-derived mononuclear cell is safe and reduces all-cause mortality in patients with a left ventricular EF of $\leq 45\%$ after successful reperfusion for MI. This study will recruit 3000 patients in over 17 European centres and is being funded by European 7 Framework with €7 million committed in funding. Results from this pivotal study will conclusively establish the efficacy of BM-MNC. A similar trial design is now required for MSC. However, before undertaking such an extensive and expansive trial, preclinical optimisation is essential.

Due to the logistics of cell therapy, such as cell isolation, cell expansion and cell delivery additional research is required to fully explore the paracrine mechanisms of MSC therapy. Paracrine delivery would circumvent many of the technical and safety issues surrounding cell delivery. MSC appear to be therapeutically beneficial in a large part due to their ability to secrete a wide variety of cytokines

and chemokines. Therefore, cell delivery may not be necessary for cardiac repair and regeneration. If a single paracrine factor or cocktail of factors could be used, issues such as what dose and when this dose should be administered arise. It could be speculated that when MSC are delivered *in vivo* their secretory profile is altered by their surrounding environment to provide the necessary local repair responses. MSC thus provide additional repair factors that cannot be supplied by an overwhelmed global body response that occurs after MI. For this concept to be established more studies such as those carried out in CRVB, in which the secretory profile of EPC under a number of physiological conditions were examined and led to the discovery of low dose IGF[164]. The major obstacle facing paracrine studies, however, is the difficulty in elucidating *in vivo* nature of cell responses. Studies that can more accurately mimic the *in vivo* physiological environment of the heart are required. Progress has been made in the tissue engineering field in which 3D engineered tissues are now available. In particular, cardiac cell sheets [288] may provide a more useful physical environment to begin to identify the *in vivo* nature of MSC with regards their secretory profile. MSC cultured in these bioengineered systems would be interacting with ECM proteins similar to those present in the myocardium. As it is an *in vitro* assay external environments can be altered to mimic that of disease states and conditioned media experiments can be utilised to determine cytokine release and response profiles. Recently research has also begun to focus on exosomes secreted from MSC. It has been suggested that cells communicate and elicit their effects by two main mechanisms-through cell to cell contact and through the release of secreted factors. However, most recently membrane secreted vesicles known as exosomes or microvesicles have been proposed to mediate the signal transfer between cells

required for tissue repair and regeneration. Exosomes were first identified in 1981 by Trams *et al* [289]. Exosomes are small vesicles of endocytic origin with a diameter of 40-100nm and are excreted by most cells in culture. They are known to contain proteins, lipids, miRNAs and RNA. Li *et al* demonstrated that exosomes are the main active component of MSC conditioned media [290] by illustrating *in vivo* that the delivery of exosomes significantly reduced infarct size in a mouse model of I/R. Interestingly, the delivery of exosome depleted conditioned media had no significant effect on infarct size [290]. Arslan and collaborators provide additional evidence of the potent cytoprotective capabilities of exosomes by showing reduction in infarct size by 45% in a mouse model of I/R. Analysis at 28 days also revealed that exosome treated animals showed significant preserved left ventricular geometry and improved contractile performance [291]. In addition to their cytoprotective properties exosomes can also influence angiogenesis and do this through direct ligand/receptor interactions or by augmenting local cytokines to induce endothelial differentiation, proliferation, migration and adhesion [292]. The biological mechanisms by which exosomes exert their benefits for the most part remain unknown. It has been suggested the pH plays a role in exosome uptake and that during ischemia cardiomyocyte pH is decreased facilitating their integration.

The main advantages of exosomes over cell therapy are their capacity to sequester a large array of factors within small vesicles bypassing the need for whole cell delivery. In addition, their lipid bi-layer prevents rapid degradation by endogenous enzymes and other hydrolases [290]. Despite the small size of exosomes, microvascular obstruction and the expression of TF needs to be assessed before IC delivery of these entities is contemplated [293]. Thus exosomes may be

a promising therapeutic prospect for future cardiac repair and regeneration. However, their mechanism of action needs to be further understood *in vitro* and their efficacy and safety needs to be validated in large animal models of MI before translation to the clinic.

The inability of MSC to elicit a more potent benefit in human subjects has been attributed to a number of factors including low cell engraftment, the hostile ischemic environment and low cell survival. Accordingly, research has tried to find ways to overcome these issues. Three main methods of *ex vivo* modification have been used to increase MSC regenerative properties, including the pre-treatment of MSC with growth factors, the pre-conditioning of MSC with external factors such as hypoxia and by genetically modifying MSC. A number of pre-treatment strategies have been explored, including exposure of MSC to growth factors such as IGF-1, FGF, and BMP2 during cell expansion which improved their cardiac retention and thus improved the efficacy of MSC transplantation [294]. Preconditioning of MSC with SDF-1 induced cell proliferation, decreased apoptosis and enhance their survival and engraftment which resulted in the reduction in infarct size and significant improvements in cardiac function [295]. It has also been demonstrated that delivery of MSC pre-treated with heat shock protein (Hsp)-70 decreases cardiac fibrosis and apoptosis with associated improved left ventricular function when compared to non-treated MSC. To date MSC have been modified to over express tumour necrosis factor receptor[296], CXCR4[297], VEGF[298], FGF[299], all of which improved cardiac function and recovery after transplantation. Modification of cells before delivery is a promising option of enhancing the effects of MSC for cardiac repair and

regeneration for the treatment of MI but methods such as gene transfer and other strategies add to the logistical and regulatory burden of getting the cells to mainstream clinical practice.

In conclusion, the field of regenerative medicine remains in a nascent state with respect to cardiac repair. Although from a clinical perspective MSC appear to be safe it is clear from findings in our study and others [277] that MSC are capable of causing adverse events especially in the setting of acute cardiac ischemia. Future studies need to address these issues by utilising either MSC by-products or by modifying MSC to lessen the occurrence of these events. MSC therapy requires future validation in large animals models to define optimal cell number and delivery strategies before going to phase II/III clinical trials.

References

1. WHO. *The top 10 causes of death*. 2011; Available from: <http://www.who.int/mediacentre/factsheets/fs310/en/index.html>.
2. Smolina, K., et al., *Determinants of the decline in mortality from acute myocardial infarction in England between 2002 and 2010: linked national database study*. BMJ, 2012. **344**: p. d8059.
3. Jhund, P.S. and J.J. McMurray, *Heart failure after acute myocardial infarction: a lost battle in the war on heart failure?* Circulation, 2008. **118**(20): p. 2019-21.
4. Zannad, F., N. Agrinier, and F. Alla, *Heart failure burden and therapy*. Europace, 2009. **11**: p. 1-9.
5. Gaziano, T.A., et al., *Growing Epidemic of Coronary Heart Disease in Low- and Middle-Income Countries*. Current Problems in Cardiology, 2010. **35**(2): p. 72-115.
6. Herrick, J.B., *Landmark article (JAMA 1912). Clinical features of sudden obstruction of the coronary arteries. By James B. Herrick*. JAMA, 1983. **250**(13): p. 1757-65.
7. Assmann, G., P. Cullen, and H. Schulte, *Simple scoring scheme for calculating the risk of acute coronary events based on the 10-year follow-up of the prospective cardiovascular Munster (PROCAM) study*. Circulation, 2002. **105**(3): p. 310-5.
8. Strong, J.P., A.W. Zieske, and G.T. Malcom, *Lipoproteins and atherosclerosis in children: an early marriage?* Nutr Metab Cardiovasc Dis, 2001. **11 Suppl 5**: p. 16-22.
9. Anderson, T.J., et al., *Systemic nature of endothelial dysfunction in atherosclerosis*. Am J Cardiol, 1995. **75**(6): p. 71B-74B.
10. Behrendt, D. and P. Ganz, *Endothelial function. From vascular biology to clinical applications*. Am J Cardiol, 2002. **90**(10C): p. 40L-48L.
11. Williams, K.J. and I. Tabas, *The response-to-retention hypothesis of early atherogenesis*. Arterioscler Thromb Vasc Biol, 1995. **15**(5): p. 551-61.
12. Glass, C.K. and J.L. Witztum, *Atherosclerosis. the road ahead*. Cell, 2001. **104**(4): p. 503-16.
13. Mestas, J. and K. Ley, *Monocyte-endothelial cell interactions in the development of atherosclerosis*. Trends Cardiovasc Med, 2008. **18**(6): p. 228-32.
14. Stary, H.C., *Natural history and histological classification of atherosclerotic lesions: an update*. Arterioscler Thromb Vasc Biol, 2000. **20**(5): p. 1177-8.
15. Stary, H.C., et al., *A definition of initial, fatty streak, and intermediate lesions of atherosclerosis. A report from the Committee on Vascular Lesions of the Council on Arteriosclerosis, American Heart Association*. Circulation, 1994. **89**(5): p. 2462-78.
16. Ross, R., *The pathogenesis of atherosclerosis: a perspective for the 1990s*. Nature, 1993. **362**(6423): p. 801-9.
17. Sakellarios, A.I., et al., *Patient-specific computational modeling of subendothelial LDL accumulation in a stenosed right coronary artery: effect of hemodynamic and biological factors*. Am J Physiol Heart Circ Physiol, 2013. **304**(11): p. H1455-70.

18. Falk, E., P.K. Shah, and V. Fuster, *Coronary plaque disruption*. Circulation, 1995. **92**(3): p. 657-71.
19. Kaplan, Z.S. and S.P. Jackson, *The role of platelets in atherothrombosis*. Hematology Am Soc Hematol Educ Program, 2011. **2011**: p. 51-61.
20. Reimer, K.A. and R.B. Jennings, *Wavefront Phenomenon of Myocardial Ischemic Cell-Death .2. Transmural Progression of Necrosis within the Framework of Ischemic Bed Size (Myocardium at Risk) and Collateral Flow*. Laboratory Investigation, 1979. **40**(6): p. 633-644.
21. Kloner, R.A., et al., *Effect of a transient period of ischemia on myocardial cells. II. Fine structure during the first few minutes of reflow*. Am J Pathol, 1974. **74**(3): p. 399-422.
22. Brodie, B.R., et al., *Importance of time to reperfusion for 30-day and late survival and recovery of left ventricular function after primary angioplasty for acute myocardial infarction*. J Am Coll Cardiol, 1998. **32**(5): p. 1312-9.
23. Beltrami, A.P., et al., *Evidence that human cardiac myocytes divide after myocardial infarction*. N Engl J Med, 2001. **344**(23): p. 1750-7.
24. Bergmann, O., et al., *Evidence for cardiomyocyte renewal in humans*. Science, 2009. **324**(5923): p. 98-102.
25. Liehn, E.A., et al., *Repair after myocardial infarction, between fantasy and reality: the role of chemokines*. J Am Coll Cardiol, 2011. **58**(23): p. 2357-62.
26. Frangogiannis, N.G., C.W. Smith, and M.L. Entman, *The inflammatory response in myocardial infarction*. Cardiovasc Res, 2002. **53**(1): p. 31-47.
27. Nahrendorf, M., M.J. Pittet, and F.K. Swirski, *Monocytes: protagonists of infarct inflammation and repair after myocardial infarction*. Circulation, 2010. **121**(22): p. 2437-45.
28. Sutton, M.G. and N. Sharpe, *Left ventricular remodeling after myocardial infarction: pathophysiology and therapy*. Circulation, 2000. **101**(25): p. 2981-8.
29. *Urokinase pulmonary embolism trial. Phase 1 results: a cooperative study*. JAMA, 1970. **214**(12): p. 2163-72.
30. Pizzetti, G., et al., *Thrombolytic therapy reduces the incidence of left ventricular thrombus after anterior myocardial infarction. Relationship to vessel patency and infarct size*. Eur Heart J, 1996. **17**(3): p. 421-8.
31. Keeley, E.C., J.A. Boura, and C.L. Grines, *Primary angioplasty versus intravenous thrombolytic therapy for acute myocardial infarction: a quantitative review of 23 randomised trials*. Lancet, 2003. **361**(9351): p. 13-20.
32. Menees, D.S., et al., *Door-to-Balloon Time and Mortality among Patients Undergoing Primary PCI*. New England Journal of Medicine, 2013. **369**(10): p. 901-909.
33. Verma, S., et al., *Fundamentals of reperfusion injury for the clinical cardiologist*. Circulation, 2002. **105**(20): p. 2332-6.
34. Hori, M. and K. Nishida, *Oxidative stress and left ventricular remodelling after myocardial infarction*. Cardiovasc Res, 2009. **81**(3): p. 457-64.
35. Nakamura, K., et al., *Inhibitory effects of antioxidants on neonatal rat cardiac myocyte hypertrophy induced by tumor necrosis factor-alpha and angiotensin II*. Circulation, 1998. **98**(8): p. 794-9.

36. Frohlich, G.M., et al., *Myocardial reperfusion injury: looking beyond primary PCI*. Eur Heart J, 2013. **34**(23): p. 1714-22.
37. Frishman, W.H., *Cardiology patient page. Beta-adrenergic blockers*. Circulation, 2003. **107**(18): p. e117-9.
38. Pfeffer, M.A., et al., *Effect of captopril on mortality and morbidity in patients with left ventricular dysfunction after myocardial infarction. Results of the survival and ventricular enlargement trial. The SAVE Investigators*. N Engl J Med, 1992. **327**(10): p. 669-77.
39. trial, B. *The effect of intracoronary reinfusion of bone marrow-derived mononuclear cells (BM-MNC) on all-cause mortality in acute myocardial infarction*. 2014; Available from: <http://www.bami-fp7.eu/>.
40. Asahara, T., et al., *Isolation of putative progenitor endothelial cells for angiogenesis*. Science, 1997. **275**(5302): p. 964-7.
41. Dowell, J.D., et al., *Myocyte and myogenic stem cell transplantation in the heart*. Cardiovasc Res, 2003. **58**(2): p. 336-50.
42. Tongers, J., D.W. Losordo, and U. Landmesser, *Stem and progenitor cell-based therapy in ischaemic heart disease: promise, uncertainties, and challenges*. Eur Heart J, 2011. **32**(10): p. 1197-206.
43. Strauer, B.E. and G. Steinhoff, *10 Years of Intracoronary and Intramyocardial Bone Marrow Stem Cell Therapy of the Heart*. Journal of the American College of Cardiology, 2011. **58**(11): p. 1095-1104.
44. Stamm, C., et al., *Autologous bone-marrow stem-cell transplantation for myocardial regeneration*. Lancet, 2003. **361**(9351): p. 45-6.
45. Wollert, K.C., et al., *Intracoronary autologous bone-marrow cell transfer after myocardial infarction: the BOOST randomised controlled clinical trial*. Lancet, 2004. **364**(9429): p. 141-8.
46. Schachinger, V., et al., *Intracoronary bone marrow-derived progenitor cells in acute myocardial infarction*. N Engl J Med, 2006. **355**(12): p. 1210-21.
47. Meyer, G.P., et al., *Intracoronary bone marrow cell transfer after myocardial infarction: eighteen months' follow-up data from the randomized, controlled BOOST (BOne marrOw transfer to enhance ST-elevation infarct regeneration) trial*. Circulation, 2006. **113**(10): p. 1287-94.
48. Meyer, G.P., et al., *Intracoronary bone marrow cell transfer after myocardial infarction: 5-year follow-up from the randomized-controlled BOOST trial*. Eur Heart J, 2009. **30**(24): p. 2978-84.
49. Janssens, S., et al., *Autologous bone marrow-derived stem-cell transfer in patients with ST-segment elevation myocardial infarction: double-blind, randomised controlled trial*. Lancet, 2006. **367**(9505): p. 113-21.
50. Lunde, K., et al., *Anterior myocardial infarction with acute percutaneous coronary intervention and intracoronary injection of autologous mononuclear bone marrow cells: safety, clinical outcome, and serial changes in left ventricular function during 12-months' follow-up*. J Am Coll Cardiol, 2008. **51**(6): p. 674-6.
51. Beltrami, A.P., et al., *Adult cardiac stem cells are multipotent and support myocardial regeneration*. Cell, 2003. **114**(6): p. 763-76.

52. Tateishi, K., et al., *Clonally amplified cardiac stem cells are regulated by Sca-1 signaling for efficient cardiovascular regeneration*. J Cell Sci, 2007. **120**(Pt 10): p. 1791-800.
53. Chugh, A.R., et al., *Administration of cardiac stem cells in patients with ischemic cardiomyopathy: the SCIPIO trial: surgical aspects and interim analysis of myocardial function and viability by magnetic resonance*. Circulation, 2012. **126**(11 Suppl 1): p. S54-64.
54. Bolli, R., et al., *Cardiac stem cells in patients with ischaemic cardiomyopathy (SCIPIO): initial results of a randomised phase 1 trial*. Lancet, 2011. **378**(9806): p. 1847-57.
55. Makkar, R.R., et al., *Intracoronary cardiosphere-derived cells for heart regeneration after myocardial infarction (CADUCEUS): a prospective, randomised phase 1 trial*. Lancet, 2012. **379**(9819): p. 895-904.
56. Friedenstein, A.J., S. Piatetzky, II, and K.V. Petrakova, *Osteogenesis in transplants of bone marrow cells*. J Embryol Exp Morphol, 1966. **16**(3): p. 381-90.
57. Friedenstein, A.J., et al., *Stromal cells responsible for transferring the microenvironment of the hemopoietic tissues. Cloning in vitro and retransplantation in vivo*. Transplantation, 1974. **17**(4): p. 331-40.
58. Pittenger, M.F., et al., *Multilineage potential of adult human mesenchymal stem cells*. Science, 1999. **284**(5411): p. 143-7.
59. Caplan, A.I., *Mesenchymal stem cells*. J Orthop Res, 1991. **9**(5): p. 641-50.
60. da Silva Meirelles, L., P.C. Chagastelles, and N.B. Nardi, *Mesenchymal stem cells reside in virtually all post-natal organs and tissues*. J Cell Sci, 2006. **119**(Pt 11): p. 2204-13.
61. Javazon, E.H., et al., *Rat marrow stromal cells are more sensitive to plating density and expand more rapidly from single-cell-derived colonies than human marrow stromal cells*. Stem Cells, 2001. **19**(3): p. 219-25.
62. Pak, H.N., et al., *Mesenchymal stem cell injection induces cardiac nerve sprouting and increased tenascin expression in a Swine model of myocardial infarction*. J Cardiovasc Electrophysiol, 2003. **14**(8): p. 841-8.
63. Bartholomew, A., et al., *Baboon mesenchymal stem cells can be genetically modified to secrete human erythropoietin in vivo*. Hum Gene Ther, 2001. **12**(12): p. 1527-41.
64. Phinney, D.G., et al., *Plastic adherent stromal cells from the bone marrow of commonly used strains of inbred mice: variations in yield, growth, and differentiation*. J Cell Biochem, 1999. **72**(4): p. 570-85.
65. Kadiyala, S., et al., *Culture expanded canine mesenchymal stem cells possess osteochondrogenic potential in vivo and in vitro*. Cell Transplant, 1997. **6**(2): p. 125-34.
66. Awad, H.A., et al., *Autologous mesenchymal stem cell-mediated repair of tendon*. Tissue Eng, 1999. **5**(3): p. 267-77.
67. Colter, D.C., et al., *Rapid expansion of recycling stem cells in cultures of plastic-adherent cells from human bone marrow*. Proc Natl Acad Sci U S A, 2000. **97**(7): p. 3213-8.
68. Wagner, W., et al., *Replicative Senescence of Mesenchymal Stem Cells: A Continuous and Organized Process*. PLoS One, 2008. **3**(5): p. e2213.
69. Rosenzweig, A., *Cardiac cell therapy--mixed results from mixed cells*. N Engl J Med, 2006. **355**(12): p. 1274-7.

70. Dominici, M., et al., *Minimal criteria for defining multipotent mesenchymal stromal cells. The International Society for Cellular Therapy position statement.* Cytotherapy, 2006. **8**(4): p. 315-7.
71. Makino, S., et al., *Cardiomyocytes can be generated from marrow stromal cells in vitro.* J Clin Invest, 1999. **103**(5): p. 697-705.
72. Saito, T., et al., *Myogenic Expression of Mesenchymal Stem Cells within Myotubes of mdx Mice in Vitro and in Vivo.* Tissue Eng, 1995. **1**(4): p. 327-43.
73. Toma, C., et al., *Human mesenchymal stem cells differentiate to a cardiomyocyte phenotype in the adult murine heart.* Circulation, 2002. **105**(1): p. 93-8.
74. Oswald, J., et al., *Mesenchymal stem cells can be differentiated into endothelial cells in vitro.* Stem Cells, 2004. **22**(3): p. 377-84.
75. Jiang, Y., et al., *Pluripotency of mesenchymal stem cells derived from adult marrow.* Nature, 2002. **418**(6893): p. 41-9.
76. Devine, S.M., et al., *Mesenchymal stem cells are capable of homing to the bone marrow of non-human primates following systemic infusion.* Exp Hematol, 2001. **29**(2): p. 244-55.
77. Wang, L., et al., *Ischemic cerebral tissue and MCP-1 enhance rat bone marrow stromal cell migration in interface culture.* Exp Hematol, 2002. **30**(7): p. 831-6.
78. Barbash, I.M., et al., *Systemic delivery of bone marrow-derived mesenchymal stem cells to the infarcted myocardium: feasibility, cell migration, and body distribution.* Circulation, 2003. **108**(7): p. 863-8.
79. Orlic, D., et al., *Bone marrow cells regenerate infarcted myocardium.* Nature, 2001. **410**(6829): p. 701-705.
80. Shake, J.G., et al., *Mesenchymal stem cell implantation in a swine myocardial infarct model: engraftment and functional effects.* Ann Thorac Surg, 2002. **73**(6): p. 1919-25; discussion 1926.
81. Silva, G.V., et al., *Mesenchymal stem cells differentiate into an endothelial phenotype, enhance vascular density, and improve heart function in a canine chronic ischemia model.* Circulation, 2005. **111**(2): p. 150-6.
82. Quevedo, H.C., et al., *Allogeneic mesenchymal stem cells restore cardiac function in chronic ischemic cardiomyopathy via trilineage differentiating capacity.* Proc Natl Acad Sci U S A, 2009. **106**(33): p. 14022-7.
83. Gneccchi, M., et al., *Paracrine mechanisms in adult stem cell signaling and therapy.* Circ Res, 2008. **103**(11): p. 1204-19.
84. Qian, Q., et al., *5-Azacytidine induces cardiac differentiation of human umbilical cord-derived mesenchymal stem cells by activating extracellular regulated kinase.* Stem Cells Dev, 2012. **21**(1): p. 67-75.
85. Koninckx, R., et al., *Human bone marrow stem cells co-cultured with neonatal rat cardiomyocytes display limited cardiomyogenic plasticity.* Cytotherapy, 2009. **11**(6): p. 778-792.
86. Roura, S., et al., *Exposure to cardiomyogenic stimuli fails to transdifferentiate human umbilical cord blood-derived mesenchymal stem cells.* Basic Res Cardiol, 2010. **105**(3): p. 419-30.
87. Kinnaird, T., et al., *Marrow-derived stromal cells express genes encoding a broad spectrum of arteriogenic cytokines and promote in vitro and in vivo arteriogenesis through paracrine mechanisms.* Circ Res, 2004. **94**(5): p. 678-85.

88. Chen, M.Y., et al., *Endothelial differentiation of Wharton's jelly-derived mesenchymal stem cells in comparison with bone marrow-derived mesenchymal stem cells*. Exp Hematol, 2009. **37**(5): p. 629-40.
89. Duffy, G.P., et al., *Bone marrow-derived mesenchymal stem cells promote angiogenic processes in a time- and dose-dependent manner in vitro*. Tissue Eng Part A, 2009. **15**(9): p. 2459-70.
90. Haynesworth, S.E., M.A. Baber, and A.I. Caplan, *Cytokine expression by human marrow-derived mesenchymal progenitor cells in vitro: Effects of dexamethasone and IL-1 alpha*. Journal of Cellular Physiology, 1996. **166**(3): p. 585-592.
91. Caplan, A.I. and D. Correa, *The MSC: an injury drugstore*. Cell Stem Cell, 2011. **9**(1): p. 11-5.
92. Meirelles Lda, S., et al., *Mechanisms involved in the therapeutic properties of mesenchymal stem cells*. Cytokine Growth Factor Rev, 2009. **20**(5-6): p. 419-27.
93. Hu, X.Y., et al., *Transplantation of hypoxia-preconditioned mesenchymal stem cells improves infarcted heart function via enhanced survival of implanted cells and angiogenesis*. Journal of Thoracic and Cardiovascular Surgery, 2008. **135**(4): p. 799-808.
94. O'Sullivan, J.F., et al., *Potent long-term cardioprotective effects of single low-dose insulin-like growth factor-1 treatment postmyocardial infarction*. Circ Cardiovasc Interv, 2011. **4**(4): p. 327-35.
95. Togel, F., et al., *Vasculotropic, paracrine actions of infused mesenchymal stem cells are important to the recovery from acute kidney injury*. Am J Physiol Renal Physiol, 2007. **292**(5): p. F1626-35.
96. Gneccchi, M., et al., *Evidence supporting paracrine hypothesis for Akt-modified mesenchymal stem cell-mediated cardiac protection and functional improvement*. Faseb Journal, 2006. **20**(6): p. 661-669.
97. Nguyen, B.K., et al., *Improved function and myocardial repair of infarcted heart by intracoronary injection of mesenchymal stem cell-derived growth factors*. J Cardiovasc Transl Res, 2010. **3**(5): p. 547-58.
98. Gneccchi, M., et al., *Paracrine Mechanisms in Adult Stem Cell Signaling and Therapy*. Circulation Research, 2008. **103**(11): p. 1204-1219.
99. Matsumoto, R., et al., *Vascular endothelial growth factor-expressing mesenchymal stem cell transplantation for the treatment of acute myocardial infarction*. Arterioscler Thromb Vasc Biol, 2005. **25**(6): p. 1168-73.
100. Frangogiannis, N.G., *Regulation of the inflammatory response in cardiac repair*. Circ Res, 2012. **110**(1): p. 159-73.
101. Murphy, M.B., K. Moncivais, and A.I. Caplan, *Mesenchymal stem cells: environmentally responsive therapeutics for regenerative medicine*. Exp Mol Med, 2013. **45**: p. e54.
102. Du, Y.Y., et al., *Immuno-inflammatory regulation effect of mesenchymal stem cell transplantation in a rat model of myocardial infarction*. Cytotherapy, 2008. **10**(5): p. 469-78.
103. Van Linthout, S., et al., *Mesenchymal stem cells improve murine acute coxsackievirus B3-induced myocarditis*. Eur Heart J, 2011. **32**(17): p. 2168-78.

104. Van Linthout, S., et al., *Mesenchymal stem cells improve murine acute coxsackievirus B3-induced myocarditis*. European Heart Journal, 2011. **32**(17): p. 2168-2178.
105. Lozito, T.P. and R.S. Tuan, *Mesenchymal Stem Cells Inhibit Both Endogenous and Exogenous MMPs via Secreted TIMPs*. Journal of Cellular Physiology, 2011. **226**(2): p. 385-396.
106. Biswas, S., et al., *Relation of anti- to pro-inflammatory cytokine ratios with acute myocardial infarction*. Korean J Intern Med, 2010. **25**(1): p. 44-50.
107. Li, L., et al., *Paracrine action mediate the antifibrotic effect of transplanted mesenchymal stem cells in a rat model of global heart failure*. Mol Biol Rep, 2009. **36**(4): p. 725-31.
108. Schievenbusch, S., et al., *Profiling of anti-fibrotic signaling by hepatocyte growth factor in renal fibroblasts*. Biochem Biophys Res Commun, 2009. **385**(1): p. 55-61.
109. Mou, S., et al., *Hepatocyte growth factor suppresses transforming growth factor-beta-1 and type III collagen in human primary renal fibroblasts*. Kaohsiung J Med Sci, 2009. **25**(11): p. 577-87.
110. Dixon, J.A., et al., *Mesenchymal cell transplantation and myocardial remodeling after myocardial infarction*. Circulation, 2009. **120**(11 Suppl): p. S220-9.
111. Mias, C., et al., *Mesenchymal Stem Cells Promote Matrix Metalloproteinase Secretion by Cardiac Fibroblasts and Reduce Cardiac Ventricular Fibrosis After Myocardial Infarction*. Stem Cells, 2009. **27**(11): p. 2734-2743.
112. Ohnishi, S., et al., *Mesenchymal stem cells attenuate cardiac fibroblast proliferation and collagen synthesis through paracrine actions*. Febs Letters, 2007. **581**(21): p. 3961-3966.
113. Li, L.L., et al., *Paracrine action mediate the antifibrotic effect of transplanted mesenchymal stem cells in a rat model of global heart failure*. Molecular Biology Reports, 2009. **36**(4): p. 725-731.
114. Guo, J., et al., *Anti-inflammation role for mesenchymal stem cells transplantation in myocardial infarction*. Inflammation, 2007. **30**(3-4): p. 97-104.
115. Griffin, M.D., et al., *Anti-donor immune responses elicited by allogeneic mesenchymal stem cells: what have we learned so far?* Immunol Cell Biol, 2013. **91**(1): p. 40-51.
116. Huang, X.P., et al., *Differentiation of Allogeneic Mesenchymal Stem Cells Induces Immunogenicity and Limits Their Long-Term Benefits for Myocardial Repair*. Circulation, 2010. **122**(23): p. 2419-2429.
117. Poncelet, A.J., et al., *Intracardiac allogeneic mesenchymal stem cell transplantation elicits neo-angiogenesis in a fully immunocompetent ischaemic swine model*. European Journal of Cardio-Thoracic Surgery, 2010. **38**(6): p. 781-787.
118. Hare, J.M., et al., *Comparison of allogeneic vs autologous bone marrow-derived mesenchymal stem cells delivered by transendocardial injection in patients with ischemic cardiomyopathy: the POSEIDON randomized trial*. JAMA, 2012. **308**(22): p. 2369-79.

119. Freyman, T., et al., *A quantitative, randomized study evaluating three methods of mesenchymal stem cell delivery following myocardial infarction*. Eur Heart J, 2006. **27**(9): p. 1114-22.
120. Kraitchman, D.L., et al., *Dynamic imaging of allogeneic mesenchymal stem cells trafficking to myocardial infarction*. Circulation, 2005. **112**(10): p. 1451-61.
121. Amado, L.C., et al., *Cardiac repair with intramyocardial injection of allogeneic mesenchymal stem cells after myocardial infarction*. Proc Natl Acad Sci U S A, 2005. **102**(32): p. 11474-9.
122. Hatzistergos, K.E., et al., *Bone marrow mesenchymal stem cells stimulate cardiac stem cell proliferation and differentiation*. Circ Res, 2010. **107**(7): p. 913-22.
123. Schuleri, K.H., et al., *The adult Gottingen minipig as a model for chronic heart failure after myocardial infarction: focus on cardiovascular imaging and regenerative therapies*. Comp Med, 2008. **58**(6): p. 568-79.
124. Williams, A.R., et al., *Durable scar size reduction due to allogeneic mesenchymal stem cell therapy regulates whole-chamber remodeling*. J Am Heart Assoc, 2013. **2**(3): p. e000140.
125. Hashemi, S.M., et al., *A placebo controlled, dose-ranging, safety study of allogenic mesenchymal stem cells injected by endomyocardial delivery after an acute myocardial infarction*. Eur Heart J, 2008. **29**(2): p. 251-9.
126. Suzuki, K., et al., *Role of interleukin-1 beta in acute inflammation and graft death after cell transplantation to the heart*. Circulation, 2004. **110**(11): p. 1219-1224.
127. Fukushima, S., et al., *Choice of Cell-Delivery Route for Skeletal Myoblast Transplantation for Treating Post-Infarction Chronic Heart Failure in Rat*. PLoS One, 2008. **3**(8).
128. Fukushima, S., et al., *Choice of cell-delivery route for skeletal myoblast transplantation for treating post-infarction chronic heart failure in rat*. PLoS One, 2008. **3**(8): p. e3071.
129. van der Spoel, T.I., et al., *Transendocardial cell injection is not superior to intracoronary infusion in a porcine model of ischaemic cardiomyopathy: a study on delivery efficiency*. J Cell Mol Med, 2012. **16**(11): p. 2768-76.
130. Van der Spoel, T.I., et al., *Transendocardial Cell Injection is Not Superior to Intracoronary Infusion in a Porcine Model of Chronic Ischemic Heart Disease: A Randomized Study on Efficiency Using Nuclear Imaging*. Circulation, 2011. **124**(21).
131. Lim, S.Y., et al., *The effects of mesenchymal stem cells transduced with Akt in a porcine myocardial infarction model*. Cardiovasc Res, 2006. **70**(3): p. 530-42.
132. Houtgraaf, J.H., et al., *Intracoronary infusion of allogeneic mesenchymal precursor cells directly after experimental acute myocardial infarction reduces infarct size, abrogates adverse remodeling, and improves cardiac function*. Circ Res, 2013. **113**(2): p. 153-66.
133. Valina, C., et al., *Intracoronary administration of autologous adipose tissue-derived stem cells improves left ventricular function, perfusion, and remodelling after acute myocardial infarction*. Eur Heart J, 2007. **28**(21): p. 2667-77.

134. Yang, Z.J., et al., *Experimental study of bone marrow-derived mesenchymal stem cells combined with hepatocyte growth factor transplantation via noninfarct-relative artery in acute myocardial infarction*. Gene Ther, 2006. **13**(22): p. 1564-8.
135. Yang, Z.J., et al., *Neovascularization and cardiomyocytes regeneration in acute myocardial infarction after bone marrow stromal cell transplantation: comparison of infarct-relative and noninfarct-relative arterial approaches in swine*. Clin Chim Acta, 2007. **381**(2): p. 114-8.
136. Vulliet, P.R., et al., *Intra-coronary arterial injection of mesenchymal stromal cells and microinfarction in dogs*. Lancet, 2004. **363**(9411): p. 783-4.
137. Grieve, S.M., et al., *Microvascular obstruction by intracoronary delivery of mesenchymal stem cells and quantification of resulting myocardial infarction by cardiac magnetic resonance*. Circ Heart Fail, 2010. **3**(3): p. e5-6.
138. Llano, R., et al., *Intracoronary Delivery of Mesenchymal Stem Cells at High Flow Rates After Myocardial Infarction Improves Distal Coronary Blood Flow and Decreases Mortality in Pigs*. Catheterization and Cardiovascular Interventions, 2009. **73**(2): p. 251-257.
139. Bach, R.R., *Initiation of coagulation by tissue factor*. CRC Crit Rev Biochem, 1988. **23**(4): p. 339-68.
140. Nemerson, Y., *Tissue factor and hemostasis*. Blood, 1988. **71**(1): p. 1-8.
141. Osterud, B. and E. Bjorklid, *Sources of tissue factor*. Semin Thromb Hemost, 2006. **32**(1): p. 11-23.
142. Key, N.S. and N. Mackman, *Tissue factor and its measurement in whole blood, plasma, and microparticles*. Semin Thromb Hemost, 2010. **36**(8): p. 865-75.
143. Zwicker, J.I., et al., *Tissue factor-bearing microparticles and thrombus formation*. Arterioscler Thromb Vasc Biol, 2011. **31**(4): p. 728-33.
144. Chen, T.S., et al., *Mesenchymal stem cell secretes microparticles enriched in pre-microRNAs*. Nucleic Acids Res, 2010. **38**(1): p. 215-24.
145. Chu, A.J., *Tissue factor, blood coagulation, and beyond: an overview*. Int J Inflam, 2011. **2011**: p. 367284.
146. Toomey, J.R., et al., *Targeted disruption of the murine tissue factor gene results in embryonic lethality*. Blood, 1996. **88**(5): p. 1583-7.
147. Chen, J., et al., *Tissue factor as a link between wounding and tissue repair*. Diabetes, 2005. **54**(7): p. 2143-54.
148. Xu, Z., et al., *Factor VII deficiency impairs cutaneous wound healing in mice*. Mol Med, 2010. **16**(5-6): p. 167-76.
149. Versteeg, H.H., et al., *Tissue factor and cancer metastasis: the role of intracellular and extracellular signaling pathways*. Mol Med, 2004. **10**(1-6): p. 6-11.
150. Pittenger, M.F., *Mesenchymal stem cells from adult bone marrow*. Methods Mol Biol, 2008. **449**: p. 27-44.
151. Barry, F.P. and J.M. Murphy, *Mesenchymal stem cells: clinical applications and biological characterization*. Int J Biochem Cell Biol, 2004. **36**(4): p. 568-84.
152. English, K., et al., *IFN-gamma and TNF-alpha differentially regulate immunomodulation by murine mesenchymal stem cells*. Immunol Lett, 2007. **110**(2): p. 91-100.

153. Klein, H.H., et al., *Temporal and spatial development of infarcts in porcine hearts*. Basic Res Cardiol, 1984. **79**(4): p. 440-7.
154. Doyle, B., et al., *Progenitor cell therapy in a porcine acute myocardial infarction model induces cardiac hypertrophy, mediated by paracrine secretion of cardiogenic factors including TGFbeta1*. Stem Cells Dev, 2008. **17**(5): p. 941-51.
155. De Luca, G., et al., *Effects of increasing doses of intracoronary adenosine on the assessment of fractional flow reserve*. JACC Cardiovasc Interv, 2011. **4**(10): p. 1079-84.
156. Gould, K.L. and K. Lipscomb, *Effects of coronary stenoses on coronary flow reserve and resistance*. Am J Cardiol, 1974. **34**(1): p. 48-55.
157. MacCarthy, P., et al., *Pressure-derived measurement of coronary flow reserve*. J Am Coll Cardiol, 2005. **45**(2): p. 216-20.
158. Pijls, N.H., et al., *Coronary thermodilution to assess flow reserve: validation in humans*. Circulation, 2002. **105**(21): p. 2482-6.
159. Basic Res CardiolMacCarthy, P., et al., *Pressure-derived measurement of coronary flow reserve*. J Am Coll Cardiol, 2005. **45**(2): p. 216-20.
160. Pijls, N.H. and B. De Bruyne, *Coronary pressure measurement and fractional flow reserve*. Heart, 1998. **80**(6): p. 539-42.
161. Leone, A.M., et al., *Maximal hyperemia in the assessment of fractional flow reserve: intracoronary adenosine versus intracoronary sodium nitroprusside versus intravenous adenosine: the NASCI (Nitroprussiato versus Adenosina nelle Stenosi Coronariche Intermedie) study*. JACC Cardiovasc Interv, 2012. **5**(4): p. 402-8.
162. Olsson, R.A., et al., *Evidence for an adenosine receptor on the surface of dog coronary myocytes*. Circ Res, 1976. **39**(1): p. 93-8.
163. Klinger, M., M. Freissmuth, and C. Nanoff, *Adenosine receptors: G protein-mediated signalling and the role of accessory proteins*. Cell Signal, 2002. **14**(2): p. 99-108.
164. Hynes, B., et al., *Potent endothelial progenitor cell-conditioned media-related anti-apoptotic, cardiogenic, and pro-angiogenic effects post-myocardial infarction are mediated by insulin-like growth factor-1*. Eur Heart J, 2013. **34**(10): p. 782-9.
165. Mandal, S.K., U.R. Pendurthi, and L.V. Rao, *Cellular localization and trafficking of tissue factor*. Blood, 2006. **107**(12): p. 4746-53.
166. Savage, B., E. Saldivar, and Z.M. Ruggeri, *Initiation of platelet adhesion by arrest onto fibrinogen or translocation on von Willebrand factor*. Cell, 1996. **84**(2): p. 289-97.
167. Zwaginga, J.J., et al., *Flow-based assays for global assessment of hemostasis. Part 1: Biorheologic considerations*. J Thromb Haemost, 2006. **4**(11): p. 2486-7.
168. Stepp, D.W., Y. Nishikawa, and W.M. Chilian, *Regulation of shear stress in the canine coronary microcirculation*. Circulation, 1999. **100**(14): p. 1555-61.
169. Weaver, M.E., et al., *A quantitative study of the anatomy and distribution of coronary arteries in swine in comparison with other animals and man*. Cardiovasc Res, 1986. **20**(12): p. 907-17.
170. Zaragoza, C., et al., *Animal models of cardiovascular diseases*. J Biomed Biotechnol, 2011. **2011**: p. 497841.

171. Dixon, J.A. and F.G. Spinale, *Large Animal Models of Heart Failure A Critical Link in the Translation of Basic Science to Clinical Practice*. Circulation-Heart Failure, 2009. **2**(3): p. 262-271.
172. Kim, W.G., et al., *Comparison of myocardial infarction with sequential ligation of the left anterior descending artery and its diagonal branch in dogs and sheep*. International Journal of Artificial Organs, 2003. **26**(4): p. 351-7.
173. Buckley, N.M., et al., *Age-Related Cardiovascular Effects of Catecholamines in Anesthetized Piglets*. Circulation Research, 1979. **45**(2): p. 282-292.
174. O'Sullivan, J.F., et al., *Multidetector computed tomography accurately defines infarct size, but not microvascular obstruction after myocardial infarction*. J Am Coll Cardiol, 2013. **61**(2): p. 208-10.
175. Theroux, P., et al., *Coronary arterial reperfusion. III. Early and late effects on regional myocardial function and dimensions in conscious dogs*. Am J Cardiol, 1976. **38**(5): p. 599-606.
176. Verdouw, P.D., et al., *Animal models in the study of myocardial ischaemia and ischaemic syndromes*. Cardiovascular Research, 1998. **39**(1): p. 121-135.
177. McCall, F.C., et al., *Myocardial infarction and intramyocardial injection models in swine*. Nature Protocols, 2012. **7**(8): p. 1479-1496.
178. Suzuki, Y., et al., *In vivo porcine model of reperfused myocardial infarction: in situ double staining to measure precise infarct area/area at risk*. Catheter Cardiovasc Interv, 2008. **71**(1): p. 100-7.
179. Garcia-Dorado, D., *Myocardial reperfusion injury: a new view*. Cardiovascular Research, 2004. **61**(3): p. 363-4.
180. Gyongyosi, M., et al., *Serial noninvasive in vivo positron emission tomographic tracking of percutaneously intramyocardially injected autologous porcine mesenchymal stem cells modified for transgene reporter gene expression*. Circ Cardiovasc Imaging, 2008. **1**(2): p. 94-103.
181. Jiang, Y., et al., *HO-1 gene overexpression enhances the beneficial effects of superparamagnetic iron oxide labeled bone marrow stromal cells transplantation in swine hearts underwent ischemia/reperfusion: an MRI study*. Basic Res Cardiol, 2010. **105**(3): p. 431-42.
182. Schneider, C., et al., *Transplantation of bone marrow-derived stem cells improves myocardial diastolic function: strain rate imaging in a model of hibernating myocardium*. J Am Soc Echocardiogr, 2009. **22**(10): p. 1180-9.
183. Wang, X., et al., *Stem cells for myocardial repair with use of a transarterial catheter*. Circulation, 2009. **120**(11 Suppl): p. S238-46.
184. Llano, R., et al., *Intracoronary delivery of mesenchymal stem cells at high flow rates after myocardial infarction improves distal coronary blood flow and decreases mortality in pigs*. Catheter Cardiovasc Interv, 2009. **73**(2): p. 251-7.
185. Perin, E.C., et al., *Comparison of intracoronary and transendocardial delivery of allogeneic mesenchymal cells in a canine model of acute myocardial infarction*. J Mol Cell Cardiol, 2008. **44**(3): p. 486-95.
186. Tomita, S., et al., *Improved heart function with myogenesis and angiogenesis after autologous porcine bone marrow stromal cell transplantation*. J Thorac Cardiovasc Surg, 2002. **123**(6): p. 1132-40.

187. Qi, C.M., et al., *Transplantation of magnetically labeled mesenchymal stem cells improves cardiac function in a swine myocardial infarction model*. Chin Med J (Engl), 2008. **121**(6): p. 544-50.
188. Amado, L.C., et al., *Multimodality noninvasive imaging demonstrates in vivo cardiac regeneration after mesenchymal stem cell therapy*. J Am Coll Cardiol, 2006. **48**(10): p. 2116-24.
189. Schuleri, K.H., et al., *Early improvement in cardiac tissue perfusion due to mesenchymal stem cells*. Am J Physiol Heart Circ Physiol, 2008. **294**(5): p. H2002-11.
190. Price, M.J., et al., *Intravenous mesenchymal stem cell therapy early after reperfused acute myocardial infarction improves left ventricular function and alters electrophysiologic properties*. Int J Cardiol, 2006. **111**(2): p. 231-9.
191. Halkos, M.E., et al., *Intravenous infusion of mesenchymal stem cells enhances regional perfusion and improves ventricular function in a porcine model of myocardial infarction*. Basic Res Cardiol, 2008. **103**(6): p. 525-36.
192. Hamamoto, H., et al., *Allogeneic mesenchymal precursor cell therapy to limit remodeling after myocardial infarction: the effect of cell dosage*. Ann Thorac Surg, 2009. **87**(3): p. 794-801.
193. Qian, H., et al., *Intracoronary delivery of autologous bone marrow mononuclear cells radiolabeled by 18F-fluoro-deoxy-glucose: tissue distribution and impact on post-infarct swine hearts*. J Cell Biochem, 2007. **102**(1): p. 64-74.
194. Li, N., et al., *Comparison of the labeling efficiency of BrdU, DiI and FISH labeling techniques in bone marrow stromal cells*. Brain Res, 2008. **1215**: p. 11-9.
195. Hamamoto, H., et al., *Allogeneic Mesenchymal Precursor Cell Therapy to Limit Remodeling After Myocardial Infarction: The Effect of Cell Dosage*. Annals of Thoracic Surgery, 2009. **87**(3): p. 794-802.
196. Meluzin, J., et al., *Autologous transplantation of mononuclear bone marrow cells in patients with acute myocardial infarction: the effect of the dose of transplanted cells on myocardial function*. Am Heart J, 2006. **152**(5): p. 975 e9-15.
197. Chen, S.L., et al., *Effect on left ventricular function of intracoronary transplantation of autologous bone marrow mesenchymal stem cell in patients with acute myocardial infarction*. Am J Cardiol, 2004. **94**(1): p. 92-5.
198. Freyman, T., et al., *A quantitative, randomized study evaluating three methods of mesenchymal stem cell delivery following myocardial infarction*. Eur Heart J, 2006. **27**(9): p. 1114-1122.
199. Penn, E.C., et al., *Comparison of intracoronary and transendocardial delivery of allogeneic mesenchymal cells in a canine model of acute myocardial infarction*. Journal of Molecular and Cellular Cardiology, 2008. **44**(3): p. 486-495.
200. Houtgraaf, J.H., et al., *Intracoronary Infusion of Allogeneic Mesenchymal Precursor Cells Directly After Experimental Acute Myocardial Infarction Reduces Infarct Size, Abrogates Adverse Remodeling, and Improves Cardiac Function*. Circulation Research, 2013. **113**(2): p. 153-166.

201. Furlani, D., et al., *Is the intravascular administration of mesenchymal stem cells safe? Mesenchymal stem cells and intravital microscopy*. Microvascular Research, 2009. **77**(3): p. 370-376.
202. Fischer, U.M., et al., *Pulmonary Passage is a Major Obstacle for Intravenous Stem Cell Delivery: The Pulmonary First-Pass Effect*. Stem Cells and Development, 2009. **18**(5): p. 683-691.
203. Toma, C., et al., *Fate Of Culture-Expanded Mesenchymal Stem Cells in The Microvasculature In Vivo Observations of Cell Kinetics*. Circulation Research, 2009. **104**(3): p. 398-U204.
204. Ankrum, J. and J.M. Karp, *Mesenchymal stem cell therapy: Two steps forward, one step back*. Trends in Molecular Medicine, 2010. **16**(5): p. 203-209.
205. Gao, J., et al., *The dynamic in vivo distribution of bone marrow-derived mesenchymal stem cells after infusion*. Cells Tissues Organs, 2001. **169**(1): p. 12-20.
206. Schrepfer, S., et al., *Stem cell transplantation: The lung barrier*. Transplantation Proceedings, 2007. **39**(2): p. 573-576.
207. Schrepfer, S., et al., *Stem cell transplantation: The lung barrier*. Transplant Proc, 2007. **39**(2): p. 573-576.
208. Savage, B., F. Almus-Jacobs, and Z.M. Ruggeri, *Specific synergy of multiple substrate-receptor interactions in platelet thrombus formation under flow*. Cell, 1998. **94**(5): p. 657-66.
209. Bonderman, D., et al., *Coronary no-reflow is caused by shedding of active tissue factor from dissected atherosclerotic plaque*. Blood, 2002. **99**(8): p. 2794-800.
210. Kretz, C.A., N. Vaezzadeh, and P.L. Gross, *Tissue factor and thrombosis models*. Arterioscler Thromb Vasc Biol, 2010. **30**(5): p. 900-8.
211. Stephenne, X., et al., *Bivalirudin in combination with heparin to control mesenchymal cell procoagulant activity*. PLoS One, 2012. **7**(8): p. e42819.
212. Lupu, C., et al., *Cellular effects of heparin on the production and release of tissue factor pathway inhibitor in human endothelial cells in culture*. Arteriosclerosis Thrombosis and Vascular Biology, 1999. **19**(9): p. 2251-2262.
213. Rumbaut, R.E. and P. Thiagarajan, in *Platelet-Vessel Wall Interactions in Hemostasis and Thrombosis*. 2010: San Rafael (CA).
214. Moll, G., et al., *Are therapeutic human mesenchymal stromal cells compatible with human blood?* Stem Cells, 2012. **30**(7): p. 1565-74.
215. Tatsumi, K., et al., *Tissue factor triggers procoagulation in transplanted mesenchymal stem cells leading to thromboembolism*. Biochemical and Biophysical Research Communications, 2013. **431**(2): p. 203-209.
216. Aberg, M. and A. Siegbahn, *Tissue factor non-coagulant signaling - molecular mechanisms and biological consequences with a focus on cell migration and apoptosis*. J Thromb Haemost, 2013. **11**(5): p. 817-25.
217. Prockop, D.J., *Marrow stromal cells as stem cells for continual renewal of nonhematopoietic tissues and as potential vectors for gene therapy*. Journal of Cellular Biochemistry, 1998: p. 284-285.
218. Bruder, S.P., D.J. Fink, and A.I. Caplan, *Mesenchymal Stem-Cells in in Bone-Development, Bone Repair, and Skeletal Regeneration Therapy*. Journal of Cellular Biochemistry, 1994. **56**(3): p. 283-294.

219. Orlic, D., et al., *Bone marrow cells regenerate infarcted myocardium*. Nature, 2001. **410**(6829): p. 701-5.
220. Gyongyosi, M., et al., *Delayed Recovery of Myocardial Blood Flow After Intracoronary Stem Cell Administration*. Stem Cell Reviews and Reports, 2011. **7**(3): p. 616-623.
221. Jaffe, R., et al., *Microvascular obstruction and the no-reflow phenomenon after percutaneous coronary intervention*. Circulation, 2008. **117**(24): p. 3152-6.
222. Kloner, R.A., C.E. Ganote, and R.B. Jennings, *The "no-reflow" phenomenon after temporary coronary occlusion in the dog*. J Clin Invest, 1974. **54**(6): p. 1496-508.
223. Rezkalla, S.H. and R.A. Kloner, *Coronary No-Reflow Phenomenon: From the Experimental Laboratory to the Cardiac Catheterization Laboratory*. Catheterization and Cardiovascular Interventions, 2008. **72**(7): p. 950-957.
224. Eeckhout, E. and M.J. Kern, *The coronary no-reflow phenomenon: a review of mechanisms and therapies*. Eur Heart J, 2001. **22**(9): p. 729-39.
225. Morishima, I., et al., *Angiographic no-reflow phenomenon as a predictor of adverse long-term outcome in patients treated with percutaneous transluminal coronary angioplasty for first acute myocardial infarction*. Journal of the American College of Cardiology, 2000. **36**(4): p. 1202-1209.
226. Salerno, M. and G.A. Beller, *Noninvasive assessment of myocardial perfusion*. Circ Cardiovasc Imaging, 2009. **2**(5): p. 412-24.
227. Grieve, S.M., et al., *Microvascular Obstruction by Intracoronary Delivery of Mesenchymal Stem Cells and Quantification of Resulting Myocardial Infarction by Cardiac Magnetic Resonance*. Circulation-Heart Failure, 2010. **3**(3): p. E5-E6.
228. Uemura, R., et al., *Bone marrow stem cells prevent left ventricular remodeling of ischemic heart through paracrine signaling*. Circulation Research, 2006. **98**(11): p. 1414-1421.
229. Hynes, B., et al., *Potent endothelial progenitor cell-conditioned media-related anti-apoptotic, cardioprotective, and pro-angiogenic effects post-myocardial infarction are mediated by insulin-like growth factor-1*. Eur Heart J, 2013. **34**(10): p. 782-789.
230. Tatsumi, K., et al., *Tissue factor triggers procoagulation in transplanted mesenchymal stem cells leading to thromboembolism*. Biochem Biophys Res Commun, 2013. **431**(2): p. 203-9.
231. Schecter, A.D., et al., *Tissue factor expression in human arterial smooth muscle cells - TF is present in three cellular pools after growth factor stimulation*. Journal of Clinical Investigation, 1997. **100**(9): p. 2276-2285.
232. Steffel, J., T.F. Luscher, and F.C. Tanner, *Tissue factor in cardiovascular diseases - Molecular mechanisms and clinical implications*. Circulation, 2006. **113**(5): p. 722-731.
233. Owens, A.P., 3rd and N. Mackman, *Microparticles in hemostasis and thrombosis*. Circulation Research, 2011. **108**(10): p. 1284-97.
234. Mendolicchio, G.L. and Z.M. Ruggeri, *New perspectives on von Willebrand factor functions in hemostasis and thrombosis*. Semin Hematol, 2005. **42**(1): p. 5-14.

235. Minami, T., et al., *Thrombin and phenotypic modulation of the endothelium*. Arteriosclerosis Thrombosis and Vascular Biology, 2004. **24**(1): p. 41-53.
236. Kranzhofer, R., et al., *Thrombin potently stimulates cytokine production in human vascular smooth muscle cells but not in mononuclear phagocytes*. Circulation Research, 1996. **79**(2): p. 286-294.
237. Johnson, K., et al., *Potential mechanisms for a proinflammatory vascular cytokine response to coagulation activation*. J Immunol, 1998. **160**(10): p. 5130-5.
238. Qi, J.F., D.L. Kreutzer, and T.H. PielaSmith, *Fibrin induction of ICAM-1 expression in human vascular endothelial cells*. Journal of Immunology, 1997. **158**(4): p. 1880-1886.
239. Skogen, W.F., et al., *Fibrinogen-Derived Peptide B-Beta-1-42 Is a Multidomained Neutrophil Chemoattractant*. Blood, 1988. **71**(5): p. 1475-1479.
240. Breitenstein, A., et al., *Amiodarone inhibits arterial thrombus formation and tissue factor translation*. Arterioscler Thromb Vasc Biol, 2008. **28**(12): p. 2231-8.
241. Celi, A., et al., *Angiotensin II, tissue factor and the thrombotic paradox of hypertension*. Expert Rev Cardiovasc Ther, 2010. **8**(12): p. 1723-9.
242. Alkistis Frentzou, G., et al., *Differential induction of cellular proliferation, hypertrophy and apoptosis in H9c2 cardiomyocytes by exogenous tissue factor*. Mol Cell Biochem, 2010. **345**(1-2): p. 119-30.
243. Gudmundsdóttir, I.J., et al., *Role of the Endothelium in the Vascular Effects of the Thrombin Receptor (Protease-Activated Receptor Type 1) in Humans*. Journal of the American College of Cardiology, 2008. **51**(18): p. 1749-1756.
244. Dorfleutner, A., et al., *Cross-talk of integrin alpha3beta1 and tissue factor in cell migration*. Mol Biol Cell, 2004. **15**(10): p. 4416-25.
245. Agis, H., et al., *Activated Platelets Increase Fibrinolysis of Mesenchymal Progenitor Cells*. Journal of Orthopaedic Research, 2009. **27**(7): p. 972-980.
246. Petitou, M., B. Casu, and U. Lindahl, *1976-1983, a critical period in the history of heparin: the discovery of the antithrombin binding site*. Biochimie, 2003. **85**(1-2): p. 83-9.
247. Rao, S.V. and E.M. Ohman, *Anticoagulant Therapy for Percutaneous Coronary Intervention*. Circulation: Cardiovascular Interventions, 2010. **3**(1): p. 80-88.
248. Narins, C.R., et al., *Relation Between Activated Clotting Time During Angioplasty and Abrupt Closure*. Circulation, 1996. **93**(4): p. 667-671.
249. Seeger, F.H., et al., *Heparin Disrupts the CXCR4/SDF-1 Axis and Impairs the Functional Capacity of Bone Marrow-Derived Mononuclear Cells Used for Cardiovascular Repair*. Circulation Research, 2012. **111**(7): p. 854-862.
250. Fujitaka, K., et al., *Heparin Mobilizes Multipotent Human Mesoangioblasts*. Circulation, 2011. **124**(21).
251. Gibson, C.M., et al., *A randomized trial to evaluate the relative protection against post-percutaneous coronary intervention microvascular dysfunction, ischemia, and inflammation among antiplatelet and*

- antithrombotic agents: the PROTECT-TIMI-30 trial.* J Am Coll Cardiol, 2006. **47**(12): p. 2364-73.
252. Ettelaie, C., et al., *Low molecular weight heparin downregulates tissue factor expression and activity by modulating growth factor receptor-mediated induction of nuclear factor-kappa B.* Biochimica Et Biophysica Acta-Molecular Basis of Disease, 2011. **1812**(12): p. 1591-1600.
 253. Breitenstein, A., et al., *Amiodarone Inhibits Arterial Thrombus Formation and Tissue Factor Translation.* Arteriosclerosis Thrombosis and Vascular Biology, 2008. **28**(12): p. 2231-U177.
 254. Bogaert, J., et al., *Determinants and impact of microvascular obstruction in successfully reperfused ST-segment elevation myocardial infarction. Assessment by magnetic resonance imaging.* Eur Radiol, 2007. **17**(10): p. 2572-80.
 255. Orn, S., et al., *Microvascular obstruction is a major determinant of infarct healing and subsequent left ventricular remodelling following primary percutaneous coronary intervention.* Eur Heart J, 2009. **30**(16): p. 1978-1985.
 256. Houtgraaf, J.H., et al., *Intracoronary Infusion of Allogeneic Mesenchymal Precursor Cells Directly Following Experimental Acute Myocardial Infarction Reduces Infarct Size, Abrogates Adverse Remodeling and Improves Cardiac Function.* Circulation Research, 2013.
 257. Pfeffer, M.A. and E. Braunwald, *Ventricular Remodeling after Myocardial-Infarction - Experimental-Observations and Clinical Implications.* Circulation, 1990. **81**(4): p. 1161-1172.
 258. D'Cruz, I.A., et al., *Differences in the shape of the normal, cardiomyopathic, and volume overloaded human left ventricle.* J Am Soc Echocardiogr, 1989. **2**(6): p. 408-14.
 259. Williams, A.R. and J.M. Hare, *Mesenchymal stem cells: biology, pathophysiology, translational findings, and therapeutic implications for cardiac disease.* Circ Res, 2011. **109**(8): p. 923-40.
 260. Marban, E. and K. Malliaras, *Mixed Results for Bone Marrow-Derived Cell Therapy for Ischemic Heart Disease.* Jama-Journal of the American Medical Association, 2012. **308**(22): p. 2405-2406.
 261. Traverse, J.H., et al., *Effect of the Use and Timing of Bone Marrow Mononuclear Cell Delivery on Left Ventricular Function After Acute Myocardial Infarction The TIME Randomized Trial.* Jama-Journal of the American Medical Association, 2012. **308**(22): p. 2380-2389.
 262. Surder, D., et al., *Intracoronary injection of bone marrow-derived mononuclear cells early or late after acute myocardial infarction: effects on global left ventricular function.* Circulation, 2013. **127**(19): p. 1968-79.
 263. Sutton, M.S., et al., *Left ventricular remodeling and ventricular arrhythmias after myocardial infarction.* Circulation, 2003. **107**(20): p. 2577-2582.
 264. Williams, A.R., et al., *Durable Scar Size Reduction Due to Allogeneic Mesenchymal Stem Cell Therapy Regulates Whole-Chamber Remodeling.* Journal of the American Heart Association, 2013. **2**(3).
 265. Ismail Siti, E.F., M. Creane, M. Harte, M. Murphy, T. O'Brien, F. Barry *Elucidating the cardioprotective role of SPARCL1 in ex vivo model of myocardial infarction,* in *Microscopy Society of Ireland.* 2013: Galway, Ireland.

266. Brekken, R.A. and E.H. Sage, *SPARC, a matricellular protein: at the crossroads of cell-matrix*. Matrix Biol, 2000. **19**(7): p. 569-80.
267. Hambrock, H.O., et al., *SC1/hevin. An extracellular calcium-modulated protein that binds collagen I*. J Biol Chem, 2003. **278**(13): p. 11351-8.
268. Sullivan, M.M., et al., *Matricellular hevin regulates decorin production and collagen assembly*. J Biol Chem, 2006. **281**(37): p. 27621-32.
269. Soderling, J.A., et al., *Cloning and expression of murine SC1, a gene product homologous to SPARC*. J Histochem Cytochem, 1997. **45**(6): p. 823-35.
270. Schellings, M.W., et al., *Absence of SPARC results in increased cardiac rupture and dysfunction after acute myocardial infarction*. J Exp Med, 2009. **206**(1): p. 113-23.
271. Chaurasia, S.S., et al., *Correction: Hevin Plays a Pivotal Role in Corneal Wound Healing*. PLoS One, 2014. **9**(1).
272. Ikonomidis, J.S., et al., *Accelerated LV remodeling after myocardial infarction in TIMP-1-deficient mice: effects of exogenous MMP inhibition*. Am J Physiol Heart Circ Physiol, 2005. **288**(1): p. H149-58.
273. Kandalam, V., et al., *TIMP2 deficiency accelerates adverse post-myocardial infarction remodeling because of enhanced MT1-MMP activity despite lack of MMP2 activation*. Circ Res, 2010. **106**(4): p. 796-808.
274. Lobb, D.C., et al., *Temporal Effects of Targeted Release of Recombinant Tissue Inhibitor of Matrix Metalloproteinase Post Myocardial Infarction: Relation to Determinants of Remodeling*, in AHA. 2013, Circulation: Dallas, TX.
275. Ma, Y., A. Yabluchanskiy, and M.L. Lindsey, *Neutrophil roles in left ventricular remodeling following myocardial infarction*. Fibrogenesis Tissue Repair, 2013. **6**(1): p. 11.
276. Krishnamurthy, P., et al., *IL-10 inhibits inflammation and attenuates left ventricular remodeling after myocardial infarction via activation of STAT3 and suppression of HuR*. Circ Res, 2009. **104**(2): p. e9-18.
277. van der Spoel, T.I., et al., *Human relevance of pre-clinical studies in stem cell therapy: systematic review and meta-analysis of large animal models of ischaemic heart disease*. Cardiovasc Res, 2011. **91**(4): p. 649-58.
278. Heldman, A.W., et al., *Transendocardial mesenchymal stem cells and mononuclear bone marrow cells for ischemic cardiomyopathy: the TAC-HFT randomized trial*. JAMA, 2014. **311**(1): p. 62-73.
279. Seeger, F.H., et al., *Heparin disrupts the CXCR4/SDF-1 axis and impairs the functional capacity of bone marrow-derived mononuclear cells used for cardiovascular repair*. Circ Res, 2012. **111**(7): p. 854-62.
280. Uygun, B.E., S.E. Stojish, and H.W. Matthew, *Effects of immobilized glycosaminoglycans on the proliferation and differentiation of mesenchymal stem cells*. Tissue Eng Part A, 2009. **15**(11): p. 3499-512.
281. Ozmen, L., et al., *Inhibition of thrombin abrogates the instant blood-mediated inflammatory reaction triggered by isolated human islets: possible application of the thrombin inhibitor melagatran in clinical islet transplantation*. Diabetes, 2002. **51**(6): p. 1779-84.
282. Contreras, J.L., et al., *Activated protein C preserves functional islet mass after intraportal transplantation: a novel link between endothelial cell*

- activation, thrombosis, inflammation, and islet cell death. *Diabetes*, 2004. **53**(11): p. 2804-14.
283. Karantalis, V., et al., *Cell-based therapy for prevention and reversal of myocardial remodeling*. *Am J Physiol Heart Circ Physiol*, 2012. **303**(3): p. H256-70.
 284. Frink, R.J., et al., *Coronary thrombosis and platelet/fibrin microemboli in death associated with acute myocardial infarction*. *Br Heart J*, 1988. **59**(2): p. 196-200.
 285. Davies, M.J., et al., *Intramyocardial platelet aggregation in patients with unstable angina suffering sudden ischemic cardiac death*. *Circulation*, 1986. **73**(3): p. 418-27.
 286. Hare, J.M., et al., *A randomized, double-blind, placebo-controlled, dose-escalation study of intravenous adult human mesenchymal stem cells (prochymal) after acute myocardial infarction*. *J Am Coll Cardiol*, 2009. **54**(24): p. 2277-86.
 287. Bartunek, J., et al., *The consensus of the task force of the European Society of Cardiology concerning the clinical investigation of the use of autologous adult stem cells for repair of the heart*. *Eur Heart J*, 2006. **27**(11): p. 1338-40.
 288. Sakaguchi, K., et al., *In vitro engineering of vascularized tissue surrogates*. *Sci Rep*, 2013. **3**: p. 1316.
 289. Trams, E.G., et al., *Exfoliation of membrane ecto-enzymes in the form of micro-vesicles*. *Biochim Biophys Acta*, 1981. **645**(1): p. 63-70.
 290. Lai, R.C., et al., *Exosome secreted by MSC reduces myocardial ischemia/reperfusion injury*. *Stem Cell Res*, 2010. **4**(3): p. 214-22.
 291. Arslan, F., et al., *Mesenchymal stem cell-derived exosomes increase ATP levels, decrease oxidative stress and activate PI3K/Akt pathway to enhance myocardial viability and prevent adverse remodeling after myocardial ischemia/reperfusion injury*. *Stem Cell Res*, 2013. **10**(3): p. 301-12.
 292. Martinez, M.C. and R. Andriantsitohaina, *Microparticles in angiogenesis: therapeutic potential*. *Circ Res*, 2011. **109**(1): p. 110-9.
 293. Park, J.A., et al., *Tissue factor-bearing exosome secretion from human mechanically stimulated bronchial epithelial cells in vitro and in vivo*. *J Allergy Clin Immunol*, 2012. **130**(6): p. 1375-83.
 294. Hahn, J.Y., et al., *Pre-treatment of mesenchymal stem cells with a combination of growth factors enhances gap junction formation, cytoprotective effect on cardiomyocytes, and therapeutic efficacy for myocardial infarction*. *J Am Coll Cardiol*, 2008. **51**(9): p. 933-43.
 295. Pasha, Z., et al., *Preconditioning enhances cell survival and differentiation of stem cells during transplantation in infarcted myocardium*. *Cardiovasc Res*, 2008. **77**(1): p. 134-42.
 296. Bao, C., et al., *TNFR gene-modified mesenchymal stem cells attenuate inflammation and cardiac dysfunction following MI*. *Scand Cardiovasc J*, 2008. **42**(1): p. 56-62.
 297. Cheng, Z., et al., *Targeted migration of mesenchymal stem cells modified with CXCR4 gene to infarcted myocardium improves cardiac performance*. *Mol Ther*, 2008. **16**(3): p. 571-9.

298. Gao, F., et al., *A promising strategy for the treatment of ischemic heart disease: Mesenchymal stem cell-mediated vascular endothelial growth factor gene transfer in rats*. Can J Cardiol, 2007. **23**(11): p. 891-8.
299. Song, H., et al., *Transfection of mesenchymal stem cells with the FGF-2 gene improves their survival under hypoxic conditions*. Mol Cells, 2005. **19**(3): p. 402-7.

Chapter 9 Appendix

9.1 MSC DiI Labelling



Vybrant™ Cell-Labeling Solutions

Experimental Protocols

Labeling of Cells in Suspension

- 1.1** Suspend cells at a density of $1 \times 10^6/\text{mL}$ in any chosen serum-free culture medium (note A).
- 1.2** Add 5 μL of the cell-labeling solution supplied per mL of cell suspension. Mix well by gentle pipetting.
- 1.3** Incubate for 1–20 minutes at 37°C . The optimal incubation time will vary depending on cell type. Typical incubation times required to produce uniform staining are shown in Table 1 (note B). For cell types other than those listed, start by incubating for 20 minutes and subsequently optimize as necessary to obtain uniform labeling.
- 1.4** Centrifuge the labeled suspension tubes at 1500 rpm for 5 minutes, preferably at 37°C .
- 1.5** Remove the supernatant and gently resuspend the cells in warm (37°C) medium.
- 1.6** Repeat the wash procedure (1.4 and 1.5) two more times.
- 1.7** Allow 10 minutes recovery time before proceeding with fluorescence measurements.

9.2 7AAD Staining



Product Information

7-Aminoactinomycin D

Product Number **A 9400**

Storage Temperature **-2-8 °C**

Product Description

Molecular Formula: $C_{42}H_{57}N_{13}O_{16}$

Molecular Weight: 1,270

CAS Number: 7240-37-1

Synonym: 7-AAD

Fluorescent Properties

Free form:

Excitation: 503 nm (0.01 M phosphate buffer,

pH 7.0 containing 0.1 mM EDTA)¹; 550 nm²

Emission: 675 nm (0.01 M phosphate buffer,

pH 7.0 containing 0.1 mM EDTA)¹; 672 nm²

DNA Complex:

Excitation: 543 nm¹; 555 nm²

Emission: 655 nm¹; 665 nm²

7-AAD is used in flow cytometry analysis of viable cells. Cell surface markers were stained by FITC and phycoerythrin-conjugated antibody. After surface staining, cells were further stained with 10 µg/ml of 7-AAD in PBS on ice for 30 minutes. After washing with PBS twice, the cells were fixed in 1% paraformaldehyde supplemented with 50 µg/ml actinomycin D. Non-apoptotic cells are 7-AAD negative.³

This material like its parent molecule, Actinomycin D, is a DNA-intercalator with growth-inhibitory properties.^{4,5}

This product has been tested for its labeling properties on transformed thymocytes that are scanned by FACS. It was possible to distinguish diploid, triploid and tetraploid sub-populations and % mitosis. When tested at fixed intervals of time, it was possible to calculate generation time.

Precautions and Disclaimer

For Laboratory Use Only. Not for drug, household or other uses.

Preparation Instructions

7-AAD is soluble in chloroform (1 mg/ml) and produce a clear, dark red solution. One milligram of 7-AAD is soluble in 50 µl of absolute methanol. A further addition of 950 µl of 1x PBS with Ca^{2+} and Mg^{2+} will achieve a concentration of 1 mg/ml.⁶

Storage/Stability

A solution prepared by adding 1mg of 7-AAD to 50 µl of absolute methanol followed by a further addition of 950 µl of 1x PBS with Ca^{2+} and Mg^{2+} was stable for several months when stored tightly closed and protected from light at 4 °C.⁶

References

1. Gill, J.E., et al., 7-Aminoactinomycin D as a Cytochemical Probe. I. Spectral Properties. *J. Histochem. Cytochem.*, **23**(11), 793-799 (1975).
2. Sengupta, S.K., et al., 7-substituted Actinomycin D analogs. Chemical and Growth-inhibitory Studies. *J. Med. Chem.*, **18**(12), 1175-1180 (1975).
3. Su, X., et al., *J. Immunology*, **156**, 4198 (1996).
4. *Cancer Chemotherapy Reports*, **58**, 35 (1974).
5. Madhavarao, M.S., et al., N7-Substituted 7-aminoactinomycin D Analogues. Synthesis and Biological Properties. *J. Med. Chem.*, **21**(9), 958-961 (1978).
6. <http://cyto.mednet.ucla.edu/7aad%20Staining%20for%20dead%20cells.htm>

HLD/RXR 8/03

9.3 Coronary Flow Research Theory[157]

Theory. The general fluid dynamic equation has been proposed to evaluate the pressure gradient induced by an epicardial coronary stenosis (1,10).

$$\Delta P = fQ + sQ^2 \quad [1]$$

The two terms of the equation correspond to different mechanisms of pressure (energy) loss across the obstruction. The constant “f” represents viscous friction at the site of the

lesion, the constant “s” represents expansion losses caused by convective acceleration of blood beyond the stenosis, and “Q” is coronary blood flow (10). The relative importance of the various components of this equation, therefore, varies according to the stenosis analyzed. At low flow rates or very long stenosis lengths, friction is the most important determinant of energy loss. However, at higher coronary flow rates (within the physiological range) and short or moderate stenosis lengths, friction loss is generally considered negligible (10). Therefore, assuming, indeed, that this term can be neglected, ΔP is only proportional to Q^2 , i.e.,

$$\Delta P \propto Q^2 \quad [2]$$

therefore,

$$\sqrt{\Delta P} \propto Q \quad [3]$$

so if:

$$CFR = Q_{\text{during hyperemia}} / Q_{\text{at rest}} \quad [4]$$

then:

$$CFR = \sqrt{\Delta P}_{\text{during hyperemia}} / \sqrt{\Delta P}_{\text{at rest}} \quad [5]$$

Values of $\sqrt{\Delta P}$ (i.e., the square root of the pressure gradient across the coronary lesion) can be obtained easily and accurately from the intracoronary pressure wire. At the same time, thermodilution CFR can be obtained, and the two methods of measuring CFR can be compared.

9.4 TF Activity Assay



INTENDED USE

The ACTICHROME® TF activity assay is a chromogenic assay intended for the measurement of human tissue factor procoagulant activity in cell lysates and human plasma. This assay is intended for research use only. It is not intended for diagnostic or therapeutic use.

EXPLANATION OF THE TEST

Tissue Factor (TF) is a 45 kD transmembrane cell surface glycoprotein known for its role in initiating coagulation for the past 90 years.¹ TF is comprised of three domains: an extracellular domain (aa 1-219), followed by a hydrophilic spanning domain (aa 220-242) and a cytoplasmic tail (aa 243-263).² It functions as a receptor and cofactor for the latent serine proteases factor VII and VIIa.^{3,4} Contact between TF and blood is sufficient to initiate the extrinsic pathway of coagulation. TF is located on the cells in the adventitia and variably on cells in cell culture.

In vitro studies reveal that once TF complexes with factor VII, factor VII is efficiently activated by factor Xa. Other proteases including factor IXa, factor XIIa and thrombin are also capable of activating factor VII. As with all vitamin K-dependent zymogens, activation requires the presence of calcium ions and phospholipids. Factor VII activation differs from the activation of other vitamin K-dependent zymogens by its binding to TF, which causes a major allosteric change, and its upregulation by TF. Formation of this TF/FVIIa complex renders the factor VII bond at Arg152 - Ile153 susceptible to cleavage by trace amounts of factor Xa and factor IXa. Activation by factor Xa is profoundly enhanced by lipidated TF but not by soluble TF (aa 1-219). TF lipidation by acidic phospholipids is more efficient than vesicles made with phosphatidylcholine (PC). This suggests that factor Xa mediated activation of factor VII requires binding of the Gla-domain to the phospholipid head groups.^{5,6}

Factor VIIa possesses little proteolytic activity in itself. Only when bound to TF does factor VIIa possess sufficient proteolytic activity to activate factor IX and factor X. Although factor VIIa possesses some activity towards peptidyl substrates in the presence of apo TF protein and calcium ions, this is not the case for physiological substrates such as factor IX and factor X. These factors require negatively charged phospholipids for full expression of factor VIIa proteolytic activity.⁷ Gamma carboxylation of the factor VII Gla-domain is crucial for manifestation of full biologic activity. Factor VII mutants lacking the Gla-domain have a markedly diminished capacity to bind to tissue factor. The EGF domain of factor VIIa (aa 51-88) is possibly a TF binding site. The interaction of factor VIIa with TF involves multiple binding sites: the N-terminal Gla-domain, the EGF domain, and amino acid residues located in the factor VII protease domain.

When monocytes and macrophages are stimulated by endotoxins, cytokines and lectins, TF is upregulated in these cells with an increase in procoagulant activity (PCA). Studies have reported patients diagnosed with Disseminated Intravascular Coagulation (DIC) as having an increase in TF plasma levels.¹⁰

Tissue Factor is released into the blood stream following disruption of the endothelium. The initiation of the coagulation pathways requires the participation of a series of molecules; TF and its ability to complex with, factor VII¹¹, factor X or factor IX, charged phospholipids and calcium (the catalytic activity of factor VIIa in comparison to VII is insignificant).¹² The TF/FVIIa complex efficiently activates both factor X and factor IX, thus

initiating both the intrinsic and extrinsic coagulation pathways.¹³ The extrinsic pathway is blocked by Tissue Factor Pathway Inhibitor, TFPI, the only effective inhibitor of TF/FVIIa allowing factor IX to activate factor X.¹⁴

PRINCIPLE OF THE METHOD

The ACTICHROME TF assay measures the peptidyl activity of human tissue factor in cell lysates and human plasma. Samples are mixed with human factor VIIa and human factor X and incubated at 37°C, during which time the tissue factor/factor VIIa complex (TF/FVIIa) is formed and the complex converts the human factor X to Factor Xa. The amount of factor Xa generated is measured by its ability to cleave SPECTROZYME® FXa, a highly specific chromogenic substrate for factor Xa, which is added to the reaction solution. The cleaved substrate releases a para-nitroaniline (pNA) chromophore into the reaction solution. The solution absorbance is read at 405 nm and compared to those values obtained from a standard curve generated using known amounts of human tissue factor.

REAGENTS

ACTICHROME TF contains sufficient reagents to perform 100 tests using a microtiter well format; 44 samples assayed in duplicate.

1. Assay Buffer: 1 vial of 5 mL, 10X concentrate
2. TF/TFPI Depleted Plasma: 2 vials, 0.5 mL (lyophilized)
3. Relipidated Human Tissue Factor: 1 vial, 500 pM (lyophilized)
4. Human Factor VIIa: 2 vials (lyophilized)
5. Human Factor X: 2 vials (lyophilized)
6. SPECTROZYME® FXa: 2 vials, 5 µmoles (lyophilized)

WARNING

The TF/TFPI Depleted Plasma provided is of human origin. Each donor unit used in the manufacture of this reagent has been tested and found to be non-reactive for Hepatitis B surface Antigen (HBsAg), Hepatitis C Virus (HCV) and Human Immunodeficiency Virus (HIV). As no known method can offer complete assurance that products derived from human blood will not transmit HBsAg, HCV, HIV or other blood-borne pathogens, this plasma should be handled as recommended for any potentially infectious human serum or blood specimen.

REAGENT RECONSTITUTION AND STABILITY

Unopened reagents are stable until the expiration date indicated on their label when stored at 2° - 8°C. Reconstituted reagents may be aliquoted and stored at -20°C for up to one month. Do not submit frozen reagents to multiple freeze-thaw cycles.

1. **Assay Buffer:** Add the contents of the vial (5 mL) to 45 mL of cold filtered deionized water and mix thoroughly.
2. **Human Factor VIIa:** Add 1.4 mL of filtered deionized water to the vial.
3. **Human Factor X:** Add 1.4 mL of filtered deionized water to the vial.
4. **SPECTROZYME® FXa:** Add 2.0 mL of filtered deionized water to the vial and mix thoroughly. Reconstituted substrate may be stored at -20°C or colder for up to 6 months.
5. **TF/TFPI Depleted Plasma:** Add 0.5 mL of Assay Buffer to the vial, mix thoroughly and place the vial on ice for 3 minutes. Add the content of the vial to an additional 9.5 mL of Assay Buffer (a 1:20 dilution) to create a 5% TF/TFPI Depleted Plasma. Place on ice for immediate use or aliquot into plastic cryotubes and store **immediately** at -20°C.
- 6a. **Tissue Factor Standard for Cell Lysate Samples:** Add 2.3 mL of Assay Buffer to the vial of Relipidated Human Tissue Factor to generate a 500 pM solution. Aliquot and immediately freeze at -20°C the stock 500 pM Tissue Factor solution that will not be used immediately. Label cryotubes and prepare standards of Tissue Factor as listed below in Table 1, by adding the specified volume of Standard to the specified volume of Assay Buffer. Discard any unused diluted standards.

- 6b. Tissue Factor Standard for Plasma Samples:** Add 2.3 mL of 5% TFPI Depleted Plasma to the vial of Relipidated Human Tissue Factor to generate a 500 pM solution. Label cryotubes and prepare standards of Tissue Factor as listed below in Table 1, by adding the specified volume of Standard to the specified volume of 5% TFPI Depleted Plasma. Discard any unused diluted standards.

Table 1 –Preparation of Tissue Factor Standards

Tissue Factor Standard Concentration	Volume of Tissue Factor Standard	Volume of Assay Buffer or 5% TF/TFPI Depleted Plasma
30 pM	20 μ L of 500 pM	313 μ L
15 pM	100 μ L of 30 pM	100 μ L
7.5 pM	100 μ L of 15 pM	100 μ L
3.75 pM	100 μ L of 7.5 pM	100 μ L
1.88 pM	100 μ L of 3.75 pM	100 μ L
0.0 pM	0 μ L	100 μ L

SPECIMEN COLLECTION AND PREPARATION

A. Cell Lysates

Cells may be lysed by repeated freeze-thaws and/or sonication in a buffer of 50 mM Tris-HCl, 100 mM NaCl, 0.1% Triton X-100, pH 7.4, and the tissue factor extracted in the buffer for 30 minutes at 37°C or for 18 hours at 2° - 8°C. Typically, samples are assayed neat but dilute with Assay Buffer if necessary. Store the extracted lysates at -70°C.

B. Plasma

Only citrate collected platelet poor plasma may be used for this assay. Do Not Use EDTA collected plasma. See "Collection, Transport and Processing of Blood Specimens for Testing Plasma-based Coagulation Assays and Molecular Hemostasis Assays; Approved Guidelines-Fifth Edition", NCCLS Document H21-A5, Vol. 28, No. 5, January 2008. Plasma collection should be performed as follows:

1. Collect 9 parts of blood into 1 part of 3.2% (0.109 M) trisodium citrate anticoagulant solution.
2. Centrifuge the blood sample at 1,500 x g for 15 minutes.
3. Plasma should be stored at room temperature and assayed within 2 hours. Alternatively, plasma may be stored at -70°C for up to 6 months.
4. Frozen plasma should be thawed rapidly at 37°C. Thawed plasmas should be stored at room temperature and assayed within 2 hours.

PROCEDURE

Materials Provided – See Reagents

Materials Required But Not Provided

96 well round bottom microtiter plate
 0.22 μ m filtered deionized H₂O
 200-1000 μ L single pipette, 10-100 μ L single pipette
 5-50 μ L eight channel multi-pipette
 Glacial acetic acid
 Microtiter plate reader at 405 nm

Assay Procedure

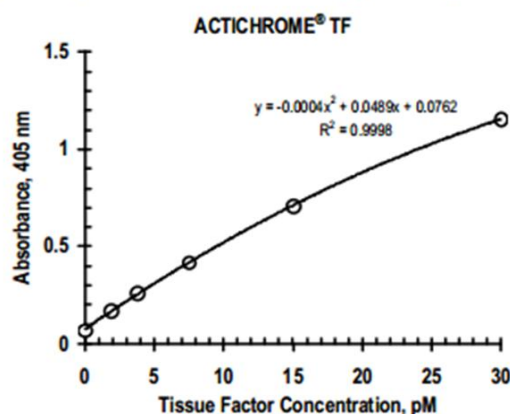
1. Add 50 μ L Assay Buffer (pH 8.4) to each well.
2. Add 25 μ L Tissue Factor Standards or test sample to each well.
3. Add 25 μ L of Human Factor VIIa to each well.
4. Add 25 μ L of Human Factor X. Cover the microwells and incubate at 37°C for 15 minutes.
5. Add 25 μ L of SPECTROZYME FXa substrate to each well and incubate at 37°C for 30 minutes. The enzyme/substrate reaction begins upon addition of the SPECTROZYME FXa, turning the solution yellow over time.

6. Stop the reaction after the 30 minutes by adding 50 μL of glacial acetic acid. Read the absorbance of the solution at a wavelength of 405 nm. For plasma samples, read the solution absorbance at 405 nm and at 490 nm. Use the $\Delta A_{405-490}$ of the sample for interpolating the tissue factor concentration.

RESULTS

Representative Standard Curve

The standard curve is constructed by plotting the mean absorbance value measured for each Tissue Factor Standard versus its corresponding concentration. A standard curve should be constructed each time the assay is performed. The following curve has been plotted using a 2nd order polynomial regression and is for demonstration purposes only.



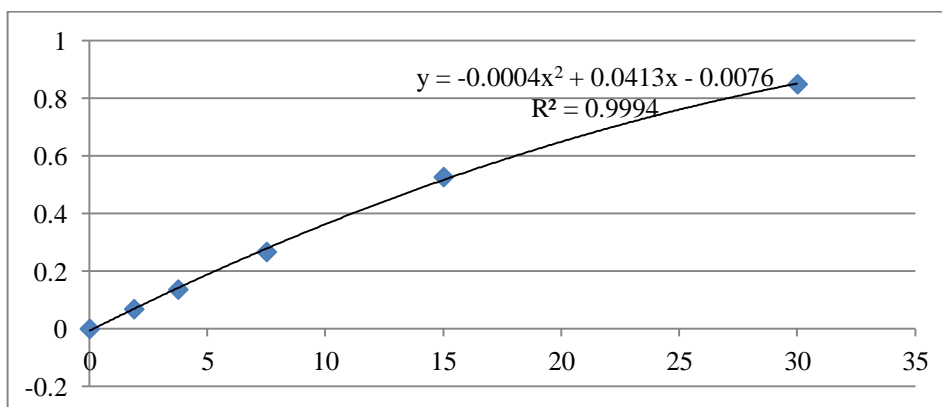
Calculation

Interpolate the Tissue Factor concentration of the test sample directly from the standard curve. If the sample has been diluted, multiply the results of the sample by the dilution factor to obtain its actual tissue factor concentration.

ANALYTICAL PERFORMANCE

Specificity: The assay recognizes native and recombinant human relipidated tissue factor. No interference from other coagulation factors has been observed.

Sensitivity: The lower limit of detection for plasma samples has been found to be approximately 2 pM (approximately 85 pg/mL), determined by adding two standard deviations to the mean OD value of the "0" standard (n=10) and interpolating the corresponding concentration from the standard curve.



Standard Curve for TF Activity (Figure 4.4)

9.5 Thrombin Generation Assay

TECHNOTHROMBIN® TGA

PRODUCT DESCRIPTION

INTENDED USE

The TECHNOTHROMBIN® TGA kit is an assay system for determination of thrombin generation over time in **platelet poor or platelet rich plasma** (PPP or PRP) upon activation of the clotting cascade by micelles of negatively charged phospholipids containing different amounts of human tissue factor and CaCl_2 . The kit can be used to monitor hemophiliacs during inhibitor bypassing therapy, to monitor anticoagulation therapy, to calculate INR values for patients and to determine states of bleeding disorders or thrombophilia as well as the activity of circulating micro particles. This broad range of applications is possible by providing different tissue factor concentrations and by monitoring the whole kinetic of thrombin generation during initiation, amplification and down regulation of thrombin formation. TECHNOTHROMBIN® TGA is therefore a universal assay kit for analyzing and monitoring the function of the haemostatic system.

TEST PRINCIPLE

TECHNOTHROMBIN® TGA is based on monitoring the fluorescence generated by the cleavage of a fluorogenic substrate by thrombin over time upon activation of the coagulation cascade by different concentrations of tissue factor and negatively charged phospholipids in plasma. From the changes in fluorescence over time, the concentration of thrombin (nM) in the sample can be calculated using the respective thrombin calibration curve. The increase in thrombin concentration with time then allows to calculate generation of thrombin in the sample and to plot such thrombin values over time for the whole coagulation process. This then results in the visualization of the different phases of clot formation.

COMPOSITION

The TECHNOTHROMBIN® TGA reagent kit for 3x16 determinations contains:

mL	reagent	description
3 x 1.5	TGA substrate (SUB)	Fluorogenic substrate 1 mM Z-G-G-R-AMC, 15 mM CaCl_2
1 x 3	TGA buffer (BUF)	Hepes-NaCl-buffer containing 0.5 % bovine serum albumin
1 x 0.5	TGA thrombin calibrator	~1,000 nM thrombin in buffer with BSA
1 x 0.5	TGA reagent C (RC) Low	RC Low conc. of phospholipid micelles containing rhTF in Tris-Hepes-NaCl buffer
1 x 0.5	TGA reagent C (RC) High	RC High conc. of phospholipid micelles containing rhTF in Tris-Hepes-NaCl buffer
1 x 1.5	TGA reagent D (RD)	RD conc. of phospholipid micelles in Tris-Hepes-NaCl buffer
1 x 1	TGA control high (CH)	Human plasma with increased thrombin generation, lyophilized.
1 x 1	TGA control low (CL)	Human plasma with decreased thrombin generation, lyophilized.

Each reagent is available on a modular basis.

The TECHNOTHROMBIN® TGA B contains:

mL	reagent	description
0.5	TGA reagent B (RB)	RB conc. of phospholipid micelles containing rhTF in Tris-Hepes-NaCl buffer

The TECHNOTHROMBIN® TGA CAL Set contains:

mL	reagent	description
1 x 3	TGA buffer (BUF)	Hepes-NaCl-buffer containing 0.5 % bovine serum albumin
1 x 0.5	TGA thrombin calibrator	~1,000 nM thrombin in buffer with BSA

MATERIAL REQUIRED (not supplied with the kit)

- Pipettes
- Distilled water
- Microtiter plates suitable for fluorescence measurement (we recommend black NUNC Maxisorp REF 475515)
- Fluorimeter, fluorescence reader (96-well format), ~360 nm/~460 nm (excitation/emission) with suitable software to monitor changes of fluorescence over time. Applications for several readers are available as download from www.technoclone.com.

WARNING AND PRECAUTIONS

- for research use only
- Every single donor plasma and every lot of the controls included is tested and found negative for HbAg, HIV 1/2 antibodies and HCV antibodies. However, general precautions should be taken by handling all human source materials as potentially infectious.
- All blood and plasma samples and products have to be handled as potentially infectious and with appropriate care and in compliance with the respective biosafety regulations and must be disposed in the same way as hospital waste.

STABILITY AND STORAGE

The expiry date printed on the labels is only applicable to storage of the unopened containers at + 2...8 °C.

Stability after reconstitution:

Reagent	RT* (20...25°C)	+2...8°C	-20°C
TGA substrate (SUB)	1 week	1 month	6 months
TGA buffer (BUF)	8 hours	1 week	1 month
TGA thrombin calibrator (CAL)	8 hours	1 week	6 months
TGA reagent B (RB), C Low (RCL), High (RCH), D (RD)	8 hours	1 week	6 months
TGA control high (CH)	4 hours	8 hours	1 month
TGA control low (CL)	4 hours	8 hours	1 month

Avoid contamination by micro-organisms.

Plasmas should be frozen only once; during storage, the vials should be tightly capped.

Stability of the sample material:

* room temperature

Sample material	RT* (20...25°C)	+2...8°C	-20°C
PPP, PRP and PFP Plasma	2 hours	4 hours	1 month

An immediate centrifugation after blood withdrawal is recommended.

Further we recommend an immediate shock freezing of the centrifuged samples.

Attention! The frozen samples should be stored in a constant environment - avoid exposing the samples to variations in temperature.

Before transportation we recommend to centrifuge and prepare the samples.

TEST PROCEDURE

PREPARATION OF SAMPLES

In the TECHNOTHROMBIN® TGA assay citrated plasma, we recommend CTAD tubes, (platelet rich, platelet poor or platelet free) can be used, depending on the specific application.

For plasma separation, mix 9 parts of venous blood and 1 part sodium citrate solution (0.11 mol/L) and centrifuge for 15 minutes at a RCF of at least 2.500 x g (corresponding to DIN 58905).

For special requirements, preparation of other plasmas might be necessary:

- for *platelet rich plasma (PRP)* centrifuge for 5 minutes at 100 x g and carefully pipette off the obtained PRP;
- for *platelet poor plasma (PPP)* centrifuge PRP for 10 minutes at 1.500 x g and carefully pipette off the obtained PPP;
- for *platelet and micro particle free plasma (PFP)*, centrifuge PPP for 30 minutes at 15.000 x g and carefully pipette off the obtained PFP or use the Technoclone micro particle filtration unit.

PREPARATION OF REAGENTS

The lyophilized reagents must be dissolved in the volume of distilled water indicated on the vials. All reconstituted reagents should reach room temperature before use.

After exactly 20 minutes of reconstitution time and thorough mixing (Vortex), reagents are ready to use.

For standardization tests a reconstitution time of 30 minutes is recommended for controls.

READER SETTING

Please use the corresponding reader application (provided under www.technoclone.com).

Temperature during measurement: 37°C

Fluorometer wavelength: ~360 nm / ~460 nm [excitation/emission]

Attention !

A pre-reading of the empty plate is suggested, to avoid any inaccuracies during the reading of your samples, which can occur due to inhomogeneous and defective plates.

READING TIMES

1.) Thrombin calibration curve: 10 min

in 30 sec measurement intervals

The thrombin calibration curve has to be done separately from sample measurement.

2.) Samples: depending on the sample material 60 min

(for FVIII inhibitor therapy 90 - 120 min)

in 1 min measurement intervals.

PERFORMANCE OF THE TEST

Samples and dissolved reagents should reach room temperature before use.

1.) Thrombin calibration curve

The thrombin calibration curve has to be done separately from sample measurement. Concentration of the thrombin calibrator (CAL) is lot dependent, consult the label on the vial.

The thrombin calibrator is diluted with TGA buffer as indicated in the table below:

1st dilution (1:2): (STD 1)	+	200 µL Thrombin Calibrator (CAL) 200 µL TGA buffer (BUF)
2nd dilution (1:4): (STD 2)	+	100 µL 1 st dilution 100 µL TGA buffer (BUF)
3rd dilution (1:20): (STD 3)	+	20 µL Thrombin Calibrator (CAL) 380 µL TGA buffer (BUF)
4th dilution (1:200): (STD 4)	+	20 µL 3 rd dilution 180 µL TGA buffer (BUF)

All calibrator dilutions have to be measured in duplicate.

Add reagents in the following sequence:

40 µL 50 µL	calibrator dilution (STD 1 - STD 4) TGA substrate (SUB)
measure for 10 min in 30 sec intervals at 37°C	

Start reading of the plate/strip immediately after pipetting the substrate.

ONLY ONE CALIBRATION CURVE HAS TO BE DONE FOR EACH LOT !

2.) Sample measurement

The reagents have to be added in the following sequence:

Measurement with:				
Reagent	TGA RB	TGA RC Low	TGA RC High	TGA RD *
sample	40 µL	40 µL	40 µL	20 µL
RB	10 µL	-	-	-
RCL	-	10 µL	-	-
RCH	-	-	10 µL	-
TGA RD	-	-	-	30 µL
TGA SUB	50 µL	50 µL	50 µL	50 µL
measure for 60 min (for FVIII inhibitor therapy 90 - 120 min) in 1 minute measurement intervals at 37°C				

Start reading of the plate immediately after pipetting the substrate.

A reagent substrate mixture can be prepared in advance.

Preparation of the mixture:

The mixture of reagent and substrate should be done in a 1+5 proportion for RC Low and RC high and in a 3+5 proportion for RD.

The mixture can be aliquoted and frozen at -20°C.

A reagent substrate mixture can be prepared in advance.

Preparation of the mixture:

The mixture of reagent and substrate should be done in a 1+5 proportion for RC Low and RC high and in a 3+5 proportion for RD.

The mixture can be aliquoted and frozen at -20°C.

When reagent/substrate mixture is used the reagents have to be added to the plate in the following sequence:

Measurement with reagent/substrate mixture:				
Reagent	RB	RC Low	RC High	TGA RD*
sample	40 µL	40 µL	40 µL	20 µL
reagent/substrate mixture	60 µL	60 µL	60 µL	80 µL
measure for 60 min (for FVIII inhibitor therapy 90 - 120 min) in 1 minute measurement intervals at 37°C				

Start reading of the plate immediately after pipetting the reagent/substrate mixture.

Attention ! We recommend to measure duplicates for each samples.

Attention ! The lamp of the Biotek Readers is loosing intensity the longer the machine is switched on. We recommend to run only 2 consecutive runs and to switch off the reader for ~ 3 hours before you start the next run.

* ATTENTION: different pipetting scheme for Reagent D

ANALYSIS OF RESULTS

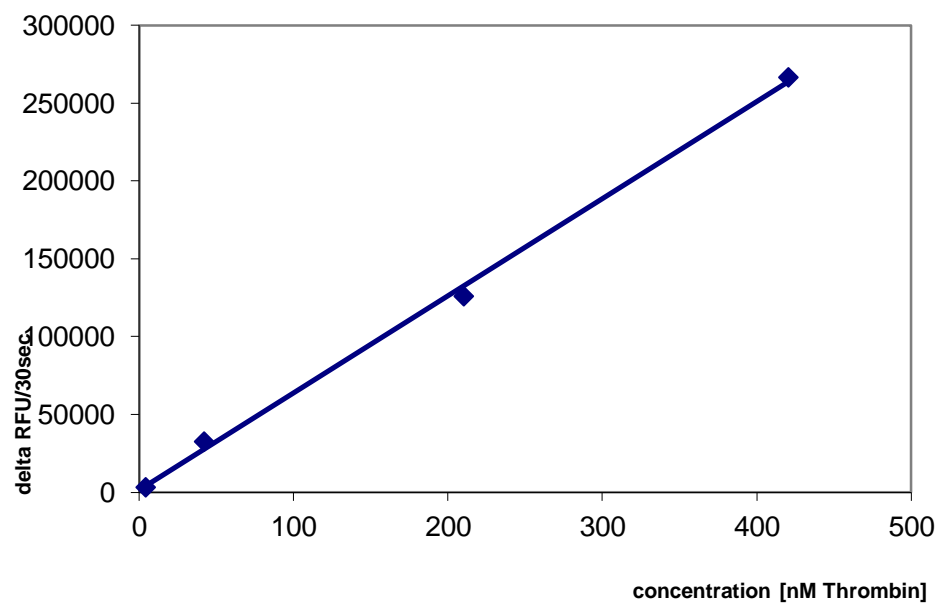
Evaluation is done automatically with the TECHNOTHROMBIN® TGA evaluation software (Software for several readers are available as download from www.technoclone.com). The software includes calibration curve and sample evaluation.

THROMBIN CALIBRATION CURVE

Using the provided evaluation software, RFU data (relative fluorescence units) measured by the fluorimeter for the different thrombin concentrations are converted into a thrombin calibration curve. This thrombin calibration curve is then used by the provided software to calculate nM thrombin present in the sample at a given time.

STANDARDIZATION

The thrombin calibrator is calibrated against the thrombin Reference Preparation of the WHO.



Standard Curve for Thrombin generation (Figure 4.5)

9.6 Sparcl1 ELISA



Sino Biological Inc.
Biological Solution Specialist

Human SPARCL1 ELISA Pair Set

(Hevin / MAST9)

Catalog Number : SEK10046

To achieve the best assay results, this manual must be read carefully before using this product and the assay is run as summarized in the General ELISA protocol.

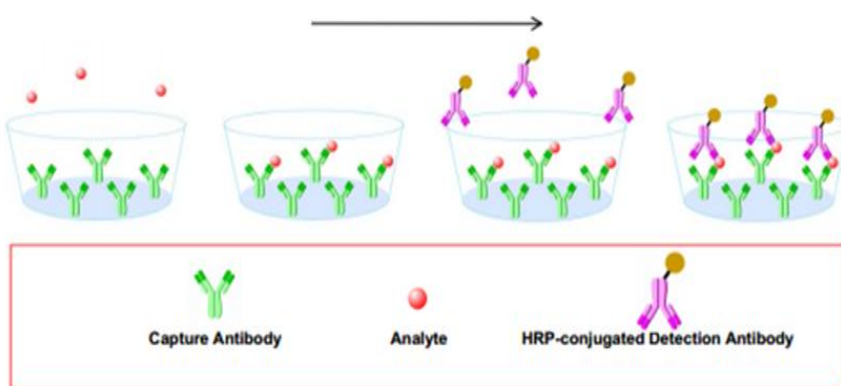
PRINCIPLE OF THE TEST

The Sino Biological ELISA Pair Set is a solid phase sandwich ELISA (Enzyme-Linked Immunosorbent Assay). It utilizes a monoclonal antibody specific for SPARCL1 coated on a 96-well plate. Standards and samples are added to the wells, and any SPARCL1 present binds to the immobilized antibody. The wells are washed and a horseradish peroxidase conjugated mouse anti-SPARCL1 monoclonal antibody is then added, producing an antibody-antigen-antibody "sandwich". The wells are again washed and TMB substrate solution is loaded, which produces color in proportion to the amount of SPARCL1 present in the sample. To end the enzyme reaction, the stop solution is added and absorbances of the microwell are read at 450 nm.

INTENDED USE

- The human SPARCL1 ELISA Pair Set is for the quantitative determination of human SPARCL1.
- This ELISA Pair Set contains the basic components required for the development of sandwich ELISAs.

ASSAY PROCEDURE SUMMARY



This Pair Set has been configured for research use only and is not to be used in diagnostic procedures.

MATERIALS PROVIDED

Bring all reagents to room temperature before use.

Capture Antibody – 1.0 mg/mL of mouse anti-SPARCL1 monoclonal antibody. Dilute to a working concentration of 2.0 µg/mL in CBS before coating.

Detection Antibody – 0.5 mg/mL mouse anti-SPARCL1 monoclonal antibody conjugated to horseradish-peroxidase. Dilute to working concentration of 1.0 µg/mL in detection antibody dilution buffer before use.

Standard – Each vial contains 160ng of recombinant SPARCL1. Reconstitute with 1 mL detection antibody dilution buffer. After reconstitution, store at -20°C to -70°C in a manual defrost freezer. A seven-point standard curve using 2-fold serial dilutions in sample dilution buffer, and a high standard of 6000 pg/mL is recommended.

SOLUTIONS REQUIRED

CBS - 0.05M Na₂CO₃ , 0.05M NaHCO₃ , pH 9.6, 0.2 µm filtered

TBS - 25mM Tris, adjust pH to 7.4 by HCl

Wash Buffer - 0.05% Tween20 in TBS, pH 7.2 - 7.4

Blocking Buffer - 2% BSA in Wash Buffer

Sample dilution buffer - 0.1% BSA in wash buffer, pH 7.2 - 7.4, 0.2 µm filtered

Detection antibody dilution buffer - 0.5% BSA in wash buffer, pH 7.2 - 7.4, 0.2 µm filtered

Substrate Solution : To achieve best assay results, fresh substrate solution is recommended

Substrate stock solution - 10 mg/ml TMB (Tetramethylbenzidine) in DMSO

Substrate dilution buffer - 0.05M Na₂HPO₄ and 0.025M citric acid ; adjust pH to 5.5

Substrate working solution - For each plate dilute 250µl substrate stock solution in 25ml substrate dilution buffer and then add 80 µl 0.75% H₂O₂ , mix it well

Stop Solution - 2 N H₂SO₄

PRECAUTION

The Stop Solution suggested for use with this Pair Set is an acid solution. Wear eye, hand, face, and clothing protection when using this material.

STORAGE

Detection Antibody should be protected from prolonged exposure to light. Aliquot the reagents and store at -20°C to -70°C in a manual defrost freezer.

GENERAL ELISA PROTOCOL

Plate Preparation

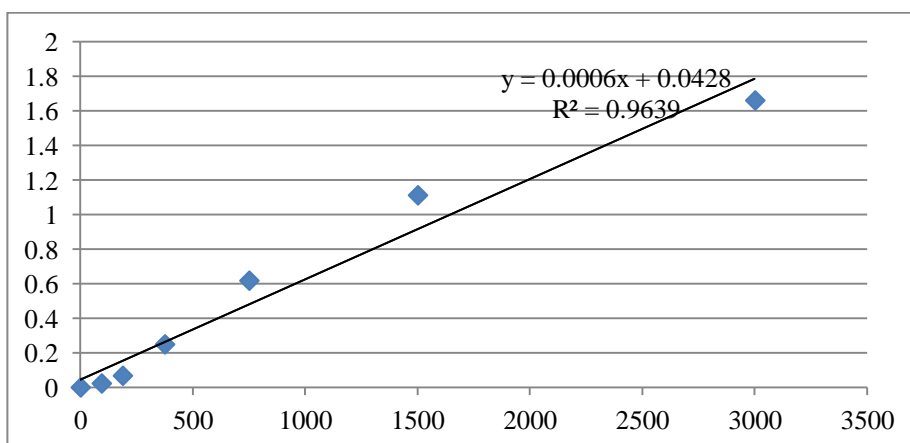
1. Dilute the capture antibody to the working concentration in CBS. Immediately coat a 96-well microplate with 100µL per well of the diluted capture antibody. Seal the plate and incubate overnight at 4°C.
2. Aspirate each well and wash with at least 300µL wash buffer, repeating the process two times for a total of three washes. Complete removal of liquid at each step is essential for good performance. After the last wash, remove any remaining wash buffer by inverting the plate and blotting it against clean paper towels.
3. Block plates by adding 300 µL of blocking buffer to each well. Incubate at room temperature for a minimum of 1 hour.
4. Repeat the aspiration/wash as in step 2. The plates are now ready for sample addition.

Assay Procedure

1. Add 100 µL of sample or standards in sample dilution buffer per well. Seal the plate and incubate 2 hours at room temperature.
2. Repeat the aspiration/wash as in step 2 of plate preparation.
3. Add 100 µL of the detection antibody, diluted in antibody dilution buffer, to each well. Seal the plate and incubate 1 hour at room temperature.
4. Repeat the aspiration/wash as in step 2 of plate preparation.
5. Add 200 µL of substrate solution to each well. Incubate for 20 minutes at room temperature (if **substrate solution is not as requested, the incubation time should be optimized**). Avoid placing the plate in direct light.
6. Add 50 µL of stop solution to each well. Gently tap the plate to ensure thorough mixing.
7. Determine the optical density of each well immediately, using a microplate reader set to 450 nm.

CALCULATION OF RESULTS

- Calculate the mean absorbance for each set of duplicate standards, controls and samples. Subtract the mean zero standard absorbance from each.
- Construct a standard curve by plotting the mean absorbance for each standard on the y-axis against the concentration on the x-axis and draw a best fit curve through the points on the graph.
- To determine the concentration of the unknowns, find the unknowns' mean absorbance value on the y-axis and draw a horizontal line to the standard curve. At the point of intersection, draw a vertical line to the x-axis and read the concentration. If samples have been diluted, the concentration read from the standard curve must be multiplied by the dilution factor.
- Alternatively, computer-based curve-fitting statistical software may also be employed to calculate the concentration of the sample.

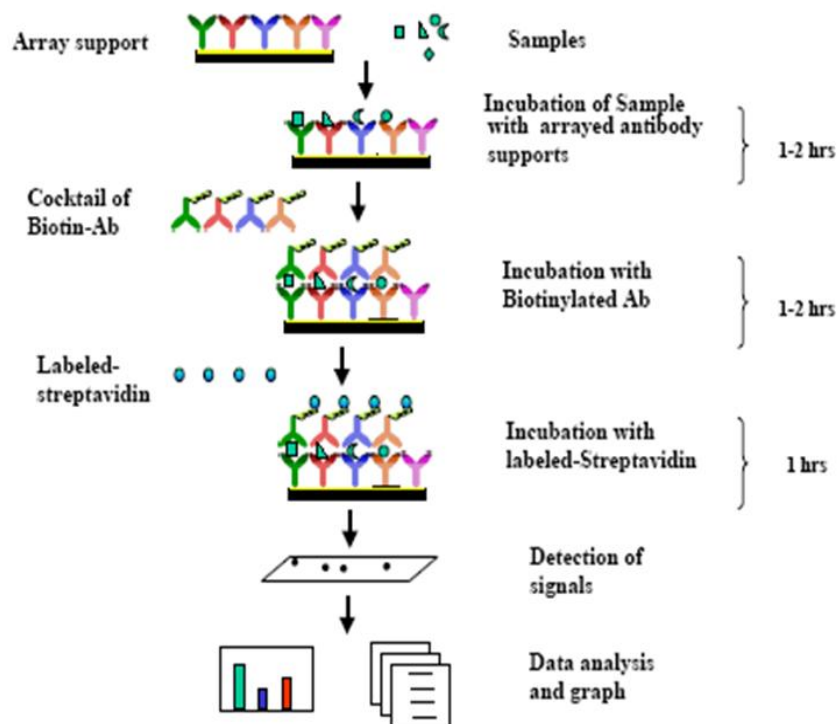


Standard Curve for Sparc11 ELISA (Figure 7.2)

9.7 CM Ctokine Arrays

RayBio® Human Cytokine Antibody Array

Here's how it works



II. Materials Provided

Upon receipt, all components of the RayBio® Human Cytokine Antibody Array kit should be stored at -20°C to -80°C. At -20°C to -80°C the kit will retain complete activity for up to 6 months. Once thawed, the array membranes and 1X Blocking Buffer should be kept at -20°C and all other component should be stored at 4°C. After thawing the reagents, the kit must be used within three months, and please use the kit within six months of purchase.

- RayBio® Human Cytokine Antibody Array membranes (2/4/8 membranes)
- Biotin-Conjugated Anti-Cytokines (1/2/4 tubes, each tube for two membranes)
- 1,000X HRP-Conjugated Streptavidin (1 tube)
- 1X Blocking Buffer (25/50 ml)
- 20X Wash Buffer I (10/20 ml)
- 20X Wash Buffer II (10/20 ml)
- 2X Cell Lysis Buffer (10/20 ml)
- Detection Buffer C (1.5/2.5 ml)
- Detection Buffer D (1.5/2.5 ml)
- Eight-Well Tray (1 each)
- Manual

Additional Materials Required

- Small plastic boxes or containers
- Orbital shaker
- Plastic sheet protector or SaranWrap
- Kodak X-Omat AR film (REF 165 1454) and film processor or Chemiluminescence imaging system

III. Overview and General Considerations

A. Preparation of Samples

- Use serum-free conditioned media if possible.
- If serum-containing media is required, use an uncultured media aliquot as a negative control sample, since many types of sera contain cytokines.
- For cell lysates and tissue lysates, we recommend using RayBio® Cell Lysis Buffer to extract proteins from cell or tissue (e.g. using homogenizer). Dilute 2X RayBio® Cell Lysis Buffer with H₂O (we recommend adding proteinase inhibitors to Cell Lysis Buffer before use). After extraction, spin the sample down and save the supernatant for your experiment. Determine protein concentration.
- We recommend using per membrane:
 - 1 ml of Conditioned media (undiluted), or
 - 1 ml of 2-fold to 5-fold diluted sera or plasma, or
 - 50-500 µg of total protein for cell lysates and tissue lysates (use ~200-250 µg of total protein for first experiment) *Dilute the lysate at least 10 fold with 1 X blocking buffer.*

Note: The amount of sample used depends on the abundance of cytokines. More of the sample can be used if the signals are too weak. If the signals are too strong, the sample can be diluted further.

○

If you experience high background, you may further dilute your sample.

B. Handling Array Membranes

- Always use forceps to handle membranes, and grip the membranes by the edges only.
- Never allow the array membranes to dry during experiments.

C. Incubation

- Completely cover the membranes with sample or buffer during incubation, and cover the eight-well tray with lid to avoid drying.
- Avoid foaming during incubation steps.
- Perform all incubation and wash steps under gentle rotation.
- Several incubation steps such as step 2 (blocking), step 3 (sample incubation), step 8 (biotin-Ab incubation) and step 11 (HRP-streptavidin incubation) may be done at 4°C for overnight, but make sure to cover the 8 well plate tightly to prevent evaporation.

IV. Protocol

A. Blocking and Incubation

1. Place each membrane into the provided eight-well tray ("-" mark is on the side printed with antibodies).
2. Add 2 ml 1X Blocking Buffer and incubate at room temperature for 30 min to block membranes. Make sure there are no bubbles between the membranes.
3. Decant Blocking Buffer from each container, and incubate membranes with 1 ml of sample at room temperature for 1 to 2 hours. Dilute sample using 1X Blocking Buffer if necessary.

Note: Incubation may be done at 4°C for overnight.

4. Decant the samples from each container, and wash 3 times with 2 ml of 1X Wash Buffer I at room temperature with shaking. Please allow 5 min per wash. Dilute 20X Wash Buffer I with H₂O.
5. Wash 2 times with 2 ml of 1X Wash Buffer II at room temperature with shaking. Allow 5 min per wash. Dilute 20X Wash Buffer II with H₂O.

6. Prepare working solution for primary antibody.

Add 100 μ l of 1x blocking buffer to the Biotin-Conjugated Anti-Cytokines tube. Mix gently and transfer all mixture to a tube containing 2 ml of 1x blocking buffer.

Note: the diluted biotin-conjugated antibodies can be stored at 4°C for 2-3 days.

7. Add 1 ml of diluted biotin-conjugated antibodies to each membrane. Incubate at room temperature for 1-2 hours.

Note: incubation may be done at 4°C for overnight.

8. Wash as directed in steps 4 and 5.

9. Add 2 ml of 1,000 fold diluted HRP-conjugated streptavidin (e.g. add 2 μ l of HRP-conjugated streptavidin to 1998 μ l 1X Blocking Buffer) to each membrane.

Note: mix the tube containing 1,000X HRP-Conjugated Streptavidin well before use since precipitation may form during storage.

10. Incubate at room temperature for 2 hours.

Note: incubation may be done at 4°C for overnight.

11. Wash as directed in steps 4 and 5.

B. Detection

*** Do not let the membrane dry out during detection. The detection process must be completed within 40 minutes without stopping.**

1. Proceed with the detection reaction.

Add 250 µl of 1X Detection Buffer *C* and 250 µl of 1X Detection Buffer *D* for one membrane; mix both solutions; Drain off excess wash buffer by holding the membrane vertically with forceps. Place membrane protein side up ("-" mark is on the protein side top left corner) on a clean plastic sheet (provided in the kit). Pipette the mixed Detection Buffer on to the membrane and incubated at room temperature for 2 minute. Ensure that the detection mixture is completely and evenly covers the membrane without any air bubbles.

2. Drain off any excess detection reagent by holding the membrane vertically with forceps and touching the edge against a tissue. Gently place the membrane, protein side up, on a piece of plastic sheet ("-" mark is on the protein side top left corner). Cover another piece of plastic sheet on the array. Gently smooth out any air bubble. Avoid using pressure on the membrane.

3. Expose the array to x-ray film (we recommend to use Kodak X-Omat AR film) and detect the signal using film developer, or the signal can be detected directly from the membrane using a chemiluminescence imaging system.

Expose the membranes for 40 Seconds. Then re-expose the film according to the intensity of signals. If the signals are too strong (background too high), reduce exposure time (e.g. 5-30 seconds). If the signals are too weak, increase exposure time (e.g. 5-20 min or overnight). Or re-incubate membranes overnight with 1X HRP-conjugated streptavidin, and redo detection in the second day.

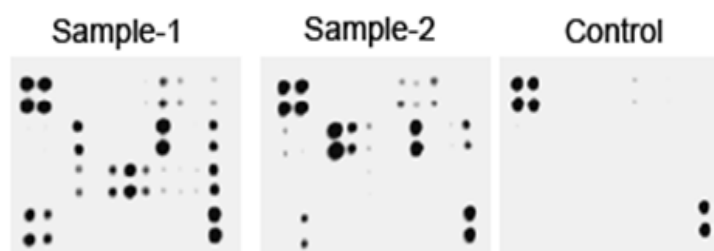
4. Save membranes in -20°C to -80°C for future references.

V. Interpretation of Results:

The following figure shows RayBio® Human Cytokine Antibody Array membranes probed with conditioned media from two different cell lines. Membranes were exposed to Kodak X-Omat film at room temperature for 1 minute. The biotin-conjugated IgG produces positive signals, which can be used to identify the orientation and to compare the relative expression levels among the different membranes.

One important parameter is background. To obtain the best results, we suggest that several exposures be attempted. We also strongly recommend using a negative control in which the sample is replaced with an appropriate mock buffer according to the array protocol, particularly during your first experiment.

Typical results using RayBio® Cytokine Antibody arrays



By comparing the signal intensities, relative expression levels of cytokines can be made. The intensities of signals can be quantified by densitometry. Positive control can be used to normalize the results from different membranes being compared. The signals also can be detected and quantitated by using a chemiluminescence imaging device.

The RayBio® Analysis Tool is a program specifically designed for analysis of RayBio® Cytokine Antibody Arrays. This tool will not only assist in compiling and organizing your data, but also reduces your calculations to a “copy and paste.” Call RayBiotech, Inc. at 770-729-2992 for ordering information.

9.8 Cardiac Functional Parameters

Infarct Zone	IZ	Region of ischemia within the myocardium as defined as regions not stained with TTC
Border Zone	BZ	Region with the infarcted myocardium defined as having 50% normal myocardium and 50% infarcted myocardium
Remote Zone	RZ	Defined as normal healthy regions within the myocardium
End Diastolic Volume	EDV	The volume of blood in each ventricle at the end of diastole usually about 120–130mL
End Systolic Volume	ESV	The volume of blood remaining in each ventricle at the end of systole usually about 50–60ml
Stroke Volume	SV	The volume of blood pumped from one ventricle of the heart with each beat. $SV = EDV - ESV$
Ejection Fraction	%EF	Represents the volumetric fraction of blood pumped out of the left and right ventricle with each heartbeat or cardiac cycle. $E_f(\%) = SV/EDV \times 100$
Heart Rate	HR	The number of heartbeats per unit of time-typically beats per minute (bpm).
Cardiac Output	CO	The volume of blood being pumped by the heart by a left or right ventricle in the time interval of one minute $CO = SV \times HR$
CT Measurements		64-slice images were analyzed with CardIQ software (AW 4.4, GE Healthcare). End-diastolic Volume (EDV) and end-systolic volume (ESV) and heart rate (HR) were calculated by slice summation using an automated contour detection. Papillary muscles and left ventricle (LV) outflow tract were not regarded as part of the LV cavity. The anatomical location for determination of the LV volume was selected at the mid mitral valve. Based on the automatic detection of the LV volume, the EDV, ESV and ejection fraction were calculated by specialised software.

